

DELINEATION OF FLOOD INUNDATION
EXTENT AS THE RESULT OF LAND USE
CHANGES IN KUANTAN RIVER BASIN



NG ZONE FHONG

اونيورسيتي ملايسيا قهغ

UNIVERSITI MALAYSIA PAHANG

Master of Science

UNIVERSITI MALAYSIA PAHANG

UNIVERSITI MALAYSIA PAHANG

DECLARATION OF THESIS AND COPYRIGHT

Author's Full Name : NG ZONE FHONG

Date of Birth : 10 DECEMBER 1991

Title : DELINEATION OF FLOOD INUNDATION EXTENT AS THE
RESULT OF LAND USE CHANGES
IN KUANTAN RIVER BASIN.

Academic Session : SEMESTER 2 2020/2021

I declare that this thesis is classified as:

- CONFIDENTIAL (Contains confidential information under the Official Secret Act 1997)*
- RESTRICTED (Contains restricted information as specified by the organization where research was done)*
- OPEN ACCESS I agree that my thesis to be published as online open access (Full Text)

I acknowledge that Universiti Malaysia Pahang reserves the following rights:

1. The Thesis is the Property of Universiti Malaysia Pahang
2. The Library of Universiti Malaysia Pahang has the right to make copies of the thesis for the purpose of research only.
3. The Library has the right to make copies of the thesis for academic exchange.

Certified by:


(Student's Signature)


(Supervisor's Signature)

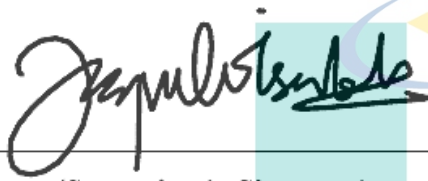
911210-05-5315
New IC/Passport Number
Date: 09/04/2021

Dr. Jacqueline Isabella Anak Gisen
Name of Supervisor
Date: 09/04/2021

NOTE: * If the thesis is CONFIDENTIAL or RESTRICTED, please attach a thesis declaration letter.

SUPERVISOR'S DECLARATION

I hereby declare that I have checked this thesis and in my opinion, this thesis is adequate in terms of scope and quality for the award of the degree of Master of Science.



(Supervisor's Signature)

Full Name : DR. JACQUELINE ISABELLA ANAK GISEN

Position : SENIOR LECTURER

Date : 9 APRIL 2021



UMP

اونيورسيتي ملايسيا قهغ

UNIVERSITI MALAYSIA PAHANG

STUDENT'S DECLARATION

I hereby declare that the work in this thesis is based on my original work except for quotations and citations which have been duly acknowledged. I also declare that it has not been previously or concurrently submitted for any other degree at Universiti Malaysia Pahang or any other institutions.



(Student's Signature)

Full Name : NG ZONE FHONG

ID Number : MAC16002

Date : 9 APRIL 2021

اونيورسيتي ملايسيا قهغ

UNIVERSITI MALAYSIA PAHANG

DELINEATION OF FLOOD INUNDATION EXTENT AS THE RESULT OF
LAND USE CHANGES IN KUANTAN RIVER BASIN



اونيورسيتي ملايسيا قهغ

UNIVERSITI MALAYSIA PAHANG

Faculty of Civil Engineering Technology

UNIVERSITI MALAYSIA PAHANG

APRIL 2021

ACKNOWLEDGEMENTS

I would like to thank Universiti Malaysia Pahang (UMP) Gambang, Pahang for giving the opportunity to further study on this research and the professionalism on conducting the postgraduate study.

My greatest thanks to Dr. Jacqueline Isabella Anak Gisen, the main supervisor of this MSc thesis, for her invaluable inputs, guidance, encouragements, and sympathies. Her support and esteemed guidance are highly appreciated, especially the hardest time of the study period. Special thanks to Dr. Abolghasem Akbari, the ex-supervisor, for his continual support and constructive comment on the related topic of the research. In addition, specific help on supporting ideas and editing technical work from the field supervisor, Mr. Cheok Hou Seng from Ranhill Bersekutu Sdn Bhd, for his expertise knowledge sharing sessions and working experiences is highly appreciated.

Thanks also go to all staffs and postgraduate students, especially from whom I have great opportunities to make real friends and to exchange knowledge in UMP. Many thanks for the financial support from Dr. Ngien Su Kong, the project leader of the FRGS grant RDU150127 to help in finishing this MSc study. Special appreciation to Dr. Doh Shu Ing for his advice and motivation along the MSc study. Moreover, sincere gratitude to all internal and external panels who have strengthened and leveled the value of this thesis. A special thank to all my supportive postgraduate friends namely Mr. Tong Foo Sheng, Mr. Tan Yeong Yu, Ms. Syeda Maria Zaidi, Ms. Yap Hiew Thong for all the love, caring, and knowledge sharing.

Furthermore, extremely grateful to Drainage & Irrigation Department (DID) of Malaysia for providing the hydrological and hydraulic information, Department of Agriculture (DOA) of Malaysia for giving land use and soil map of Kuantan, and Department of Survey and Mapping Malaysia (JUPEM) for supplying the tidal report.

Valuable support from the beloved family has encouraged me to overcome all the barriers, with your love, I believe I can do the best. It is never enough to just say.

“Thank You” but please accept my great and sincere appreciation for what you all have done for me.

Last but not least, a big love to myself for the determination, passion, tolerance, and wisdom towards this MSc study.

ABSTRAK

Banjir merupakan bencana alam yang paling dahsyat di dunia. Masalah banjir seperti kehilangan nyawa dan harta benda serta penyelenggaraan kerosakan banjir telah mengejutkan pihak berkuasa tempatan dan agensi kerajaan di Malaysia. Salah satu banjir yang terburuk di Kuantan telah berlaku pada bulan Disember 2013 akibat hujan monsoon lebat berterusan. Ia telah menyebabkan sekitar 14,044 orang berpindah, kerosakan besar dari segi elektrik, struktur jalan, bangunan dan barang-barang. Kajian pengurusan risiko banjir kurang dilakukan di Kuantan River Basin (KRB). Oleh itu, kajian banjir teliti khususnya penjana peta banjir (FIM) di KRB sangat diperlukan bertujuan perancangan bandar masa depan. Kajian ini bertujuan mensimulasikan hidrograf banjir berdasarkan peristiwa hujan lebat dan untuk membangunkan FIM di KRB. Rangkaian saluran sungai KRB ditakrifkan dari Model Ketinggian Digital misi Shuttle Radar Topography Mission (SRTM) dengan resolusi 30 meter menggunakan aplikasi ArcGIS. HEC-GeoHMS digunakan untuk mengekstrak parameter hidrologi sebagai input untuk pemodelan hidrologi. Kaedah SCS Unit Hydrograph dan SCS-CN telah dilaksanakan dalam Sistem Pemodelan Hidrologi (HEC-HMS) untuk menganalisis aliran hujan. Hasil dari model hidrologi kemudiannya digunakan dalam Sistem Analisis Sungai 1D-2D (HEC-RAS) untuk simulasi ramalan paras air sungai dan FIM. Hidrograf banjir yang telah disimulasikan dari pemodelan hidrologi akan dibandingkan dengan data sebenar. Selepas proses penentuan dan pengesahan, simulasi menghasilkan purata ralat ramalan Nash Sutcliffe, E sebanyak 0.641 dan Root Mean Square Error, RMSE sebanyak 70.9 m³/s. Bagi hasil pemodelan hidraulik 1D, ia menunjukkan bahawa paras air di hulu dan hilir sungai Kuantan dalam purata ralat ramalan E sebanyak 0.716 dan RMSE sebanyak 0.493 m. Untuk pemodelan hidraulik 2D, kawasan banjir yang diramalkan pada tahun 2013 menunjukkan hampir 70% kesamaan berbanding kawasan banjir sebenar. Kawasan banjir menggunakan guna tanah pada tahun 2013 hampir 50% lebih besar berbanding tahun 2010. Secara keseluruhannya, hidrograf banjir dan kawasan banjir agak mencukupi dihasilkan oleh SRTM-DEM dalam pemodelan hidrologi dan hidraulik.

اونيورسيتي ملايسيا قهق

UNIVERSITI MALAYSIA PAHANG

ABSTRACT

Flood is undoubtedly the most devastating natural disaster in Malaysia. Flood induced problems such as loss of life, property damages, and infrastructure disruptions have distressed the local authorities and government agencies in Malaysia including the Kuantan District. One of the worst floods that occurred in Kuantan took place in December 2013 which was caused by extreme monsoon rain. This massive flood resulted in the evacuation of around 14,044 people and major damages to the electricity, road structure, buildings, and properties. Although flood event happens in a yearly basis in the Kuantan River Basin (KRB), there are still lack of flood risk management studies conducted in this region. Hence, a comprehensive flood study, especially the generation of flood inundation map (FIM) in (KRB) is highly needed for the future urban planning purpose. This study aims to simulate the flood hydrograph based on extreme rainfall events, and to develop the FIM for KRB. Watershed and river networks of the KRB were delineated from the Shuttle Radar Topography Mission Digital Elevation Model (SRTM-DEM) with a resolution of 30 m using ArcGIS application. ArcGIS integrated application, the Geospatial Hydrologic Modelling Extension (HEC-GeoHMS) was used to extract the hydrological parameters as the input for the hydrological modelling. For the rainfall-runoff analysis, the SCS Unit Hydrograph transformation method and SCS-CN loss method were implemented in the Hydrologic Modelling System (HEC-HMS). Runoff results from the hydrological model were then applied in the 1D-2D River Analysis System (HEC-RAS) for the unsteady-flow simulation to simulate and predict the river water level and overbank flow which were subsequently used to generate FIM. The flood hydrographs that have been simulated from the hydrological modelling was compared with the observed data. After the process of calibration and validation, it was noted that the simulation produced the same pattern of flow discharge to the observed with an average Nash Sutcliffe efficiency, NSE of 0.641 and Root Mean Square Error, RMSE of 70.9 m³/s. For the result of the 1D hydraulic modelling, it indicates that the water levels simulated at the upstream and downstream of the Kuantan river was fitted with the observed levels with an average E of 0.716 and RMSE of 0.493 m. Meanwhile, for the 2D hydraulic modelling, the generated flood inundated areas in the year 2013 demonstrates almost 70% similarity to the observed flood areas. The flood extent using land use in year 2013 is almost 50% larger compared to that in year 2010. Based on the modelling analysis and outcome, it can be concluded that generation of flood hydrograph and flood inundation extent is sufficient by SRTM-DEM in hydrological and hydraulic modelling.

UNIVERSITI MALAYSIA PAHANG

TABLE OF CONTENT

DECLARATION

TITLE PAGE

ACKNOWLEDGEMENTS

ii

ABSTRAK

iii

ABSTRACT

iv

TABLE OF CONTENT

v

LIST OF TABLES

ix

LIST OF FIGURES

x

LIST OF ABBREVIATIONS

iv

CHAPTER 1 INTRODUCTION

1

1.1 Study Background

1

1.2 Problem Statement

3

1.3 Objectives of the Study

5

1.4 Scope of the Study

5

1.5 Significance of the Study

6

CHAPTER 2 LITERATURE REVIEW

8

2.1 Introduction

8

2.2 Types of Flood

8

2.3 Causes of Flood

10

2.4 Flood Impacts

11

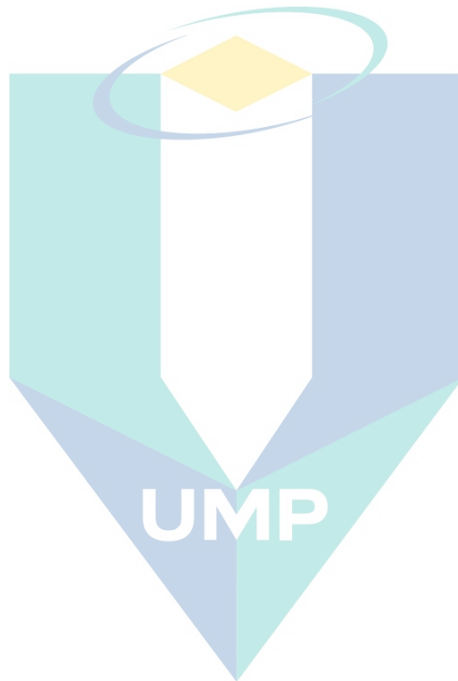
2.5 History of Recent Major Flood Events in Malaysia

12

2.5.1	Kuantan Flood Event	14
2.6	Geographic Information, Hydrology and Hydraulic Processes	15
2.6.1	Geographic Information Analysis	15
2.6.2	Hydrological Modelling	18
2.6.3	Hydraulic Modelling	31
2.6.4	Flood Inundation Map (FIM)	38
2.7	Research Overview	38
CHAPTER 3 METHODOLOGY		40
3.1	Introduction	40
3.2	Preliminary Study	43
3.2.1	Study Area	43
3.2.2	Field Visit	44
3.2.3	Storm Event Selection	44
3.3	Data Collection	55
3.3.1	Hydrological Data	55
3.3.2	River Survey	58
3.4	ArcGIS and HEC-GeoHMS	59
3.4.1	Watershed Delineation	59
3.4.2	Curve Number	61
3.4.3	HEC-GeoHMS Extension	62
3.5	Application of HEC-HMS Hydrological Modelling	66
3.5.1	Basin Model	66
3.5.2	Meteorological Model	67
3.5.3	Control Specification	69
3.5.4	Calibration and Validation	69

3.6	Application of HEC-RAS Hydraulic Modelling	69
3.6.1	Hydraulic Data Input	70
3.6.2	Hydraulic Model Run	71
3.6.3	Flood Inundation Map Based on Historical Flood Events	74
3.7	Flood Inundation Map Based on Landuse Changes Impact	74
3.8	Model Performance Evaluation	75
CHAPTER 4 RESULTS AND DISCUSSION		77
4.1	Introduction	77
4.2	Watershed and River Network Delineation	78
4.2.1	Delineation of Kuantan River Network	78
4.2.1	Generation of Kuantan River Basin	85
4.2.2	Generating Curve Number	89
4.2.3	Generating Basin Model Components for Hydrologic Modelling	93
4.3	HEC-HMS Rainfall-Runoff Modelling	93
4.3.1	HEC-HMS Model Simulation	93
4.4	Hydraulic Modelling	101
4.4.1	1D-2D Unsteady Simulation	101
4.4.2	Comparison of Flood Inundation Map (FIM) with Historical Flood Event	106
4.4.3	Flood Inundation Map (FIM) based on Land Use Changes	117
CHAPTER 5 CONCLUSION AND RECOMMENDATIONS		119
5.1	Introduction	119
5.2	Recommendations	120
REFERENCES		122

APPENDIX A Survey fieldwork pictures	130
APPENDIX B Hydraulic parameters	132
APPENDIX C Hydrological parameters	133



اونيورسيتي مليسيا قهغ

UNIVERSITI MALAYSIA PAHANG

LIST OF TABLES

Table 2.1	Major Recent Flood History in Malaysia	13
Table 2.2	Runoff Volume Models	21
Table 2.3	Surface Runoff Models	21
Table 2.4	Baseflow Models	21
Table 2.5	Channel Routing Models	21
Table 2.6	CN-conversion formulae	25
Table 2.7	Classes of Antecedent Moisture Conditions (AMC)	25
Table 3.1	Location of rainfall, streamflow, and water level stations in KRB	56
Table 3.2	Description of Hydrologic Soil Group Classification	62
Table 3.3	The Landuse changes between year 2010 and 2013	75
Table 4.1	The characteristics of the main basin and sub-basins as stated above in the paragraph	86
Table 4.2	The Characteristics of the River Network for KRB	88
Table 4.3	The calibration parameters used in the calibration on 29 th December 2010 to 2 nd January 2011	96
Table 4.4	The calibration parameters used in the calibration on 16 th to 19 th March 2014	99
Table 4.5	Summary of model prediction on discharge	101
Table 4.6	Summary of model prediction on the 1D water level	106

اونيورسيتي ملايسيا قهغ

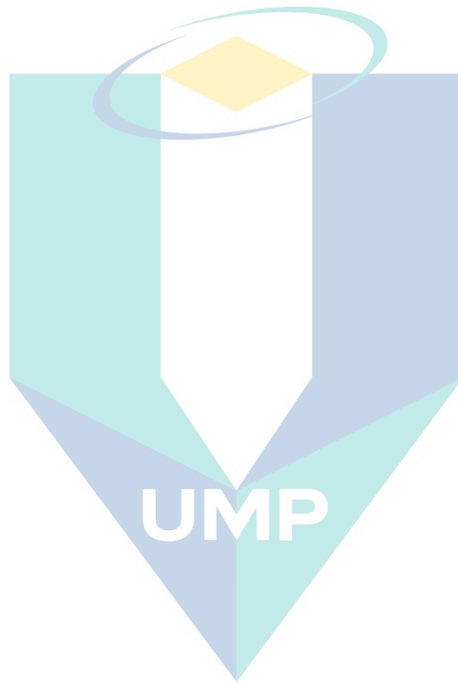
UNIVERSITI MALAYSIA PAHANG

LIST OF FIGURES

Figure 1.1	Plan view of the flooded area at the centre of Kuantan District in December 2013	4
Figure 2.1	The wind direction of South-West and North-East monsoon in Malaysia	12
Figure 2.2	Figure Representation of Terms in Energy Equation	34
Figure 2.3	Channel and floodplain flows	35
Figure 3.1	Flowchart of Flood Inundation Modelling at KRB	42
Figure 3.2	Kuantan River Basin in Malaysia	43
Figure 3.3	Average total monthly precipitation for the year 2000 to 2016	45
Figure 3.4	Average total yearly precipitation for the year 2000 to 2016	45
Figure 3.5	The maximum discharge at Bukit Kenau station (3930401) for the year 2000 to 2013	45
Figure 3.6	Total Precipitation for the event from 29 th December 2010 to 2 nd January 2011	47
Figure 3.7	Streamflow for the event from 29 th December 2010 to 2 nd January 2011	48
Figure 3.8	Precipitation for the event from 26 th to 30 th March 2011	49
Figure 3.9	Streamflow for the event from 26 th to 30 th March 2011	50
Figure 3.10	Precipitation for the event from 1 st to 5 th December 2013	51
Figure 3.11	Streamflow for the event from 1 st – 5 th December 2013	52
Figure 3.12	Precipitation for the event from 16 th to 19 th March 2014	53
Figure 3.13	Streamflow for the event from 16 th to 19 th March 2014	54
Figure 3.14	Hydrological stations within KRB	57
Figure 3.15	Location of the cross-sections surveyed point along the Kuantan River	58
Figure 3.16	The cross-sectional view at chainage CH10000 and CH 500	59
Figure 3.17	Process flow of DEM pre-processing	60
Figure 3.18	Land Use Map in 2010 for KRB	63
Figure 3.19	Land Use Map in 2013 for KRB	64
Figure 3.20	Hydrologic Soil Group (HSG) Map for KRB	65
Figure 3.21	Rainfall Distribution by Thiessen Polygon Method	68
Figure 3.22	Terrain created based on the SRTM DEM for KRB	73
Figure 4.1	Reconditioned DEM for KRB	79
Figure 4.2	Filled DEM for KRB	80
Figure 4.3	Flow Direction DEM for KRB	81

Figure 4.4	Flow Accumulation DEM for KRB	82
Figure 4.5	Delineated river network in the Kuantan River Basin	83
Figure 4.6	Delineated sub-basins and river network	84
Figure 4.7	The adjusted curve number map of the year 2010 at KRB	90
Figure 4.8	The adjusted curve number map of the year 2013 at KRB	91
Figure 4.9	Basin Model Component in HECHMS	92
Figure 4.10	The simulated vs observed data on 29 th December 2010 to 2 nd January 2011 at Bukit Kenau Station	95
Figure 4.11	The simulated vs observed flood hydrograph on 26 th to 30 th March 2011 at Bukit Kenau Station	97
Figure 4.12	The simulated vs observed flood hydrograph on 16 th to 19 th March 2014 at Bukit Kenau Station	98
Figure 4.13	The simulated vs observed flood hydrograph on 1 st to 5 th December 2013 at Bukit Kenau Station	101
Figure 4.14	The simulated vs observed stage hydrograph on 29 th December 2010 to 2 nd January 2011 at Bukit Kenau Station	102
Figure 4.15	The simulated vs observed stage hydrograph on 29 th December 2010 to 2 nd January 2011 at Kuantan Bypass station	103
Figure 4.16	The simulated vs observed stage hydrograph on 26 th to 30 th March 2011 at Bukit Kenau Station	103
Figure 4.17	The simulated vs observed stage hydrograph on 26 th to 30 th March 2011 at Kuantan Bypass Station	104
Figure 4.18	The simulated vs observed stage hydrograph on 1 st to 5 th December 2013 at Bukit Kenau Station	104
Figure 4.19	The simulated vs observed stage hydrograph on 1 st to 5 th December 2013 at Kuantan Bypass Station	105
Figure 4.20	Generated FIM on 29 th December 2010 to 2 nd January 2011	107
Figure 4.21	Generated FIM on 26 th – 30 th March 2011	107
Figure 4.22	Generated FIM on 1 st to 5 th December 2013	108
Figure 4.23	Hardcopy of Digital Flood Inundation Map (FIM) in the year of 2013 from DID flood report	110
Figure 4.24	Generated flood area from HECRAS (in red filled) with the observed flooded locations from Figure 4-22 (in red line) in the year 2013	111
Figure 4.25	Generated FIM from HECRAS (in red colour) with the observed flooded locations extracted from DID flood report in the year 2013	112
Figure 4.26	Scene 1 at the area around Perkampungan Sg. Isap Perdana and Sg. Isap Damai during a flood event in the year 2013 taken from the historical aerial photos and google earth view	114
Figure 4.27	Scene 2 at the area around Sg. Isap during a flood event in the year 2013 from the historical aerial photos and google earth view	115

Figure 4.28	Scene 3 at Tunas Manja near Sg Isap during a flood event in the year 2013 from the historical aerial photos and google earth view	116
Figure 4.29	Flood Inundation Map based on 2010 landuse	118
Figure 4.30	Flood Inundation Map based on 2013 landuse	118



اونيورسيتي ملايسيا قهغ

UNIVERSITI MALAYSIA PAHANG

LIST OF SYMBOLS

ΔT	Computational Time Step [s]
ΔX	Cell Size [m]
μ	Hydraulic Diffusivity [m ² /s]
A	Watershed Area [m ²]
a	Velocity Weighting Coefficient [-]
B	Top Width of Water Surface [m]
c	Wave Velocity [m/s]
C_c	2.08, Conversion Constant [-]
C_f	Bottom Friction Coefficient [-]
C_i	Coefficient of Routing Parameter [-]
CN	Curve Number [-]
C_r	Courant Number [-]
D	Rainfall Duration [hr]
dy/dx	Pressure Gradient [-]
f	Coriolis Parameter [-]
g	Gravitational Acceleration [m/s ²]
h_e	Energy Head Loss [m]
I_a	Initial Abstraction [mm]
I_t	Inflow Hydrograph Ordinate at Time t [m ³ /s]
K	Conveyance of Subdivision [-]
K_c	Conveyance in the Channel [-]
K_f	Conveyance in the Floodplain [-]
K_r	Travel Time of the Flood Wave Through Routing Reach [hr]
l	Longest Flow Length [m]
n	Manning Roughness Coefficient [-]
no	Total Number of Data Ordinates [-]
NSE	Nash-Sutcliffe Efficiency [-]
O_i	Observed Data at ith Ordinate [-]
O_t	Outflow Hydrograph Ordinate at Time t [m ³ /s]
P	Rainfall Depth [mm]
P_e	Accumulated Precipitation Excess [mm]
P_i	Estimated Data at ith Ordinate [-]
Q_B	Baseflow [m ³ /s]
Q_c	Flow in Channel [m ³ /s]

q_L	Lateral Inflow [m^3/s]
Q_o	Reference Flow [m^3/s]
Q_{peak}	Inflow Peak [m^3/s]
R	Hydraulic Radius [m]
r^2	Coefficient of Determination [-]
RMSE	Root Mean Square Error [-]
S	Potential Maximum Retention [mm]
S_f	Slope of the Energy Gradeline [-]
S_o	Bottom Slope [-]
S_t	Storage in the Reach [m^3]
t_c	Time of Concentration [hr]
t_{lag}	Basin Lag Time [hr]
T_p	Time to Peak [hr]
U_p	Peak Discharge [m^3/s]
V	Flood Wave Velocity [m/s]
v	Velocity [m/s]
ν_t	Horizontal Eddy Viscosity Coefficient [-]
X	Dimensionless Weight ($0 \leq X \leq 0.5$) [-]
Y	Depth of Water at Cross Section [m]
Y_s	Average Slope Gradient [%]
Z	Elevation of Main Channel Inverts [m]

اونیورسیتی ملیسیا قہق

UNIVERSITI MALAYSIA PAHANG

LIST OF ABBREVIATIONS

AMC	Antecedent Moisture Condition
ASTER	Advanced Spaceborne Thermal Emission and Reflection Radiometer
DEM	Digital Elevation Model
DID	Department of Irrigation and Drainage
DOA	Department Of Agriculture
DSM	Digital Surface Model
DTM	Digital Terrain Model
FIM	Flood Inundation Map
GIS	Geospatial Information System
GUI	Graphical User Interface
HEC-GeoHMS	Hydrologic Engineering Center -Geospatial Hydrologic Modelling Extension
HEC-HMS	Hydrologic Engineering Center-Hydrologic Modelling System
HEC-RAS	Hydrologic Engineering Center- River Analysis System
IFSAR	Interferometric Synthetic Aperture Radar
IKONOS	Eikōn Observation Satellite
KRB	Kuantan River Basin
LIDAR	Light Imaging Detection And Ranging
LPDAAC	Land Processes Distributed Active Archive Center
NASA	National Aeronautics and Space Administration
NGA	National Geospatial-Intelligence Agency
NRCS	Natural Resources Conservation Service
SAR	Synthetic-Aperture Radar
SPOT	Satellite Pour l'Observation de la Terre
SRTM	Shuttle Radar Topography Mission
SWMM	Storm Water Management Model
UH	Unit Hydrograph
USGS	United States Geological Survey

CHAPTER 1

INTRODUCTION

1.1 Study Background

Flood is a natural disaster caused by overflowing of water in lowland area or water ponding. Factors contributing to flood events can be due to heavy rainfall or dam failure and clogging of drainage system. Floods often lead to the loss of life, properties damaged, and infrastructure disruptions (Hammond, Chen, Djordjević, Butler, & Mark, 2015). In Malaysia, the east coast region of the peninsula experienced floods problems annually during the northeast monsoon season. Kuantan as one of the cities located at the east coast has become one of the flood-prone area for many years. In this region, flood occurs due to factors such as heavy rainfall intensities, highly developed land, poor drainage system, and low capacity of river storage which contribute to excess surface runoff (Shahirah & Saru, 2012).

In the effort to solve the flood problems in the Kuantan City, the responsible local authorities and governmental agencies have implemented several flood mitigation and risk management measures including both structural and non-structural measures. In general, the structural measures are such as the construction of the flood control structure, reservoir, artificial levee, and channelization (Liao, Chan, & Huang, 2019). For the non-structural methods, they are usually used to fill the limitation of structural measures in term of the legal agreement, guidelines, laws and regulations, policies as well as training and awareness through educational programs in multiple levels based on the target groups for example hydrologist, hydraulic modeler, and flood risk manager. In Malaysia, the non-structural approaches adopted include the development of flood mitigation design manuals such as the Urban Storm Water Management Manual (MSMA) and Erosion and Sediment Control Plan (ESCP), the establishment of the Flood Inundation Map (FIM), flood hazard map, flood forecasting warning system, flood damage assessment, and flood

insurance program (Chan, 2015). The frequent flood techniques adopted in Kuantan or Malaysia are Flood/Earth Bunding, Detention Pond, Flood Forecasting, Flood Warning, Flood Siren system, Flood Study on PISMA, IRBM, Landuse Zoning in both structural and non-structural measures.

In recent years, FIM has become increasingly popular and important in flood mitigation efforts. FIM delivers information such as the area and water depth of the potential flooding region which are the major components for flood mitigation and risk management purpose (Mehebab, Raihan, Nuhul, & Haroon, 2016). The flood extent simulated can ease the local authorities in identifying and conducting maintenance at the affected zone. Furthermore, FIM can also be used to alert the people living in the flood risk zones, served as decision making tool for upgrading emergency plan and to assist insurance companies in flood risk assessment (Ernst et al., 2010). Similar to any other mitigation approaches either structural or non-structural, hydrological and hydraulic modelling are the pre-requisite processes in generating FIM. Thus, hydrology and hydraulic studies based on the appropriately selected rainfall -runoff events and hydraulic structures respectively are crucial in flood inundation modelling.

Flood inundation modelling involves complex processes with integration of topography datasets extraction, hydrological modelling, and hydraulic modelling. Through these processes, the potential flood water level fluctuation over time can be predicted for a certain rainfall event. Any constrictions or factors affecting the runoff pattern or time such as man-made structures or vegetation, are to be included in the models to ensure the water level and flow pattern simulated can represent the real situation appropriately which can be done by the software computation.

There are many flood extent models being discussed by using numerical hydraulic software and yet expand the power of a computer in flood inundation modelling (Di Baldassarre, Schumann, Bates, Freer, & Beven, 2010). HEC-HMS is a commonly used hydrological modelling tool to perform rainfall-runoff transformation. The transformation outcome in term of excess runoff served as the input of water discharge in the hydraulic modelling. FIM needs both hydrologic and hydraulic components to simulate because a hydrological model which is the rainfall-runoff model is used as an input of water discharge of every sub-basin into hydraulic modelling. HEC-RAS is one of hydraulic modelling software that can be applied to compute and delineate flood wave

along the open channel and floodplain based on time, which subsequently generate flood extent over the floodplain (Olayinka & Irivbogbe, 2017). HEC-HMS and HEC-RAS which are developed by US Army Corps of Engineers are the most economical and helpful tools applied in flood inundation modelling since both models are available as free sources.

As a conclusion, this research mainly focused on the development of FIM for the Kuantan River Basin (KRB). FIM requires information from both hydrology and hydraulic aspects. In the following chapter, literature review of flood inundation modelling is categorized into hydrology and hydraulic subtopics to be described further in detail.

1.2 Problem Statement

The main problem of this study is the increasing flood damages burden to the government due to frequent flood occurrence at east coast region during northeast monsoon season. Kuantan District has the most devastating flood events in the year 2012 and 2013 and these events have greatly attracted the attention of the local authorities and government agencies regarding the issues and damages incurred. The flood causes were due to continuous heavy rain with poor drainage system within the Kuantan town.

One of the most significant flood events in the Kuantan District occurred in December 2013. This flood event was caused by the continuous heavy rainfall for four days in which the condition was worsened by the increasing urbanization till reduced the imperviousness of the ground and consequently increase the runoff volume. The massive flood event has led to failure of the water and electricity supply affected in many areas in the district. It was reported that there were about 14,044 people evacuated from the affected areas and major damages on electricity, road structure, buildings, and properties (Bernama, 2013). As a consequence, the government suffered significant financial burden for compensating all the damages caused by the floods. Figure 1.1 shows the condition of the extreme flood event in Kuantan District in December 2013.



Figure 1.1 Plan view of the flooded area at the centre of Kuantan District in December 2013

Source: Bernama (2013)

There are several flood risk management research studies that have been carried out for the river basins in Peninsular Malaysia for example the Kelantan River Basin, Dungun River Basin, and Pahang River Basin (Ghani, Chang, Leow, & Zakaria, 2012; Hafiz et al., 2013; Pradhan & Youssef, 2011). However, not much has been done for the KRB.

Comprehensive flood study in KRB is still lacking for future urban planning purpose. Flood inundation modelling techniques which is helpful in simulating the possible scenarios of flood extent for future flood mitigation project and flood risk management is highly recommended to be practiced by government agencies, flood mitigation authorities and researchers (Klijn, Kreibich, De Moel, & Penning-Rowsell, 2015).

1.3 Objectives of the Study

- a. To analyze and delineate the topographical characteristics of the river basins and river network in Kuantan River Basin using GIS application.
- b. To predict and simulate the flood flow hydrograph patterns during extreme event in the Kuantan River networks adopting open-sourced hydrological model.
- c. To develop flood inundation maps and assess the impact of land use changes towards flood extends in the Kuantan River Basin through 1D-2D hydraulic modelling.

1.4 Scope of the Study

In this research, the scope of the study area is limited to the KRB only. Land use maps for the year 2010 and 2013 of the KRB were selected to examine the land use changes effect on the surface roughness or loss parameter known as the runoff curve number (CN). The compiled land use datasets were combined with the SRTM-DEM of 30 m in ArcGIS version 10.4 application for preprocessing stage.

Sub-basins and river networks in the KRB were delineated using ArcGIS and the hydrological parameters obtained were utilized in the HEC-HMS hydrological model for all the sub-basins. However, due to the lack of streamflow observation data (only one station available upstream) in KRB, the hydrological and calibration processes covered only the upstream part of the basin. For the downstream region, the calibration and validation of the model were done by via HEC-RAS hydraulic modelling.

The criteria of the flood events selected in this study are discussed in Section 3.2.3 where some events were based on the DID flood report. There were total of four (4) flood events chosen consisting the events from 29th December 2010 to 2nd January 2011, 26th to 30th March 2011, 1st to 5th December 2013; and 16th to 19th March 2014. It is worth to note that the complete hydrological data, landuse data information, and recorded historical report of the flood event on-site are very limited, hence the flood events for calibration and validation process has been carefully categorized based on the available type of data. In this study, the events from 29th December 2010 to 2nd January 2011 and

16th to 19th March 2014 were applied for the calibration process for two reasons: 1.) data available to compare the observed and simulated water level and streamflow; and 2.) analyses for different landuse data of 2010 and 2013. For the validation purpose, the event from 26th to 30th March 2011 and 1st to 5th December 2013 were utilized because recorded historical flood report is available for the year 2013.

Since Sg. Kuantan is the main river in KRB and floods mostly occurred along this main river especially the downstream areas (urban area), the river flow profile considered in this study is limited to the main stem. As for the tributaries, the output flood hydrographs from the hydrological simulation were inserted as the inflow at each confluence points accordingly. Besides river flow, tidal effect was also inserted in the hydraulic simulation at the estuary region. Nevertheless, the hydraulic structure such as bridges and barrage were not considered in the hydraulic modelling due to lack of survey information.

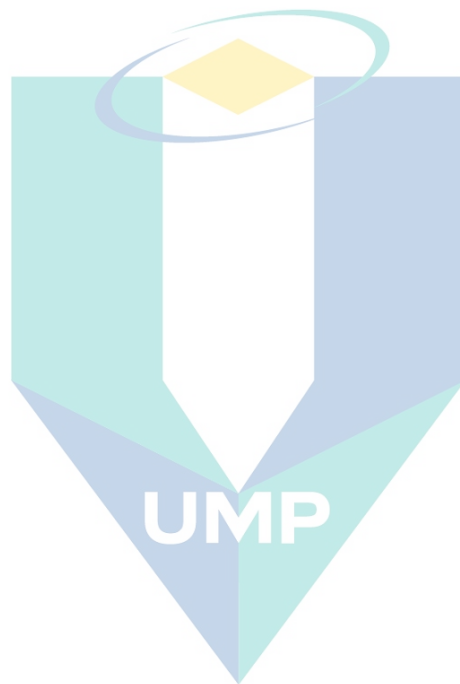
1.5 Significance of the Study

Flood related studies in Malaysia have been carried out for decades by industries, governmental agencies, and various researchers. In the early decades, mitigation on flood issues mostly focused on structural measures. Only until the recent decades, non-structural measures such as flood risk management studies, establishment of the FIM, flood hazard map, flood forecasting and warning system as well as flood response system have become equally important in flood mitigations. Although these soft engineering approaches have been implemented for some time in Malaysia, there are still many areas yet to be covered including the KRB.

Based on the flood history reports of KRB, the generation of FIM is crucial for this basin. FIM provides valuable information on potential flood areas which can be used to identify and gazette floodplain reserves from development such as the construction of infrastructures and buildings. Besides that, FIM can be integrated into the flood warning system to enhance the system efficiency. Highly affected areas identified from FIM can be prioritized in the flood warning system in term of management.

Hydrology and hydraulic flood modelling are very important in flood mitigation design particularly for areas that has minimal gauging devices. In KRB, there are 11 rainfall stations within KRB but only one streamflow station available which is located

at the upstream part of the basin. Hence, to simulate the flood extent at the downstream region, combination of hydrological and hydraulic modelling is essential. The outcome from the models can be examined to identify the appropriate flood prevention measures in term of efficiency and cost.



اونيورسيتي ملايسيا قهغ

UNIVERSITI MALAYSIA PAHANG

CHAPTER 2

LITERATURE REVIEW

2.1 Introduction

Flooding impact on the loss of live and properties, country economic crisis, and living lifestyle disruption of local residences (Mohammed, Edwards, & Gale, 2018; Rahman, Tarmudi, Rosdy, & Muhiddin, 2017). In Malaysia, monsoonal and flash flood occurred frequently due to the receiving of total annual rainfall of 2500 mm in tropical country (Ros, Shahrin, & Chuan, 2019). Ros et al. (2019) reported that the Malaysia government had spent more than RM 3 billion on structural measures to mitigate flooding since 1970's until now. Even the installation of flood warning systems at flood prone area are yet sufficient to cater the flood impact during the actual time occurrence (Mohammed et al., 2018). Thus, it is advisable to perform flood modelling first for the propose flood mitigation work.

2.2 Types of Flood

Flood possesses a random amplitude of wave propagating to the downstream outlet towards the sea. As the water is fully occupied in the main river, the excess water will then spill onto the adjacent shallow gradient floodplains. These floodplains may act as a temporary water storage and extra routes for flow conveyance (Ghimire, 2019). There are different types of the flood in nature for example flash floods, coastal floods, urban floods, and pluvial flood (Mohor, Hudson, & Thieken, 2020).

Coastal or tidal flood surge occurs in the areas that lie on the coast of the sea or large body of open water. It is typically the result of extreme tidal conditions caused by severe weather. Storm surge propagates large volume of water onshore and when associated with tropical storm would create severe damages. Impacts of coastal flooding

can be categorized into three levels: minor, moderate, and major (Maddox, 2014). The minor level indicates a slight amount of beach erosion, but no major damage is expected; the moderate level can be considered if a fair amount of beach erosion occurs as well as damage to some homes and businesses; and the major level leads to serious threat to life and property (Technologies, 2012). Besides the storm, coastal flooding is also highly affected by the sedimentation accumulation especially at the river mouth or estuary region. Insufficient flushing forces from the river allow the sediment to settle at the lowland riverbed causing shallow river bed. These phenomena subsequently induced overflowing of tidal surge and flood water to the channel banks.

Fluvial, or riverine flooding, occurs when excessive rainfall over an extended period causes a river to exceed its capacity. The damage from a river flood may include the formation of break and swamp. There are two main types of riverine flooding which consist of the overbank flooding and flash flooding. Reported by Maddox (2014), Overbank flooding occurs when the water rises overflows over the edges of a river or stream. It is the most common flooding and can occur in any size of channel from small streams to huge rivers. On the other hand, flash flooding is the second type of riverine flooding that characterized by an intense, high-velocity torrent of water that occurs in an existing river channel. Flash floods are very dangerous and destructive not only because of the force of the water, but also the hurtling debris that is often swept up in the flow. The severity of a river flood is determined by the amount of precipitation in an area, duration for precipitation to accumulate, previous saturation of local soils, and the terrain surrounding the river system (Chan, 2015).

Pluvial flooding can happen in any urban area even higher elevation areas that lie above coastal and river floodplains. There are two common types of pluvial flooding. The first type occurs when intense rain saturates an urban drainage system forcing water to flow out into streets and nearby structures. The second type is the runoff from rainfall on hillsides which is the excess rainfall. Pluvial flooding often occurs in combination with coastal and fluvial flooding. Although the rainfall depth is a few centimeters deep, a pluvial flood do cause significant property damage (Maddox, 2014).

2.3 Causes of Flood

Causes of flood can be categorized into three categories: hydrological, meteorological, and anthropogenic. Based on the flood records, most of the intense flood cases are caused by meteorological phenomena (Shahirah & Saru, 2012). According to Moore (2012), meteorological factors such as cyclones, prolonged and intense rainfall, typhoons, storms, and tidal surges have caused the result of extreme, intense and long duration floods. Besides that, hydrological causes such as ice and snow melt, impermeable surfaces, saturated land, poor infiltration rates, and land erosion also may lead to the increase of runoff. The anthropogenic on the other hand is basically caused by human activities in the water catchments. Human actions associated with land use change such as deforestation, intensive agriculture, and urbanization are the most important factor contributed to flooding followed by the population growth, socio-economic and development activities, climate change, and global warming.

Urbanization is another factor contributing to flood. Land use demand for housing and commercial have induced the removal of vegetation and forest area. As the land acquisition extended into to river reserved zones without proper planning of landuse zoning, it reduces the flood water storage areas which subsequently causes flooding to occur. Furthermore, this also increases runoff volume to the downstream area since excess rainwater is unable to infiltrate into the soil directly (FaghihMina & Ying, 2015).

Climate change is interrelated with the urban development where greenhouse effect and urban heat island will be the main factors that change the volume of precipitation and condition of climate. Due to the alteration of climate and weather, the increase in precipitation and the snowmelt from the iceberg mostly at north and south pole area led to a major impact on the climatology of floods. Thus, the land use changes contribute great impact towards the flood occurrences.

Land use changes are also one of the factors contributing to flood event. Flood occurs based on river profile condition, topographic condition, human activities, natural phenomenon, and environmental structure. All these factors may lead to the change of land use from time to time (Akbari, Mozafari, Fanodi, & Hemmesy, 2014). Two types of major activities that change the land use significantly are urbanization and deforestation. As the land use changed, it changes the soil properties mainly on the surface

imperviousness which might alter the surface runoff rate. The Curve Number (CN) representation the runoff and infiltration rate which depend on the different land use type and hydrological soil group. This parameter is one of the calibration parameters in hydrological modelling.

Increase in land impervious area resulted in more excess runoff which subsequently increase the flow in urban area or suburban area. The excess rainfall may become the excess runoff directly on the ground during wet season and then convey into the nearby drainage system. This excess runoff had occupied the drain capacity instead of storing in the ground due to the impervious surface in urban area (urbanization). In the coastal region, the unplanned urbanization due to the poor drainage system and high tidal cause flash floods and tidal floods.

In Malaysia, the causes of flood are mainly due to the land use changes and high rainfall intensity. Flash flood and monsoon flood are the most frequent disaster occurred gives many negative impacts that disrupted the quality of life and economic growth in the country (Taib, Jaharuddin, & Mansor, 2016)

2.4 Flood Impacts

In general, there are two types of flood damage: direct and indirect damages. Direct damages are defined as the physical damages caused by the flood water for example damage of properties, assets, and infrastructures. Meanwhile, indirect damages are the real-time or after disaster loss of income and cost of alternative accommodation. Flood impact can also be categorized into tangible and intangible losses. Tangible losses are related to monetary values whereas intangible losses are the damages that cannot be evaluated or measured (Akasah & Doraisamy 2015).

Over the decade, floods have caused tremendous losses and damages globally. Maintenance cost, repair fees, and compensation for the community welfare required substantial amount of funds. This has imposed huge burden to the governments. Buildings and infrastructures are the most affected by floods, and the maintenance for it is high. The damaged infrastructure led to the inconvenience to public transportation. Thus, victims suffered on waiting during the evacuation period.

Flood water acts as a medium to carry sediments runoff from the surface to the river along the channel. The sediments sometimes contained toxic substances which is harmful to human life. This situation may become worse near industrial area and cities due to the pollution from the water discharge from factories and industry buildings. Which may affect to human health. Hence, the severity of flood impact must be taken into consideration to reduce the consequences towards human life and environment.

2.5 History of Recent Major Flood Events in Malaysia

In Malaysia, DID has classified flood into two types known as flash flood and monsoon flood. Based on the hydrological perspectives, the difference between these two floods is the period taken by the river flow to recede to the normal level. Flash floods take only hours to adjust to the normal water level, while monsoon flood can last for months. Monsoon winds, especially the North-East monsoon in November to March is largely responsible for the extensive floods on the east coast of the Peninsular Malaysia. On the west coast, flood is more localized and associated with the South-West monsoon in May to September and two relatively short transitional periods known as the inter-monsoon seasons in April and October (Alias et al., 2020). Figure 2.1 indicates the wind pattern during South West and North East Monsoons in Malaysia (Gasim, Toriman, & Abdullahi, 2014).

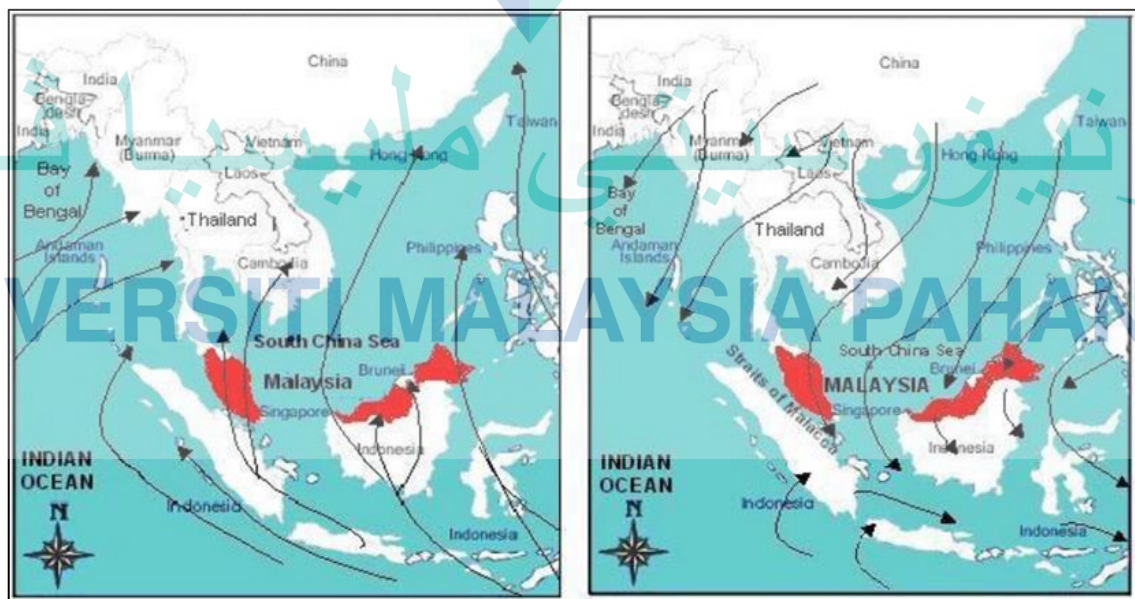


Figure 2.1 The wind direction of South-West and North-East monsoon in Malaysia

Source: Chan (2015)

Table 2.1 Major Recent Flood History in Malaysia

No	Flood Date	Flood Location	Sources
1	January 1971	Kuala Lumpur hit by flash floods.	(Leigh & Low, 1978)
2	December 1996	Floods brought by Tropical Storm Greg in Keningau with 241 casualties.	(Gasim et al., 2014)
3	2000	Floods caused by heavy rains in Kelantan and Terengganu with 15 casualties.	(Gasim et al., 2014)
4	26 February 2006	Shah Alam hit by flash floods.	(Zamri, 2009)
5	19 December 2006	Muar, Johor Bahru, Skudai, and Segamat were hit by flash floods with a total of 46 casualties in these 3 disaster events.	(Gasim et al., 2014)
6	10 January 2007		
7	December 2008		
8	10 June 2007	Kuala Lumpur hit by flash floods.	(Nor & Rakhecha, 2008)
9	December 2007	Kelantan, Terengganu, Pahang, and Johor were hit by flash floods.	
10	November 2010	Kedah and Perlis flooded due to heavy rainfall after a tropical depression with a total of 4 casualties.	(Gasim et al., 2014)
11	December 2014	Kelantan, Terengganu, Pahang, Perak, and Perlis were hit by flash floods including some areas in Sabah.	(Akasah & Doraisamy, 2015)

The flood types in Malaysia are mainly the monsoon flood and flash flood as shown in Table 2.1. Most of the flash flood incidents occurred at the major cities and towns such as Kuala Lumpur, Shah Alam, Muar, Skudai and Segamat, whereas monsoon flooding frequently occurred at the west and east coast of the Peninsula including Kelantan, Terengganu, Kedah, Perlis, Pahang and Perak. The critical flood events were listed from year 1971 to year 2014. The causes of flood were commonly due to low lying area, high tide, poor drainage system, continuous heavy rainfall during the monsoon

period which worsen the flood condition. The east coast region encountered frequent flood issue during monsoon season such as Kuantan in Pahang State.

2.5.1 Kuantan Flood Event

Kuantan city is a mixed development city which consists of commercial, domestic, tourist spot, agriculture and forest reserved areas. Based on its geographic location (east coast of the Malaysia Peninsula), it is affected by the monsoon flooding that occurs annually. Monsoon flooding occurred frequently in the month of December and January due to the North-East monsoon wind. According to the flood report recorded by DID, there were several major floods occurred in 30th to 31st December 2010, 6th to 7th January 2011, 23th November to 11th December 2011, 24th to 31st December 2012, 2nd to 5th December 2013, 18th December 2014 to 11th January 2015, and 23rd to 28th December 2015 in this region. The cause of flood was mainly due to continuous rain with high rainfall intensity and high tide.

It was reported by the state police that during the flood event in December 2013, the water and electricity supply has been cut off in most areas in Kuantan while seven roads were inundated up to one meter high in the town area (Chong, Pan, Leong, Bahri, & Ahmad Khan, 2014). On the other event in January 2015, the East Coast Expressway (LPT) has been closed to vehicles for weeks because the highway was flooded. In the same event, flood warning for residents in the vicinity of Sg Belat, the main tributary of Sg Kuantan has been triggered as the river level has exceeded the critical level at 4.07 metres. At the end of the year 2015, Tariq (2015) reported that there were 39 of villagers had been evacuated after day-long rains flooded their homes near Sg Soi (tributary of the Sg Belat area). The flooding was caused by continuous rain and poor drainage system whereby the drains were filled with debris.

There are many others flood events in Kuantan City which mainly caused by continuous heavy rain and poor drainage system. It is crucial for government to conduct study on the flood mitigation and improvement on the existing drainage system which known as the flood issue. The flood damages could be reduced if the flood mitigation and flood risk assessment successfully conducted in Kuantan River Basin.

2.6 Geographic Information, Hydrology and Hydraulic Processes

Flood inundation modelling is one of the fundamental process in flood mitigation studies. The output of the flood inundation map shall be presented in geographical system to be further analysed in google earth or any geographical information system (GIS) software. Both hydrological and hydraulic modelling are the elements to generate flood map. The models shall be set in the same projection system so that the result reflect to the actual situation or location.

Hydrological modeling is to transform the natural rainfall into the excess runoff calculation after losses and routed by the ground or surface whereas hydraulic modelling is to simulate the flow condition along specific location structures for capacity adequacy checking and many more. Both models are incorporate to provide accurate results to assist in the development of sustainable flood risk management solutions.

Solutions to prevent flood by either structural or non- structural method were highly needed. However, before any mitigation is adopted, hydrological and hydraulic studies must be carried out to determine the best solution to overcome the flood problem. Many flood factors such as storm, excessive rainfall, tidal action, dam failure, or channel obstruction (Shahirah & Saru, 2012) has to be considered in the hydrological and hydraulic modelling.

2.6.1 Geographic Information Analysis

In hydrological study, pre-processing of the geographic information such as watershed delineation and hydrological parameterization are necessary before the rainfall-runoff transformation modelling. Watershed delineation is a process to generate the sub-basins and river networks in a catchment. (Dingman, 2015) stated that these applications are enhanced using GIS because hydrology is inherently spatial in nature. Geospatial Information System (GIS) is commonly applied for the watershed delineation, hydrological parameters extraction, and floodplain mapping. The digital representation of topography, soils, and land use may be accomplished using GIS data and methodology

2.6.1.1 DEM

As an alternative to the traditional topographical map, satellite image captured by remote sensing is preferred by researchers in performing studies on flood inundation modelling because this technique is effective and cost as well as time saving. Remote sensing is vital in flood inundation mapping particularly for the validation and calibration process and it can be practiced in any study area (Domeneghetti, Schumann, & Tarpanelli, 2019).

Digital Elevation Model, DEM provides the grid of elevation data while Digital Terrain Model, DTM is a model of bare earth with the elevation data, and Digital Surface Model, DSM is an image of bare earth, treetops, and buildings with elevation data per pixels. Among all the digital models, DTM possesses a higher quality in measuring elevation data among the others (Breytenbach & Van Niekerk, 2020).

DEM is the key source in hydrological modelling and flood inundation mapping (Manfreda, Leo, & Sole, 2011). It is generally generated by various techniques through photogrammetry, ground survey, surface sensing, cartography and satellite sensing (Akbari et al., 2014). There are several resolutions of DEM in various scale depending on the techniques used to capture the information. Airborne laser technology such as Light Detection and Ranging (LIDAR), Interferometric Synthetic Aperture Radar (IFSAR), IKONOS, and Spot DEM are those that have high resolution. LIDAR resolution can be as precise as 5 m grid and has been used in many flood related projects globally.

Besides providing information on the surface elevation and earth cover, DEM with optimum resolution can also be used to generate riverine cross-sections when no survey data is available. (Bajracharya, Shrestha, & Shrestha, 2017) has demonstrated the riverine cross-section extraction from SRTM and then compare the generated cross section with the actual river cross-section conducted by the survey which has an vertical accuracy of approximately +10 m. The extracted cross-section was used in flood modelling because no survey data is available at that region. (Wang, Yang, & Yao, 2012) stated that Advanced Spaceborne Thermal Emission and Reflection Radiometer (ASTER) global DEM and SRTM can be used for flood inundation modelling which gives acceptable result if the higher resolution DEM is not available. In term of the DEM vertical accuracy, (Czubski, Kozak, & Kolecka, 2013; Forkuor & Maathuis, 2012; Hirt,

Filmer, & Featherstone, 2010; Rawat, Mishra, Sehgal, Ahmed, & Tripathi, 2013) have proved that SRTM is better than ASTER-GDEM. SRTM simulated a better flood hydrograph than that by Global DEM according to the research by (Bhuyian, Kalyanapu, & Hossain, 2017).

2.6.1.2 SRTM-DEM

Shuttle Radar Topography Mission (SRTM) was launched in conjunction with the National Aeronautics and Space Administration (NASA) and the National Geospatial-Intelligence Agency (NGA) to acquire radar data which were used to create the first near-global set of land elevations.

At the early stage, SRTM data for regions outside the United States were sampled for public release at 3 arc-seconds, which is 1/1200th of a degree of latitude and longitude, or about 90 m. Then, the radar data is improved to 1 arc-second, or about 30 m, and released to public usage. This newly sampled data reveals the full resolution of the original measurements. The SRTM 30 m resolution are available without charges to users worldwide and can be retrieved from the Land Processes Distributed Active Archive Center (LPDAAC) website (Forkuor & Maathuis, 2012).

2.6.1.3 ArcGIS and HEC-GeoHMS

ArcGIS is a GIS software for mapping, compiling geographic data, analyzing mapped information, and storing geodatabase. It has great function of storing spatial and non-spatial data to be analyzed where the result can be presented in the exact location on Google Earth. This software was chosen to perform watershed delineation process, hydrological parameter extraction, and hydrological modelling file export coupling with the geospatial hydrology toolkit extension, HEC-GeoHMS.

Hec-GeoHMS tool allows engineers and hydrologists to visualize the spatial information, document watershed characteristics, perform spatial analysis, delineate sub-basins and streams, construct inputs to hydrologic models, and assist with report preparation. All the processes required the DEM which provide the elevation information in pixel form to perform the hydrological analysis processes. The first step is the pre-processing of DEM which is the watershed delineation process followed by the post-processing process such as the calculation of hydrologic parameters and the generation

of hydrological modelling file which can be open in the rainfall-runoff modelling software HEC-HMS.

2.6.2 Hydrological Modelling

In the 1960s and 1970s, the introduction of the digital computer into water engineering works has created many sophisticated hydrological models mainly for flood control, contaminant transport, hydraulic design, and water quality management respectively. The invention of hydrologic models which interact with hydrologic data, digital terrain data and mapping software have allowed complex problems to be solved especially in the urban area. These models enhance the analysis of urban stormwater, floodplain and watershed hydrology, drainage design, reservoir design and operation, flood frequency analysis, and large river basin management (Chen, Shams, Carmona-Moreno, & Leone, 2010).

Hydrologic model represents the real-world river system and the modelling process aids in understanding, predicting, and managing water resources. Furthermore, it is a technique that simulates the behavior and flow of water along a river system. The simulation is generated by transforming actual rainfall input into overland flow output where the routing system, losses, and gains of water are considered in the modelling (Maxwell, Condon, & Kollet, 2015).

There are several hydrologic modelling software available in the market nowadays such as HEC-HMS, MIKE-SHE, soil water assessment tool (SWAT), and artificial neural network (ANN) (Abdulkareem, Pradhan, Sulaiman, & Jamil, 2018). HEC-HMS is frequently used by many previous researchers and expert which is a very reliable system for rainfall-runoff modelling and requires no licensing (Alaghmand, Abdullah, Abustan, Said, & Vosough, 2012; Razi, Ariffin, Tahir, & Arish, 2010; Romali, Yusop, & Ismail, 2018). Zope, Eldho, & Jothiprakash (2016) have practiced on the impact of landuse changes on urban flood modelling using HEC-HMS integrating with HEC-GeoHMS extension and the result was shown that lower return periods led to a maximum change in peak discharge/volume of runoff compared to higher return periods for change in land use conditions. The integrated radar rainfall had been adopted as the input in the flood hydrograph estimation for SMART control operation purpose using HEC-HMS model (Ramly et al., 2020). At Klang watershed, two different loss model

namely SCS curve number and Green-Ampt methods were compared in term of simulated direct runoff and peak discharge where no significant difference (Kabiri, Chan, & Bai, 2013).

2.6.2.1 HEC-HMS Models Application

HEC-HMS is a deterministic model that contained a large set of methods to simulate watershed, channel, and water-control structure behavior, thus calculate the resulting storm hydrograph for a given pattern of rainfall intensity (Akbari, 2011). It simulates the rainfall-runoff processes of dendritic watershed systems and perform in a wide range of geographic areas for solving problems including large river basin water supply and flood hydrology, and small urban or natural watershed runoff (Duhan & Kumar, 2017).

HEC-HMS is the “Windows” based hydrologic model that supersedes HEC-1 with many improvements over its predecessor. The US Army Corps of Engineers has developed it. The significant advantage of HEC-HMS is the user-friendly graphical user interface (GUI) for the model schematic and results presentation. A GIS background map can be overlaid as an overview reference for visualization purpose.

The physical representation of the watershed is accomplished with a basin model, meteorologic model, control specification, data series, and model run (Tassew, Belete, & Miegel, 2019). These hydrological elements are connected in a dendritic network to simulate the runoff processes. Basin model comprises of the basin and channel characteristics parameters such as runoff, surface roughness, baseflow (initial storage), and channel routing mechanism. For the meteorologic model, it includes the hydrological data processing such as the time series of rainfall and distribution. Prior to model execution or model run, the boundary condition for the temporal series has to be done in the control specifications section. The temporal boundary condition setup must be in reference to the time series indicated in the meteorologic model. Detail explanations on the HEC-HMS components are discussed in the next sections.

2.6.2.2 Basin Model

A basin model in HEC-HMS describes the physical characteristics of watersheds and river channels. The physical landscape is modeled by a series of hydrologic elements arranged in a dendritic, link-node manner. Hydrologic elements include sub-basins, reaches, junctions, reservoirs, diversions, sources, and sinks are connected in the basin model. For each element, various methods of computation can be selected for the model run. The following methods are shown in detail.

Various methods are available for estimating the runoff volume, transforming excess precipitation into surface runoff, computing baseflow contributions to sub-basin outflow, and flow routing. Outflow from a sub-basin is computed from rainfall data by subtracting losses, transforming excess precipitation, and adding baseflow. Table 2.2 to Table 2.5 show the runoff volume model, surface runoff model, baseflow model, and channel routing model in HEC-HMS respectively. Runoff volume indicates the resultant runoff from the precipitation after consideration of loss from evaporation, infiltration, intercepted or stored in the subsoil surface. Surface runoff is the transformed discharge from the excess precipitation via empirical or conceptual models. Baseflow defined as the flow within the channel that is not generated from the excess rainfall during a storm. Channel routing is required to predict the actual hydrograph as water moves through different condition of channel properties which might change the shape of the hydrograph (Castro & Maidment, 2020).

The selection of different types of model were based on the suitability of the estimation runoff volume, surface runoff, baseflow, and channel routing assumption. In the KRB study, it is the flood event-based model. The land use changes impact play an important role in the prediction of runoff where SCS curve number calculation shall be adopted in this model. As a result, SCS curve number (runoff volume model); SCS unit hydrograph (Surface runoff model); Constant monthly (Baseflow model); and Muskingum-Cunge (Channel routing model) was set.

Table 2.2 Runoff Volume Models

Model	Category
Initial and constant-rate	Event, lumped, empirical, fitted parameter
SCS curve number	Event, lumped, empirical, fitted parameter
Gridded SCS CN	Event, distributed, empirical, fitted parameter
Green and Ampt	Event, distributed, empirical, fitted parameter
Deficit and constant rate	Continuous, lumped, empirical, fitted parameter
Soil Moisture Accounting	Continuous, lumped, empirical, fitted parameter
Gridded Soil Moisture Accounting	Continuous, distributed, empirical, fitted parameter

Table 2.3 Surface Runoff Models

Model	Category
Clark Unit Hydrograph	Event, lumped, empirical, fitted parameter
Snyder Unit Hydrograph	Event, lumped, empirical, fitted parameter
SCS Unit Hydrograph	Event, lumped, empirical, fitted parameter
User Defined Unit Hydrograph	Event, lumped, empirical, fitted parameter
Kinematic Wave	Event, lumped, conceptual, measured parameter
ModClark	Event, distributed, empirical, fitted parameter

Table 2.4 Baseflow Models

Model	Category
Constant Monthly	Event, lumped, empirical, fitted parameter
Exponential Recession	Event, lumped, empirical, fitted parameter
Linear Reservoir	Event, lumped, empirical, fitted parameter

Table 2.5 Channel Routing Models

Model	Category
Kinematic Wave	Event, lumped, conceptual, measured parameter
Lag	Event, lumped, empirical, fitted parameter
Modified Puls	Event, lumped, empirical, fitted parameter
Muskingum	Event, lumped, empirical, fitted parameter
Muskingum-Cunge	Event, lumped, quasi-conceptual, measured parameter

A reservoir acts as water storage to reduce and attenuate the resultant flow towards downstream area as well as water supply purpose. This element is included to produce the actual outflow hydrograph based on a monotonically increasing storage-outflow relationship. There are three types of stage-flow relationship in a reservoir: 1) storage versus outflow, b) elevation versus storage versus outflow, and c) elevation versus area versus outflow. The inflow data is entered to relate storage to outflow of the reservoir (Rahman, Balkhair, Almazroui, & Masood, 2017).

2.6.2.3 Rainfall-runoff Loss Method - SCS CN Method

In the sub-basin element, there are several mathematical models that can be applied to perform the infiltration losses. The infiltration method is specified for each sub-basin in the basin model for example Soil Conservation Service Curve Number (SCS CN) method, initial and constant method, soil moisture accounting method, and Green and Ampt method. SCS CN loss method is the most popular because of its ability to be applied in ungauged areas, and it has large empirical database. This was then supported by (Pampaniya & Tiwari, 2017; Sardoii, Rostami, Sigaroudi, & Taheri, 2012) in two separated studies, found and claimed that the SCS CN method is better than Initial loss and constant rate method when comparing the result of observation and simulation flow changes. Moreover, SCS CN method and initial and constant method provides good accuracy in runoff volume and peak flow simulation than the Green and Ampt method (Zema, Labate, Martino, & Zimbone, 2017).

In the SCS CN method, accumulated excess precipitation is estimated as a function of cumulative precipitation, soil cover, land cover/use, and antecedent moisture based on statistical correlations as presented in Equation 2.1 to Equation 2.3.

$$P_e = \frac{(P - I_a)^2}{P + S - I_a} \quad 2.1$$

$$I_a = 0.2S \quad 2.2$$

$$S = \frac{25400}{CN} - 254 \quad 2.3$$

where P_e (mm) is the accumulated rainfall excess, P (mm) is the accumulated rainfall depth, I_a (mm) is the initial abstraction, and S (mm) is the potential maximum retention. The single-value of CN for a watershed can be generated using ArcGIS by extracting the information from the soil and land use maps.

For accuracy in runoff prediction using the popular SCS-CN method, correct estimation of Antecedent Moisture Condition (AMC) dependent CN -values is necessary. (Farran & Elfeki, 2020) have proposed the new formulae of CN expression according to AMC I and AMC III respectively. Table 2.6 shows the CN -conversion formulae from AMC II to AMC I or AMC III accordingly.

Although CN value can be calculated from ArcGIS, it still must be considered the estimated AMC of five days antecedent rainfall prior to the rainfall event of interest. Table 2.7 presents the AMC range for the dormant and growing seasons based on the total five-day antecedent rainfall by (Miliani, Ravazzani, & Mancini, 2011). Akbari, Samah, & Daryabor (2016) stated that the AMC can also be categorized into three conditions, for example (AMCI) dry condition, (AMCII) moderate condition, and (AMCIII) wet condition.

(Fu, Zhang, Wang, & Luo, 2011) compared the SCS CN approach with the ratio of I_a/S is reduced to 0.05 from the original value of 0.2. According to Akbari et al. (2016), the revised SCS-CN approach reveals a stretching effect on the CN value which is capable of providing a reasonable indication for flood runoff simulation. Equation 2.4 shows the revised computation for the rainfall excess.

$$P_e = \begin{cases} 0 & \text{if } P \leq 0.05 \times S \\ \frac{(P - 0.05 \times S_{0.05})^2}{P + 0.95 \times S_{0.05}} & \text{if } P > 0.05 \times S \end{cases} \quad 2.4$$

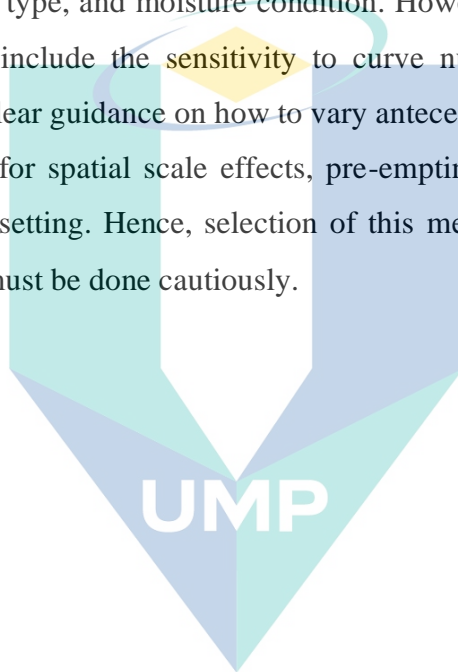
The relationship between $S_{0.05}$ and $S_{0.2}$ obtained as Equation 2.5

$$S_{0.05} = 1.33 \times (S_{0.2})^{1.15} \quad 2.5$$

Then, the revised $CN_{0.05}$ can be estimated by Equation 2.6.

$$CN_{0.05II} = \frac{100}{1.879 \times \left[\frac{100}{CN_{0.2II}} - 1 \right]^{1.15} + 1} \quad 2.6$$

Mishra & Singh (2013) stated that the SCS CN method are simple, predictable, stable, reliable and responsive to major runoff-producing watershed properties such as land use changes, soil type, and moisture condition. However, the disadvantages of the SCS CN discovered include the sensitivity to curve number, varying accuracy for different biomes, no clear guidance on how to vary antecedent condition, the absence of an explicit provision for spatial scale effects, pre-empting a regionalization based on geologic and climate setting. Hence, selection of this method on the suitability of the study area condition must be done cautiously.



اونيورسيتي ملايسيا قهغ

UNIVERSITI MALAYSIA PAHANG

Table 2.6 CN-conversion formulae

Methods	AMC I	AMC III
Sobhani (1976)	$CN_I = \frac{CN_{II}}{2.334 - 0.01334CN_{II}}$	$CN_{III} = \frac{CN_{II}}{0.4036 + 0.005964CN_{II}}$
Hawkins, Hjelmfelt Jr, & Zevenbergen (1985)	$CN_I = \frac{CN_{II}}{2.281 - 0.01281CN_{II}}$	$CN_{III} = \frac{CN_{II}}{0.427 + 0.00573CN_{II}}$
Chow, Maidment, & Mays (1962)	$CN_I = \frac{4.2CN_{II}}{10 - 0.058CN_{II}}$	$CN_{III} = \frac{23CN_{II}}{10 + 0.13CN_{II}}$
Neitsch, Arnold, Kiniry, & Williams (2011)	$CN_I = CN_{II} - \frac{20(100 - CN_{II})}{\{100 - CN_{II} + \exp[2.533 - 0.0636(100 - CN_{II})]\}}$	$CN_{III} = CN_{II} \exp\{0.00673(100 - CN_{II})\}$
Proposed CN expression by Mishra, Jain, Babu, Venugopal, & Kaliappan (2008)	$CN_I = \frac{CN_{II}}{2.2754 - 0.012754CN_{II}}$	$CN_{III} = \frac{CN_{II}}{0.430 + 0.0057CN_{II}}$

Table 2.7 Classes of Antecedent Moisture Conditions (AMC)

AMC	Total Five-Days Antecedent Rainfall, (mm)	
	Dormant Season	Growing Season
I	Less than 13	Less than 36
II	13 to 28	36 to 53
III	More than 28	More than 53

Source: Kamran & Rajapakse (2018)

2.6.2.4 Rainfall-runoff Transform Method – SCS Unit Hydrograph

The transform method is also specified for each sub-basin in the basin model for example Clark UH method, Snyder UH method, SCS UH method, User Defined UH, and Kinematic Wave method. According to Majidi & Shahedi (2012), the study has proven that runoff rate estimation can be simulated more accurately using SCS UH method. In this study, SCS UH method was selected for transforming the runoff to the UH.

This model is based on averages of dimensionless hydrograph developed from many UHs from gaged watersheds ranging in size and geographic location. At the heart of the SCS UH model is a dimensionless, single-peaked UH. According to several literatures, the magnitude and timing of the hydrograph peak are a function of the lag time and area of each sub-basin as shown in Equations 2.7 to Equation 2.9 (Rahman et al., 2017; Verma, Jha, & Mahana, 2010; Yang, Du, Cheng, & Xu, 2017):

$$U_p = C \frac{A}{T_p} \quad 2.7$$

$$T_p = \frac{D}{2} + t_{lag} \quad 2.8$$

$$t_{lag} = \frac{l^{0.8} \times \left(\frac{25400}{CN} - 254 + 1 \right)^{0.7}}{1900 \times y^{0.5}} \quad 2.9$$

where A (m^2) is the watershed area, C (-) is the conversion constant, U_p (m^3/s) is the UH peak discharge, T_p (hr) is the time to peak, D (hr) is the excess rainfall duration, l (m) is the longest flow length, y (%) is the average slope gradient, t_{lag} (hr) is the basin lag time, and CN (-) is the average curve number. The SCS dimensionless UH can be used to generate a curved hydrograph by using the same t_{lag} and U_p as the triangular hydrograph and found that time of concentration, $t_c = 1.67 t_{lag}$ (Kabiri et al., 2013).

2.6.2.5 Baseflow Method – Constant Monthly

Baseflow in the hydrological simulation is considered as the indirect runoff. Due to the lack of information regarding baseflow in general, it can be estimated through field inspection. Groundwater flow and rainfall precipitation are the two elements that

contribute to baseflow especially in the large tropical watershed region. Thus, baseflow are one of the factors in rainfall-runoff modelling.

(De Silva, Weerakoon, & Herath, 2014) claimed that the constant monthly is the simplest baseflow method. It indicates the constant baseflow in monthly interval. The user-specified flow is added to the direct runoff computed from rainfall for each time step of the simulation. The parameters of this model are in monthly based which is the best estimation for empirical model.

2.6.2.6 Routing Method- Muskingum-Cunge

Routing without attenuation may be accomplished with the lag method while the Muskingum, Muskingum-Cunge, and modified Puls routing methods may be used to simulate the effects of attenuation as. The Muskingum method and Muskingum-Cunge method are widely used for flood routing due to their high accuracy and reliable relationship between parameters and geometry (Rahman et al., 2017). For river channel routing, the Muskingum-Cunge model would be used as it is capable of routing slow-rising flood waves through reaches with flat slopes. Furthermore, the Muskingum-Cunge parameters are physically based and can be directly estimated from river cross-sectional data compared to other models.

Muskingum-Cunge model is the improved principles from the classical Muskingum method introducing the physical-numerical assumptions to calculate the routing parameters. This model is based upon the solution of the following form of the continuity equation, (with lateral inflow, q_L , included) as Equation 2.10:

$$\frac{\partial A}{\partial t} + \frac{\partial Q}{\partial x} = q_L \quad 2.10$$

And the diffusion form of the momentum equation as Equation 2.11:

$$S_f = S_o - \frac{\partial y}{\partial x} \quad 2.11$$

The wave celerity and the hydraulic diffusivity are expressed as Equations 2.12 and Equation 2.13

where c (m/s) is the wave celerity; and μ (m²/s). = hydraulic diffusivity.:

$$c = \frac{\partial Q}{\partial A} \quad 2.12$$

and

$$\mu = \frac{Q}{2BS_o} \quad 2.13$$

where the B (m) = top width of the water surface.

A finite difference approximation of the partial derivatives yields as Equation 2.14:

$$O_t = C_1 I_{t-1} + C_2 I_t + C_3 I_{t+1} + C_4 (q_L \Delta x) \quad 2.14$$

The coefficients are as Equation 2.15 to Equation 2.18:

$$C_1 = \frac{\frac{\Delta t}{K_t} + 2X}{\frac{\Delta t}{K_t} + 2(1-X)} \quad 2.15$$

$$C_2 = \frac{\frac{\Delta t}{K_t} - 2X}{\frac{\Delta t}{K_t} + 2(1-X)} \quad 2.16$$

$$C_3 = \frac{2(1-X) - \frac{\Delta t}{K_t}}{\frac{\Delta t}{K_t} + 2(1-X)} \quad 2.17$$

$$C_4 = \frac{2\left(\frac{\Delta t}{K_t}\right)}{\frac{\Delta t}{K_t} + 2(1-X)} \quad 2.18$$

The parameters Kt and X are listed as Equations 2.19 and Equation 2.20:

$$K_t = \frac{\Delta x}{c} \quad 2.19$$

$$X = \frac{1}{2} \left(1 - \frac{Q}{BS_o c \Delta x} \right) \quad 2.20$$

However, these parameters c , Q , and B will be altered over time as well as the coefficients C_1 , C_2 , C_3 , and C_4 . HEC-HMS has recomputed them at each time, Δt and distance step, Δx using the algorithm suggested by (Reshma, Kumar, Babu, & Kumar, 2010) to ensure model stability and accuracy. HEC-HMS computes Δx after Δt as Equation 2.21:

$$\Delta x = c \Delta t \quad 2.21$$

The value is constrained as Equation 2.22 so that:

$$\Delta x < \frac{1}{2} \left(c \Delta t + \frac{Q_o}{BS_o c} \right) \quad 2.22$$

Here Q_o (m^3/s) = reference flow, computed from the inflow hydrograph as Equation 2.23:

$$Q_o = Q_B + \frac{1}{2} (Q_{peak} - Q_B) \quad 2.23$$

where Q_B (m^3/s) = baseflow; and Q_{peak} (m^3/s) = inflow peak.

The Muskingum-Cunge model in HEC-HMS used in this study represent the physical characteristics of the channel in term of channel width; slope; roughness. It is better to be applied in routing method with limited information condition.

2.6.2.7 Reservoir Routing

Outflow structures reservoir routing consists of several uncontrolled outlet structures such as culverts, orifices, spillways, and dam tops. The elevation-storage

method with appropriate paired data function defines the storage characteristics of the reservoir.

(Gumindoga, Rwasoka, Nhapi, & Dube, 2017) stated that reservoir routing is the process of determining the reservoir stage, the storage volume of the outflow hydrograph corresponding to a known hydrograph of inflow into the reservoir. The reservoir routing basically attenuates the peak outflow and lag the time to peak for the outflow where the change of storage can be written as the mass conservation equation as presented in Equation 2.24:

$$I_t \Delta t - O_t \Delta t = \Delta S_t \quad 2.24$$

where I_t (m^3/s) = average upstream flow; O_t (m^3/s) = average downstream flow; and ΔS_t (m^3) = change in reach storage. If the subscripts 1 and 2 are used for inflow and outflow to the reservoir at time t (s) and $t + \Delta t$ (s) respectively, then the equation can be written as Equation 2.25:

$$\frac{1}{2}(I_1 + I_2)\Delta t - \frac{1}{2}(O_1 + O_2)\Delta t = S_2 - S_1 \quad 2.25$$

Where I_1 (m^3/s), I_2 (m^3/s), O_1 (m^3/s), and S_1 (m^3), are known at any time t (s), values for S_2 (m^3) and O_2 (m^3/s) are unknown.

2.6.2.8 Meteorologic Model

The meteorological model represents the temporal and spatial variation of precipitation inputs to the basin model. Historic and synthetic precipitation methods such as rain gauge or gridded precipitation data are included to distribute the rainfall over the basin. Thiessen polygons, inverse distance weighting, and user-specified hyetograph are available for gage weighting techniques.

2.6.2.9 Control Specification and Model Run

The control specifications in HMS model run describe the simulation time frame, temporal resolution or time step of the model. The purpose of this function is to set the

exact modelling time control and time interval to be saved in the simulation for further data analysis. All the results such as discharge, runoff volume, peak time in each basin element (junction or reach) will be presented in the form of a graph (time versus flow), summary table (peak flows and time to peak), and time series (inflow and outflow for each time step). The outcomes were adopted as the initial boundaries (input) into hydraulic modelling.

2.6.3 Hydraulic Modelling

Hydraulic modelling is performed to understand the stormwater flow; flood conditions and evaluate the performance of the mitigation structures design. Flows input of the hydraulic model are derived from the results of hydrologic analysis, either as a separate process to the hydraulic modelling or embedded in the same model. Efficient hydraulic modelling allows optimization of mitigating structures design, which subsequently reduce construction and maintenance costs, and ensure the reliability of the structures Brunner (2016). There are many different hydraulic models available in the industries up to date such as HEC-RAS, MIKE 11, Flood Modeller, XP-SWMM, and TUFLOW.

In hydraulic modelling, adequate information representing the floodplain areas such as topography and bathymetry, the calibrated hydrographs for each reach of interest, and river cross section survey data are crucial. Lack of topographic and bathymetric information will produce low accuracy on the results in term of illustration of the flooded areas. For 1D modelling, the water flow simulation is only in x direction which is linear to the channel flow. For 2D modelling, the water flow analysis is in both x and y direction where x direction is linear to the channel whereas y direction is perpendicular to the channel. 2D modelling describes the multi-direction floodwater flow pattern in term of x and y. However, 1D-2D modelling was used in this study where 1D model will be linked with 2D model to generate FIM. This is due to the inadequate width of cross sections represent the floodplain and the better resolution of satellite topographic data to perform flood inundation modelling such as LIDAR or IFSAR. As a result, 1D channel modelling is calibrated after linked with the floodplain satellite image to generate FIM.

Vozinaki, Morianou, Alexakis, & Tsanis (2017) stated that combined 1D-2D modelling performs better than 1D modelling using HEC-RAS model coupled with high-

resolution topographic data. Furthermore, HEC-RAS 5.0.1 has the ability for flood inundation analysis in a 1D-2D environment for decision-makers to explore in advance the possibility of flood velocity, depth, arrival time, recession and duration at a specific location in the floodplain (Patel, Ramirez, Srivastava, Bray, & Han, 2017).

2.6.3.1 HEC-RAS

The Institute for Water Resource, Hydrologic Engineering Center of U.S. Army Corps of Engineers has developed HEC-RAS. USAC (2010) stated that this model performs one-dimensional river flow analysis for steady flow water surface profile computations, unsteady flow simulation, movable boundary sediment transport computations and water quality analysis. The water surface profiles were evaluated based on defined recurrence frequency flows or validated flow obtained from HEC-HMS.

HEC-RAS is one of the most popular models which solves energy based on Saint-Venant equation with an iterative procedure called the standard step method (USAC, 2010). This model is widely used for river hydraulic modelling (Goodell & Warren, 2014; Khattak et al., 2016; Quiroga, Kure, Udo, & Mano, 2016). HEC-RAS basically computes the energy loss due to sudden contraction and expansion in cross section, or any obstacle. It is a public downloadable software from the US Army Corps of Engineers website for free.

In term of the model governing equation, the selection of time steps can be determined by using the Courant number equation. Quiroga et al. (2016) mentioned that the stability of the model will be dependent on the Courant–Friedrichs–Lewy condition as Equation 2.26 and Equation 2.27:

$$C_r = \frac{V\Delta T}{\Delta X} \leq 1.0 \quad \text{max} \quad C_r = 3.0 \quad 2.26$$

$$\Delta T \leq \frac{\Delta X}{V} \quad \text{with} \quad C_r = 1.0 \quad 2.27$$

where C_r (-) is the Courant Number, V (m/s) is the wave speed, ΔT (s) is the computational time step and ΔX (m) is the average cell size. Courant number must be less than or equal to 1 so that the model is stable.

2.6.3.2 1D Steady Flow Theory

HEC-RAS is widely used for 1D steady water surface profile calculations in river or concrete channels. Water surface profiles are computed from one cross section to the next by solving the Energy equation with an iterative procedure called the standard step method as Equation 2.28:

$$Z_2 + Y_2 + \frac{a_2 V_2^2}{2g} = Z_1 + Y_1 + \frac{a_1 V_1^2}{2g} + h_e \quad 2.28$$

Where:

Z_1, Z_2 (m) = elevation of the main channel inverts

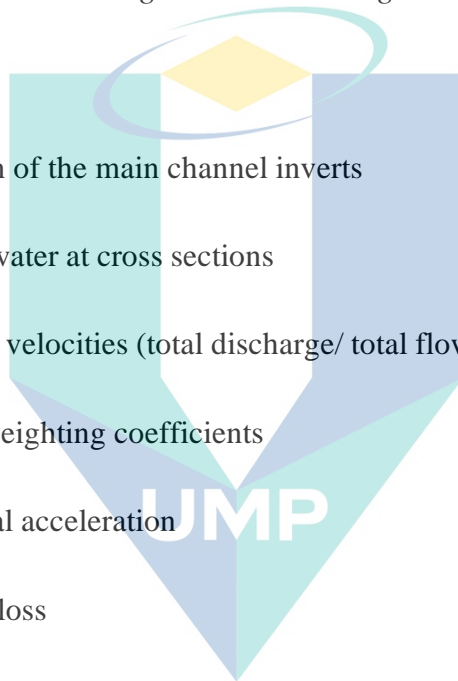
Y_1, Y_2 (m) = depth of water at cross sections

V_1, V_2 (m/s) = average velocities (total discharge/ total flow area)

a_1, a_2 (-) = velocity weighting coefficients

g (m²/s) = gravitational acceleration

h_e (m) = energy head loss



اونيورسيتي مليسيا قهغ

UNIVERSITI MALAYSIA PAHANG

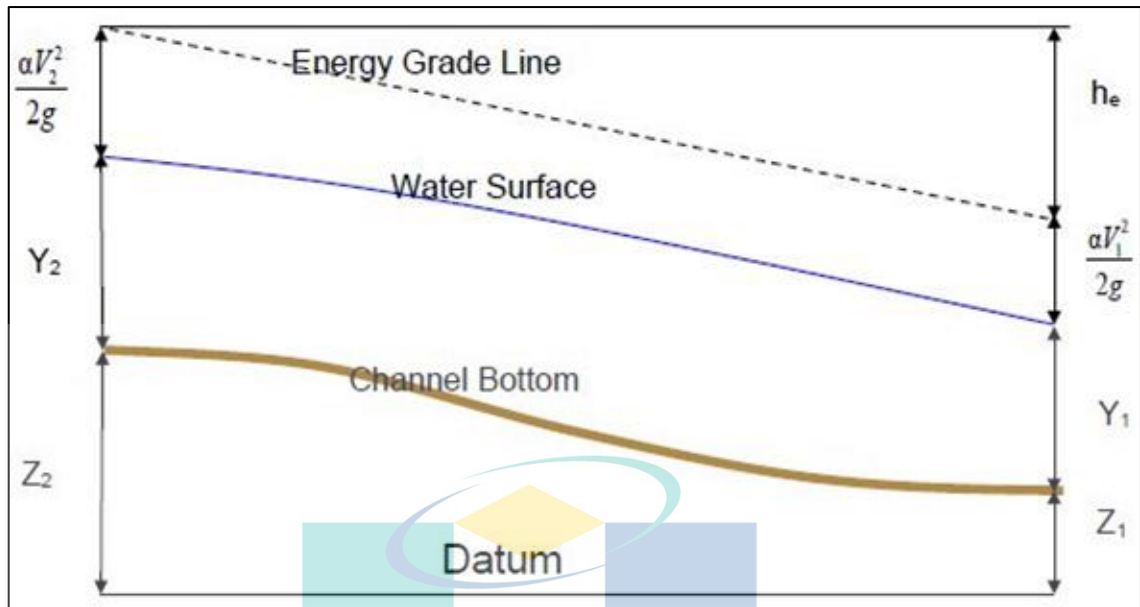


Figure 2.2 Figure Representation of Terms in Energy Equation

Source: USAC (2010)

HEC-RAS subdivide flow into the overbank areas using the input cross-section n -value breakpoints (locations where n -values change) as the basis for subdivision in Figure 2.2. Conveyance is calculated within each subdivision from Equation 2.29 and Equation 2.30:

$$Q = KS_f^{1/2} \quad 2.29$$

$$K = \frac{1.486}{n} AR^{2/3} \quad 2.30$$

Where:

K (-) = conveyance of subdivision

n (-) = Manning's roughness coefficient for subdivision

A (m²) = flow area for subdivision

R (m) = hydraulic radius for subdivision (area/wetted perimeter)

S_f (-) = slope of the energy grade line

2.6.3.3 1D Unsteady Flow Theory

The principle of conservation of mass (continuity) and momentum are the two main physical laws which govern the flow of water in a stream. These laws are expressed mathematically in the form of partial differential equations known as the continuity and momentum equations. Figure 2.3 represents the two-dimensional (2D) characteristics between the channel and floodplain flows. When the river water is increasing, it overflows from the channel into the floodplain or low areas and vice versa.

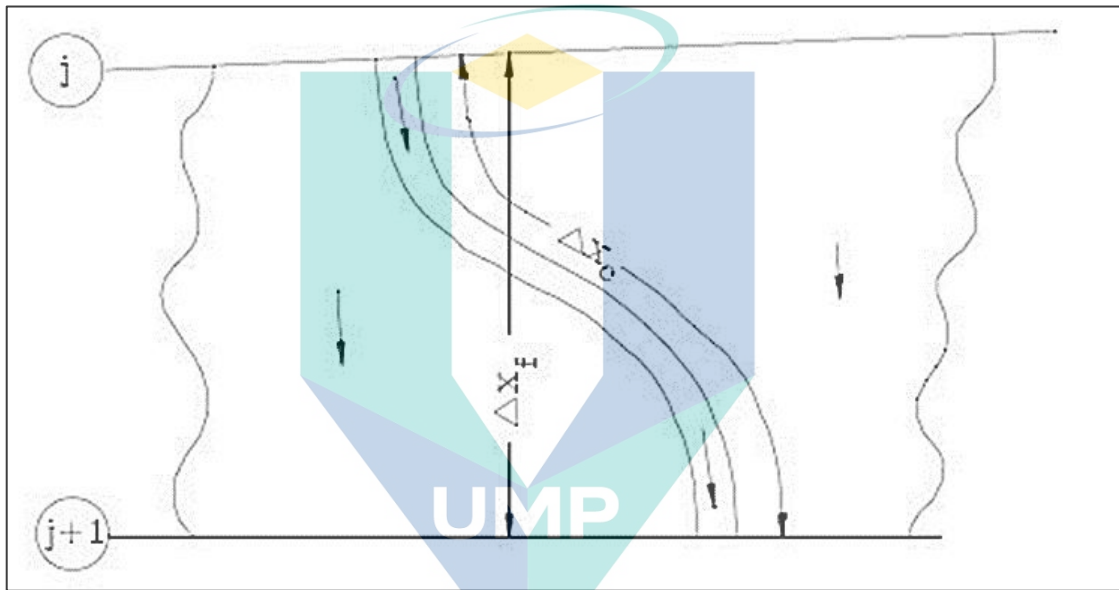


Figure 2.3 Channel and floodplain flows

Source: Brunner (2016)

A common approach is to ignore overbank conveyance entirely if the overbank is used only for storage. The horizontal water surface at each cross section is normal to the direction of flow; such that the exchange of momentum between the channel and the floodplain was negligible and that the discharge was distributed according to the conveyance as Equation 2.31:

$$Q_c = \Phi Q$$

2.31

Where:

Q_c (m³/s) = flow in channel

Q (m³/s) = total flow

Φ (-) = $K_c / (K_c + K_f)$

K_c (-) = conveyance in the channel

K_f (-) = conveyance in the floodplain

With these assumptions, the one-dimensional equations of motion can be combined into a single set as Equation 2.32 and Equation 2.33:

$$\frac{\partial A}{\partial t} + \frac{\partial(\Phi Q)}{\partial x_c} + \frac{\partial[(1-\Phi)Q]}{\partial x_f} = 0 \quad 2.32$$

$$\frac{\partial Q}{\partial t} + \frac{\partial(\Phi^2 Q^2 / A_c)}{\partial x_c} + \frac{\partial[(1-\Phi)^2 Q^2 / A_f]}{\partial x_f} + gA_c \left[\frac{\partial Z}{\partial x_c} + S_{fc} \right] + gA_f \left[\frac{\partial Z}{\partial x_f} + S_{ff} \right] = 0 \quad 2.33$$

in which the subscripts c (-), f (-), fc (-), ff (-) refer to the channel, floodplain, channel friction, floodplain friction respectively. These equations were approximated using implicit finite differences and solved numerically using the Newton-Raphson iteration technique. The model was successful and produced the desired effects in test problems.

2.6.3.4 2D Unsteady Hydrodynamic Flow Theory

2D unsteady flow for channel and flood modelling uses the Shallow Water equations. The combining equation with mass conservation is known as the Diffusive Wave Approximation of the Shallow Water equations. In the sections below, sub-grid bathymetry equations are derived in the context of both; full Shallow Water equations and Diffusion Wave equations. If the flow is incompressible, the unsteady differential form of the mass conservation (continuity) as Equation 2.34:

$$\frac{\partial H}{\partial t} + \frac{\partial(hu)}{\partial x} + \frac{\partial(hv)}{\partial y} + q = 0 \quad 2.34$$

where t (s) is time, u (m/s) and v (m/s) are the velocity components in the x -direction and y -direction respectively and q (m³/s) is a source/sink flux term. The shallow water equations are as Equation 2.35 and Equation 2.36:

$$\frac{\partial u}{\partial t} + u \frac{\partial u}{\partial x} + v \frac{\partial u}{\partial y} = -g \frac{\partial H}{\partial x} + v_t \left(\frac{\partial^2 u}{\partial x^2} + \frac{\partial^2 u}{\partial y^2} \right) - c_f u + fv \quad 2.35$$

$$\frac{\partial v}{\partial t} + u \frac{\partial v}{\partial x} + v \frac{\partial v}{\partial y} = -g \frac{\partial H}{\partial y} + v_t \left(\frac{\partial^2 v}{\partial x^2} + \frac{\partial^2 v}{\partial y^2} \right) - c_f v + fu \quad 2.36$$

Where u (m/s) and v (m/s) are the velocities in the Cartesian directions, g (m²/s) is the gravitational acceleration, v_t (m²/s) is the horizontal eddy viscosity coefficient, c_f (-) is the bottom friction coefficient, R (m) is the hydraulic radius and f (-) is the Coriolis parameter (Brunner, 2016; USAC, 2010).

2.6.3.5 1D-2D Unsteady Flow Theory

Running a combined 1D-2D unsteady flow model in HEC-RAS where the 1D and the 2D computations are directly coupled on a time step by time step basis iteratively. This allows direct feedback from 1D to 2D elements and from 2D to 1D elements for each time step. This makes the linking of the 1D and 2D very accurate when it comes to sending flow through a breach (using a lateral structure), or any others. This direct feedback allows the software to calculate headwater more accurately, tailwater, flow, and any submergence that is occurring at a hydraulic structure on a time step by time step basis.

There are many researchers carried out floodplain modelling using HEC-RAS. Most of the studies concluded that HEC-RAS provides a realistic result which can be used for flood modelling purpose in flood forecasting in Alberta (Peace River), flood hazard assessment in Pakistan (Swat River), floodplain mapping in Iran (Polasjan River) and prediction of stages in Surat City (Lower Tapi River) (Khattak et al., 2016; Salajegheh, Bakhshaei, Chavoshi, Keshtkar, & Najafi Hajivar, 2010; Timbadiya, Patel, & Porey, 2011; Yerramilli, 2012). Therefore, HEC-RAS is chosen for this research.

2.6.4 Flood Inundation Map (FIM)

FIM is important in flood studies because it serves as the non-structural measure to reduce flood risk (Choi, Choi, & Kim, 2013). This map presents the flood information regarding flooded areas and flood depth visually. Flood inundation map is useful for transformation into flood hazard map and flood risk map. These maps are crucial for flood damage assessment, flood risk analysis, flood mitigation planning, urban development planning, flood insurance rate studies, emergency action plans, and ecological studies. The targeted groups who hugely applied the flood risk map are the municipal council and related government agencies to ensure improvement in the quality of life (Goodell & Warren, 2014; Sahoo & Sreeja, 2015).

Development of FIM basically requires four main data components namely: the terrain data which is needed to build the model; discharge or bulk flow data as the input data for water inflow and water outflow purpose; appropriate friction parameter among all types of surface cover; and the observed data such as streamflow and water level data for calibration and validation (Paiva, Collischonn, & Tucci, 2011). The performance of flood inundation modelling is based on the topography data for example, a lower resolution of digital elevation model may underestimate or overestimate the predicted inundation areas and volume. Although higher resolution topographic dataset is highly preferable, this type of data is very costly.

Generally, flood inundation modelling can be performed in 1D modelling, 2D modelling, or 1D-2D modelling approaches based on the objectives of respective studies and also the data acquisition list (Kourtis, Bellos, & Tsihrintzis, 2017). In the last decades, 1D-2D modelling has drawn attention from many researchers due to its better accuracy in term of the data availability. In this study, 1D-2D modelling has chosen to generate a better FIM rather than 1D or 2D modelling due to the better options as describe in Section 2.6.3.5 and also the data acquisition availability. The coarser terrain satellite image will act as the floodplain area whereas the actual river survey data is representing in 1D modelling where both elements will be link together for 1D-2D flood modelling.

2.7 Research Overview

In overall, both hydrological and hydraulic modelling are interrelated and play crucial role in flood modelling. The variety of the software and methods available for

both hydrological and hydraulic model have been reviewed. In this study, the fundamental theories for both elements were discussed.

In hydrological modelling, HEC-HMS was found to be the best option in this study because of its user-friendly application and public domain software for rainfall runoff modelling in industry sector. The selection of the infiltration, transform, routing, and baseflow method were reviewed in term of accuracy, functionality, and availability according to the output result. As a summary, SCS CN loss method and SCS unit hydrograph method were chosen as they correlate with the land use changes topographically. Muskingum Cunge method was the best for KRB since it can be used in flat ungauged region for river routing calculation. For the initial storage, monthly constant was applied for the baseflow method by referring the initial flow in hydrograph before the rising limb occurred referred to Section 2.6.2.5.

In hydraulic modelling, 1D-2D modelling was chosen due to the insufficient river survey cross section width and lower resolution terrain availability. In term of accuracy, 1D-2D modelling is the best among 1D or 2D modelling. Therefore, this method was applied in this study referred to Section 2.6.3.5. In addition, the hydraulic model HEC-RAS was proved to be widely used for flood modelling in many researches.

In term of flood impact by the landuse changes, the imperviousness parameter has been set as the main changes in the hydrological modelling to generate different set of peak hydrographs to be used as the initial boundary input at all confluences to Kuantan River. The flood inundation map produced the flood extent and flood depth information to be further assessment on the flood impact based on landuse changes.

Based on all literature review, most of the researchers used different model to compare the flood inundation area, flood depth, and flood mitigation purpose. There were only few researchers compare the flood impact due to landuse changes in general but in hydrological parameters such as streamflow Akbari et al. (2014); Ali, Khan, Aslam, & Khan (2011); Amini, Ali, Ghazali, Aziz, & Akib (2011); Zope et al. (2016). Therefore, the flood extent area will be compared between two different landuse condition accordingly.

CHAPTER 3

METHODOLOGY

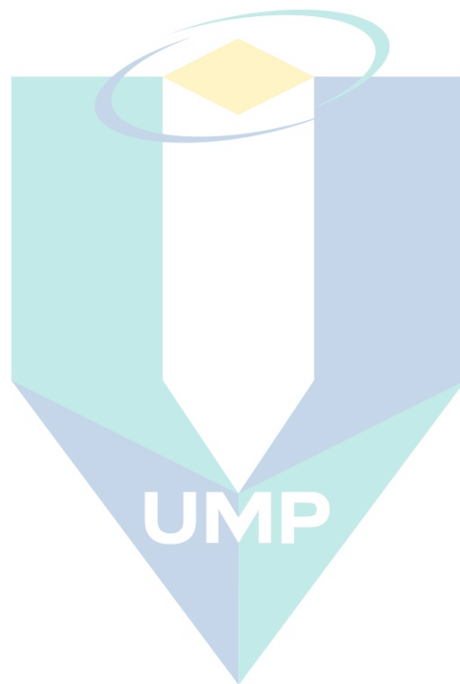
3.1 Introduction

This chapter describes the processes involved in conducting this research which include preliminary survey, data collection, data analysis, hydrological modelling, hydraulic modelling, and development of flood inundation map. Preliminary survey was carried out to get an idea on the basin condition such as restriction of bridges, dam condition, location of water level and streamflow stations, and type of land use. Various data in this study were collected from different government agencies and online sources that were mainly used for preparing data input for the hydrological and hydraulic modelling.

Before the hydrology and hydraulic modelling were conducted, some catchment characteristics for the KRB were extracted through GIS application. Among the information generated is the delineated river network, watershed, loss coefficients, and hydrological scheme. All these processed data have served as the input for the hydrological modelling. For the hydrological model, the HEC-HMS 4.1 was selected to perform the rainfall-runoff simulation and estimate discharge from precipitation.

Results obtained from the hydrological model were applied in the hydraulic modelling. In this study, HEC-RAS version 5.0.3 was chosen. At this stage, river cross-sectional data is crucial and essential to represent the hydraulic structure for the flood analysis. Hence, river cross-section data were collected from previous report and also GIS analysis. Flood level and flow pattern generated from the 1D hydraulic modelling were then applied into the 2D floodplain modelling to generate the flood inundation map for the KRB based on selected flood events. Lastly, the flood extent in the generated flood inundation maps were compared according to the effect of landuse changes.

Performance of all the models were evaluated statistical through several methods namely the Nash-Sutcliffe model efficiency (NSE) and Root Mean Square Error (RMSE) by comparing both simulated and observed data with the equation as discussed in Section 3.8. The accuracy and error analysis were done for both the calibration and validation. Figure 3.1 presents the methodology flowchart showing the processes involved in completing this study.



اونيورسيتي مليسيا قهغ

UNIVERSITI MALAYSIA PAHANG

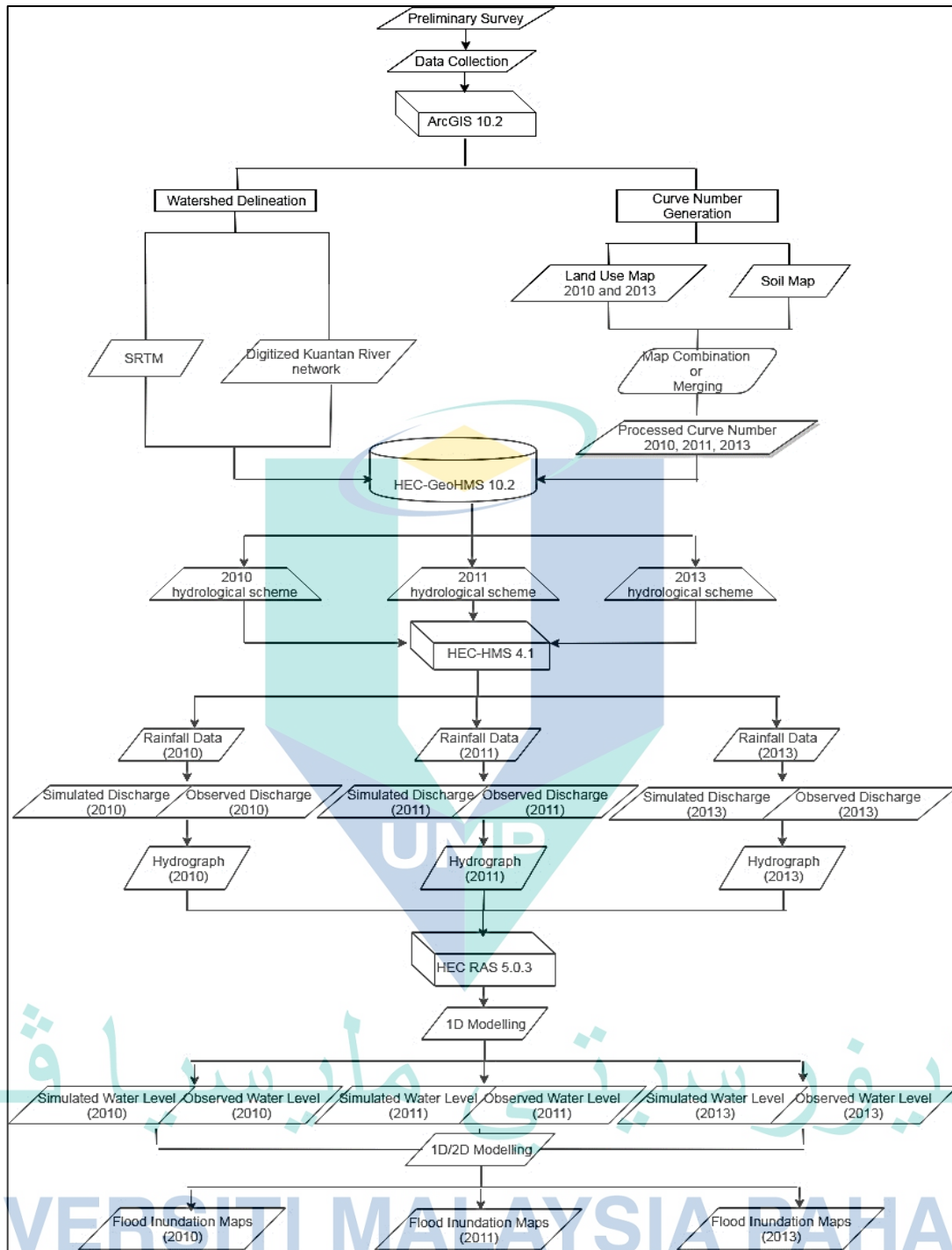


Figure 3.1 Flowchart of Flood Inundation Modelling at KRB

3.2 Preliminary Study

3.2.1 Study Area

KRB is situated at the north-eastern of Pahang state in Peninsular Malaysia. This basin has a surface catchment area of 1630km² (Zaidi, Akbari, & Ishak, 2014) initiated from the Mukim Ulu Kuantan to Tanjung Lumpur and outlet point to the South China Sea. The catchment was in elongated shape where the upstream of the catchment land covers are mainly forest and agriculture activities. The urbanized in KRB were located at downstream region spread out over the estuary. Along Sg. Kuantan, there are many tributaries flowing through the major rural, urban, industrial areas and agricultural areas of the Kuantan District. The tributaries of Sg. Kuantan are Sg. Cereh, Sg. Keliu, Sg. Terapai, Sg. Bunga, Sg. Jin, Sg. Berapit, Sg. Kabong, Sg. Kenau, Sg. Nada, Sg. Reman, Sg. Siput, Sg. Caru, Sg. Panching, Sg. Riau, Sg. Danau, Sg. Gading, Sg. Pandan, Sg. Rambutan, Sg. Pinang, Sg. Tiram, Sg. Belat, Sg. Galing, and Sg. Salak (Edre, Hayati, Salmiah, & SI, 2015). The KRB river map was as shown in Figure 3.2.

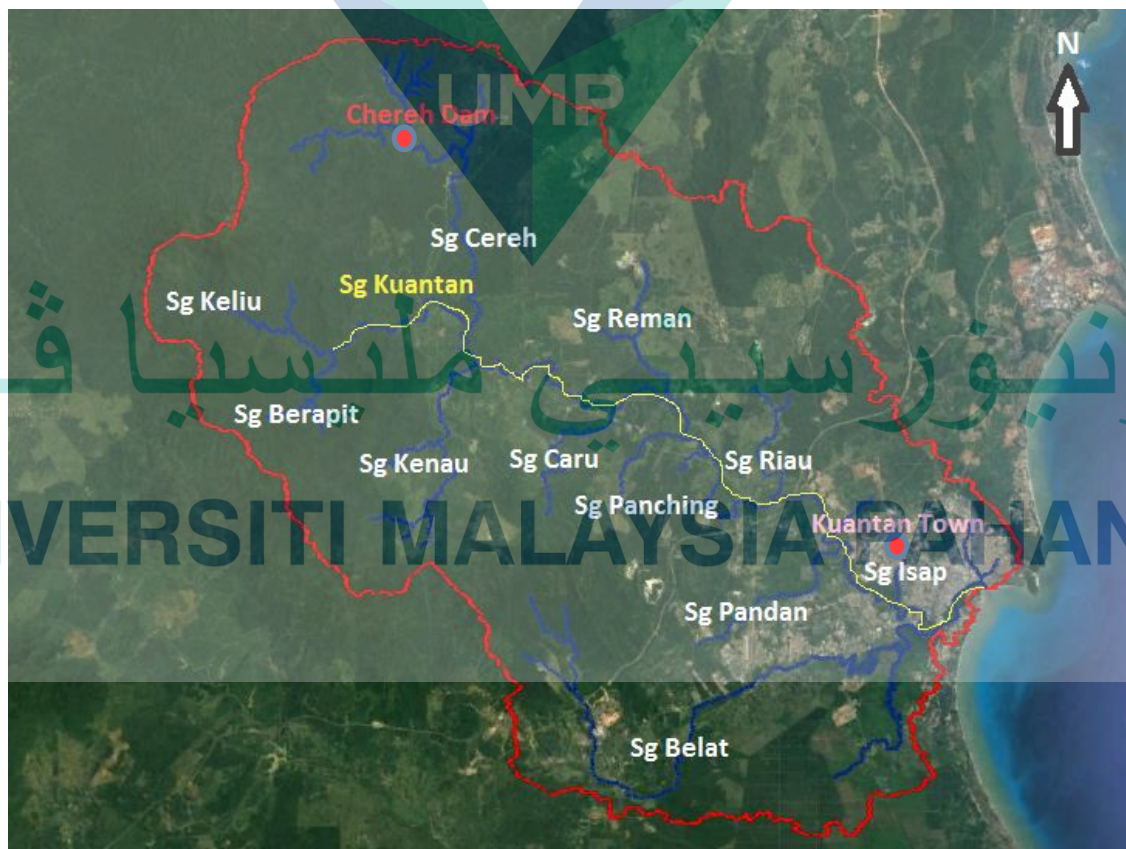


Figure 3.2 Kuantan River Basin in Malaysia

3.2.2 Field Visit

List of hydrological stations was identified from the national hydrological network provided in the DID online database. The coordinate of the rainfall, streamflow, and water level stations within the KRB were counterchecked on field with the assistance of DID personnel to ensure the locations provided in the database are not off grid. Additionally, the surroundings along the main river were observed and documented to identify the type of land use in the basin and any existing hydraulic structures. These observations are important to determine the floodplain roughness and flow constrictions in flood modelling. The site visits activities are presented in Appendix A.

3.2.3 Storm Event Selection

In this study, four (4) storm events have been selected based on several criteria include: a) highest discharge; b) highest total precipitation; c) availability of land use map; and d) completeness of the hydrological data. Preliminary analyses on the hydrological data were conducted for the selection process. Figure 3.3 and Figure 3.4 display the total precipitation in the form of histograms on the monthly and yearly basis, respectively. Additionally, the maximum streamflow from the year 2000 to 2013 is shown in

From Figure 3.3, the highest average total monthly precipitation observed for all stations for the year 2000 to 2016 falls in December followed by the month of November and January. Heavy rainfall occurred in these months because of the northeast monsoon. In the yearly basis, the year 2001 showed the highest total average precipitation with an amount of about 2500 mm as shown in Figure 3.4. High precipitation in the KRB is also due to the climate condition in this tropical region. Since there is only one streamflow station available in the KRB, only the station at Bukit Kenau was considered in this research.

Based on the analyzed data presented in Figure 3.5, the highest yearly discharge was in 2001 in -line with the precipitation pattern. Apart from the year 2001, high streamflow was also observed followed in the year 2003, 2004, 2006, 2009, and 2013, when flood events occurred in these years.

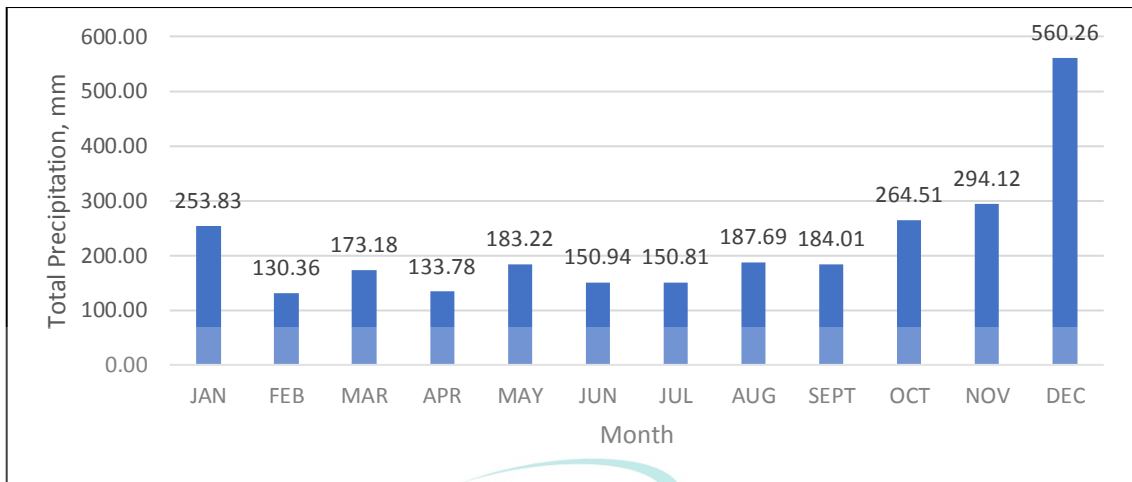


Figure 3.3 Average total monthly precipitation for the year 2000 to 2016

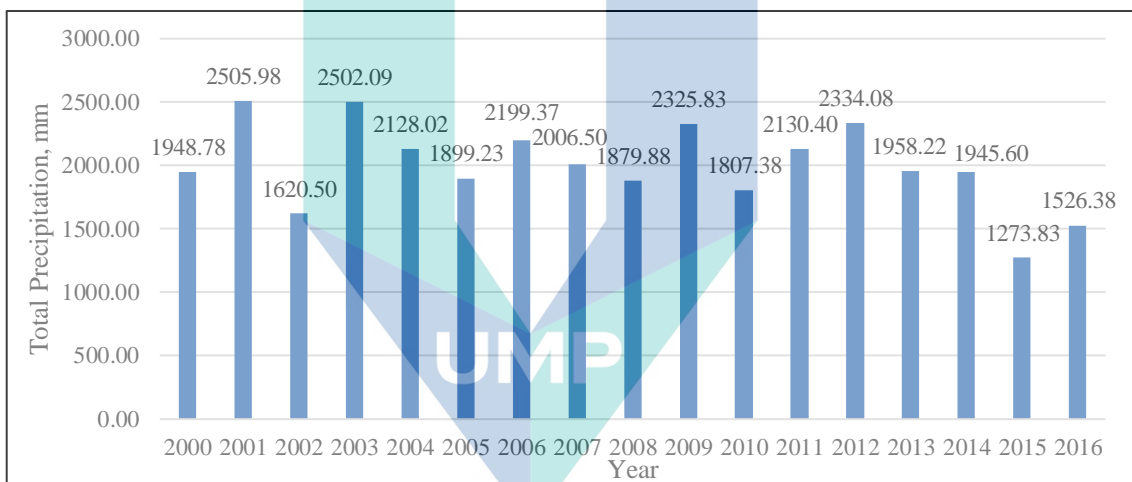


Figure 3.4 Average total yearly precipitation for the year 2000 to 2016

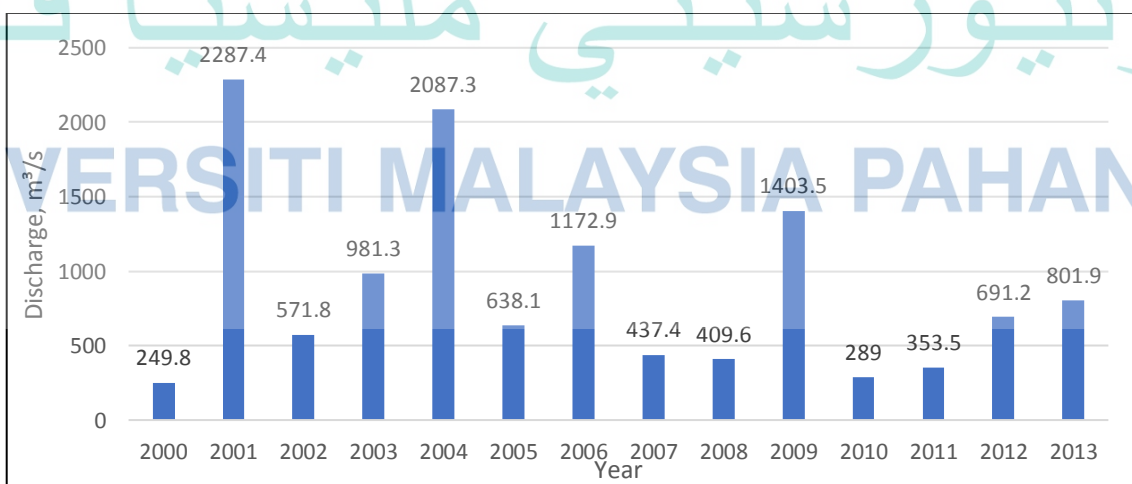


Figure 3.5 The maximum discharge at Bukit Kenau station (3930401) for the year 2000 to 2013

Besides hydrological aspect, the availability of the land use map in KRB was also crucial in selecting the storm events. Based on the year of land use map available, which in this case was the year 2010 and 2013, the rainfall, streamflow, and water level data were reviewed to ensure the completeness of the data for these years. Then the months with the highest flow and precipitation were chosen as the flood events in the modelling process.

The selected flood events were within the months of December and January are 29th December 2010 to 2nd January 2011; 26th to 30th March 2011; 1st to 5th December 2013, and 16th to 19th March 2014 in reference to the selection criteria discussed. Two (2) flood events dates (29th December 2010 to 2nd January 2011 and 1st to 5th December 2013) have been checked and verified with the flood report from DID Pahang. As for the other extreme rainfall events, they were selected based on the data completeness. All the observed data of rainfall, streamflow, and water level were presented in Appendix C1, C2, and C3 respectively.

After the collection of the required data, the flood data from DID Pahang in which the flood record is within the Kuantan River Basin. Total rainfall at all available rainfall stations and streamflow station (Bukit Kenau) patterns for all the flood events selected were displayed in Figure 3.6 to Figure 3.13.

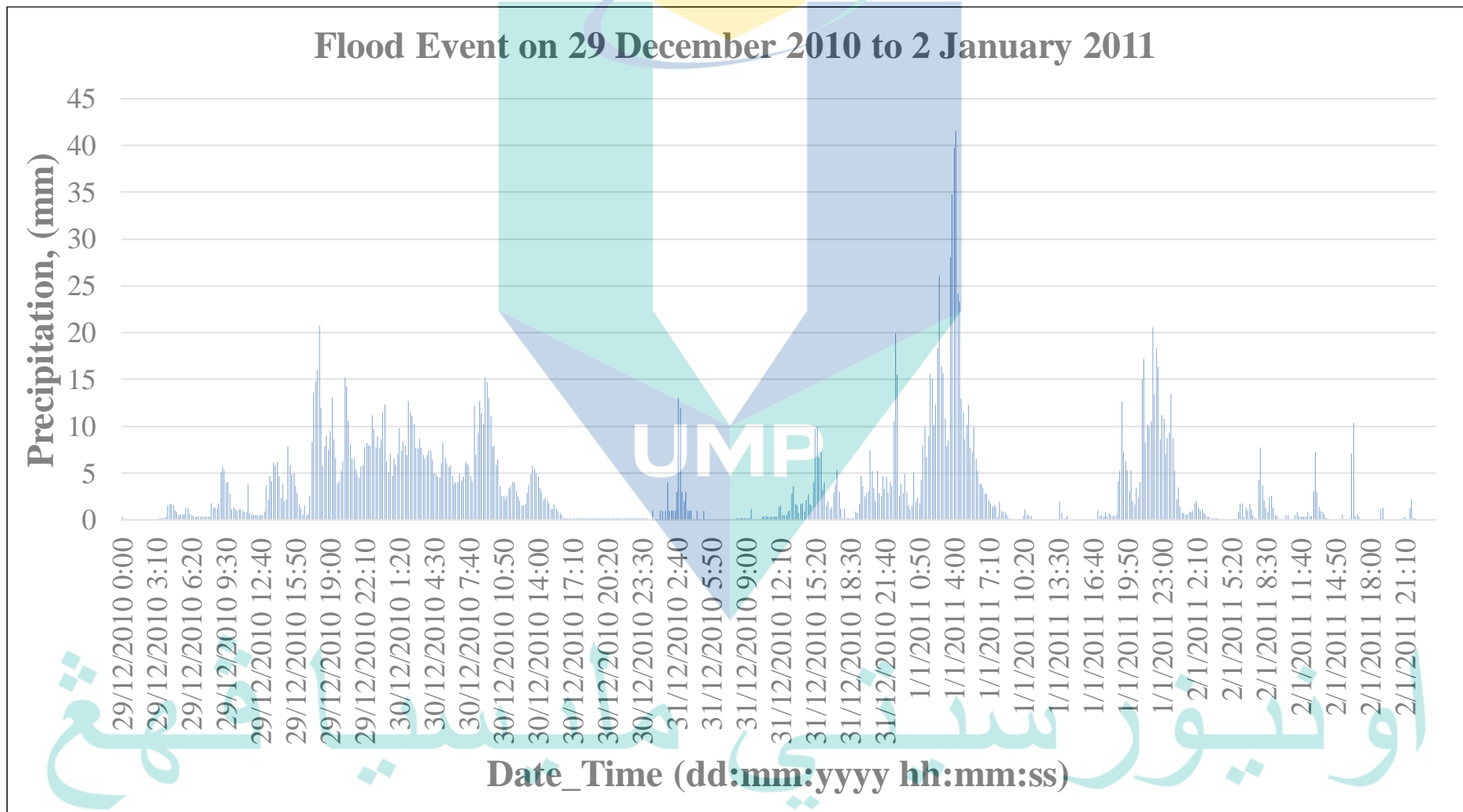


Figure 3.6 Total Precipitation for the event from 29th December 2010 to 2nd January 2011

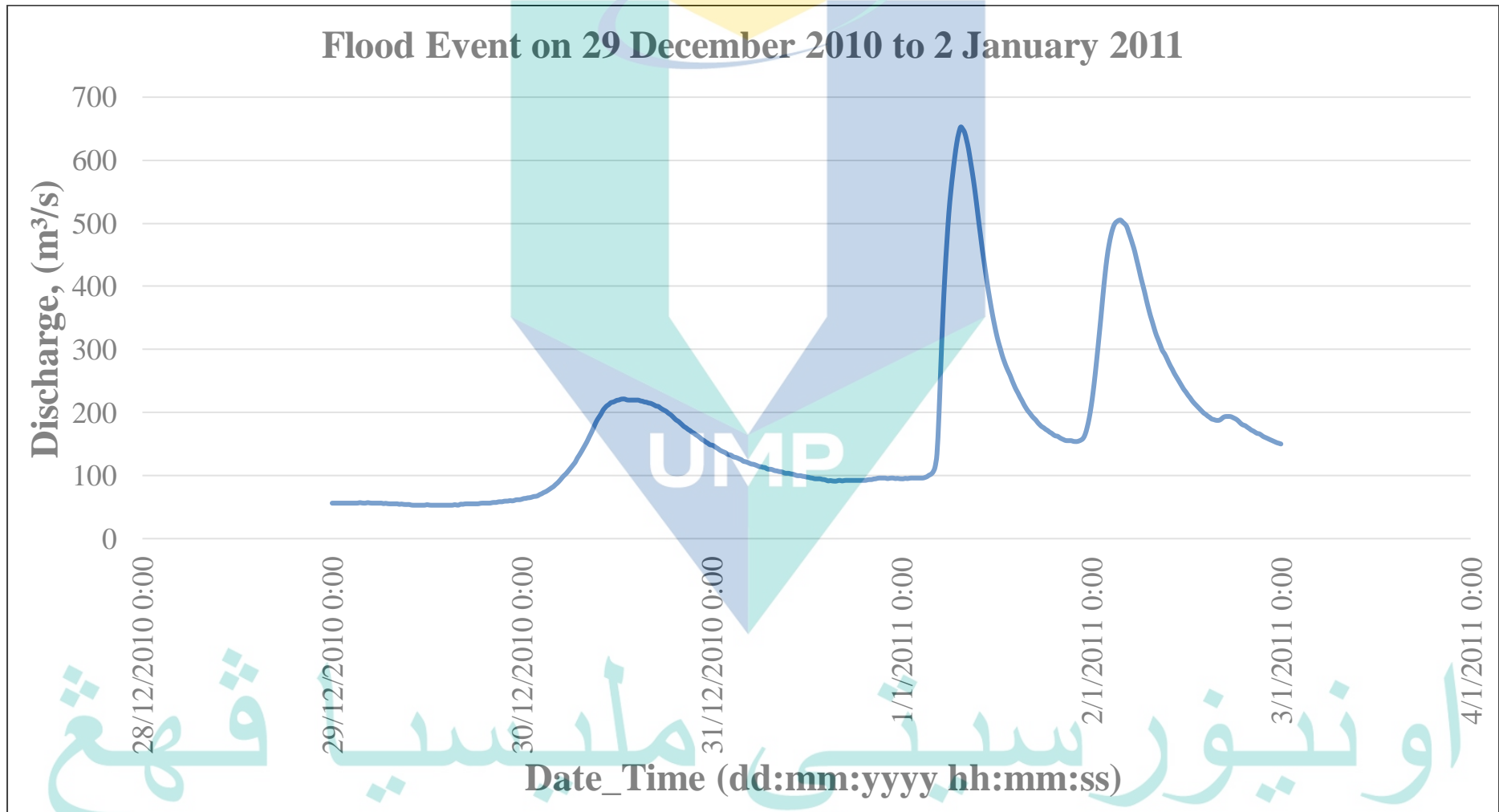


Figure 3.7 Streamflow for the event from 29th December 2010 to 2nd January 2011

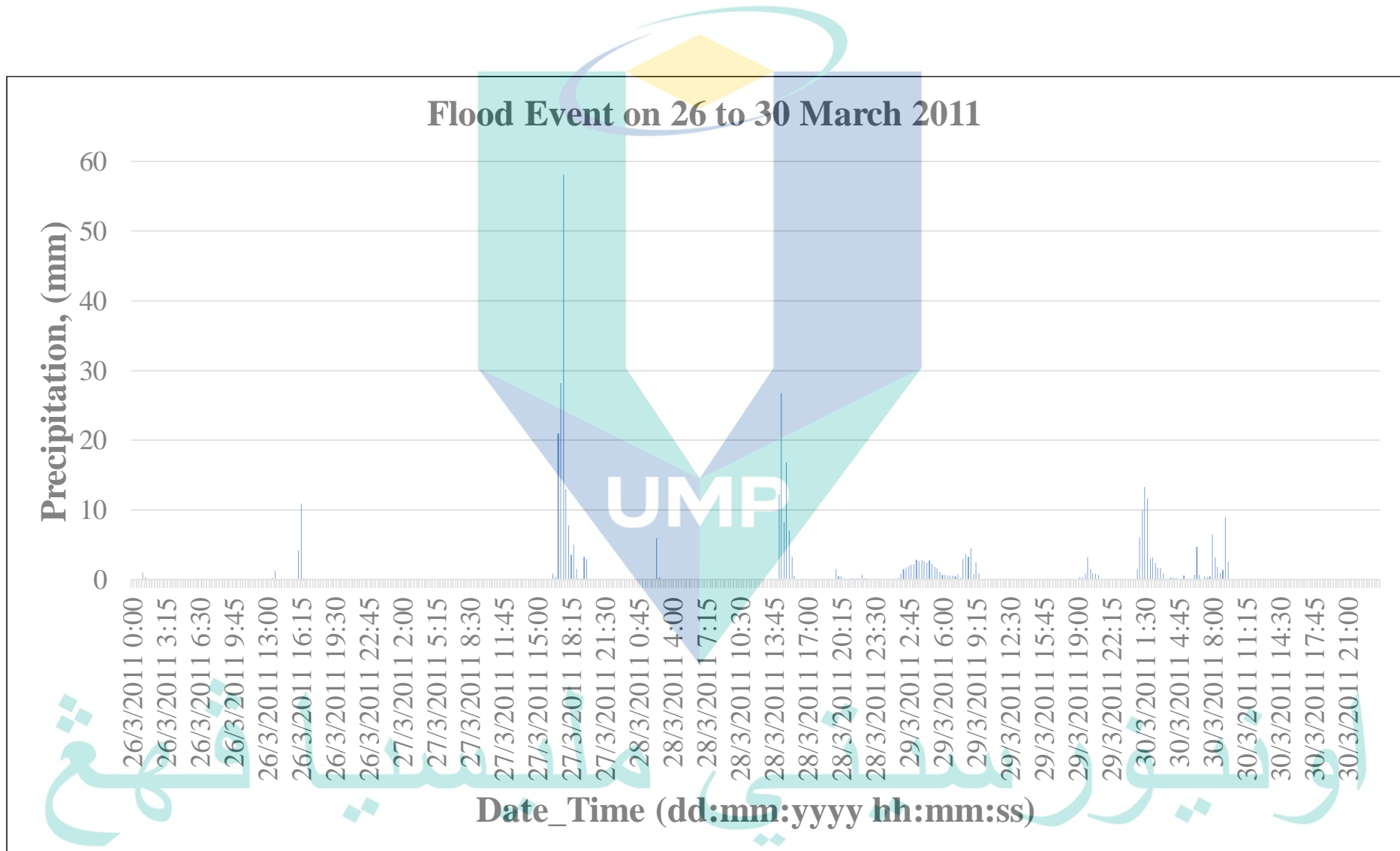


Figure 3.8 Precipitation for the event from 26th to 30th March 2011

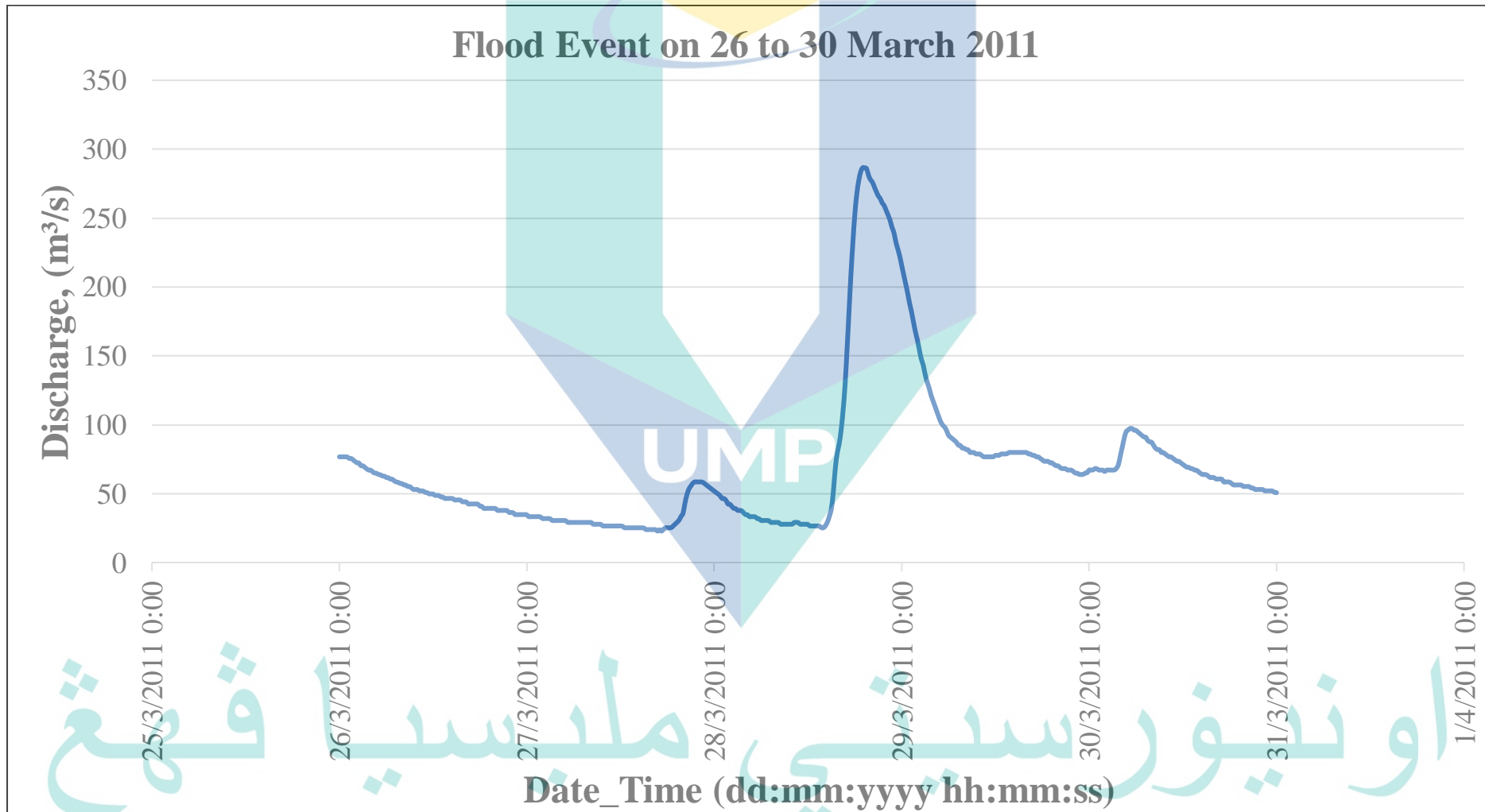


Figure 3.9 Streamflow for the event from 26th to 30th March 2011

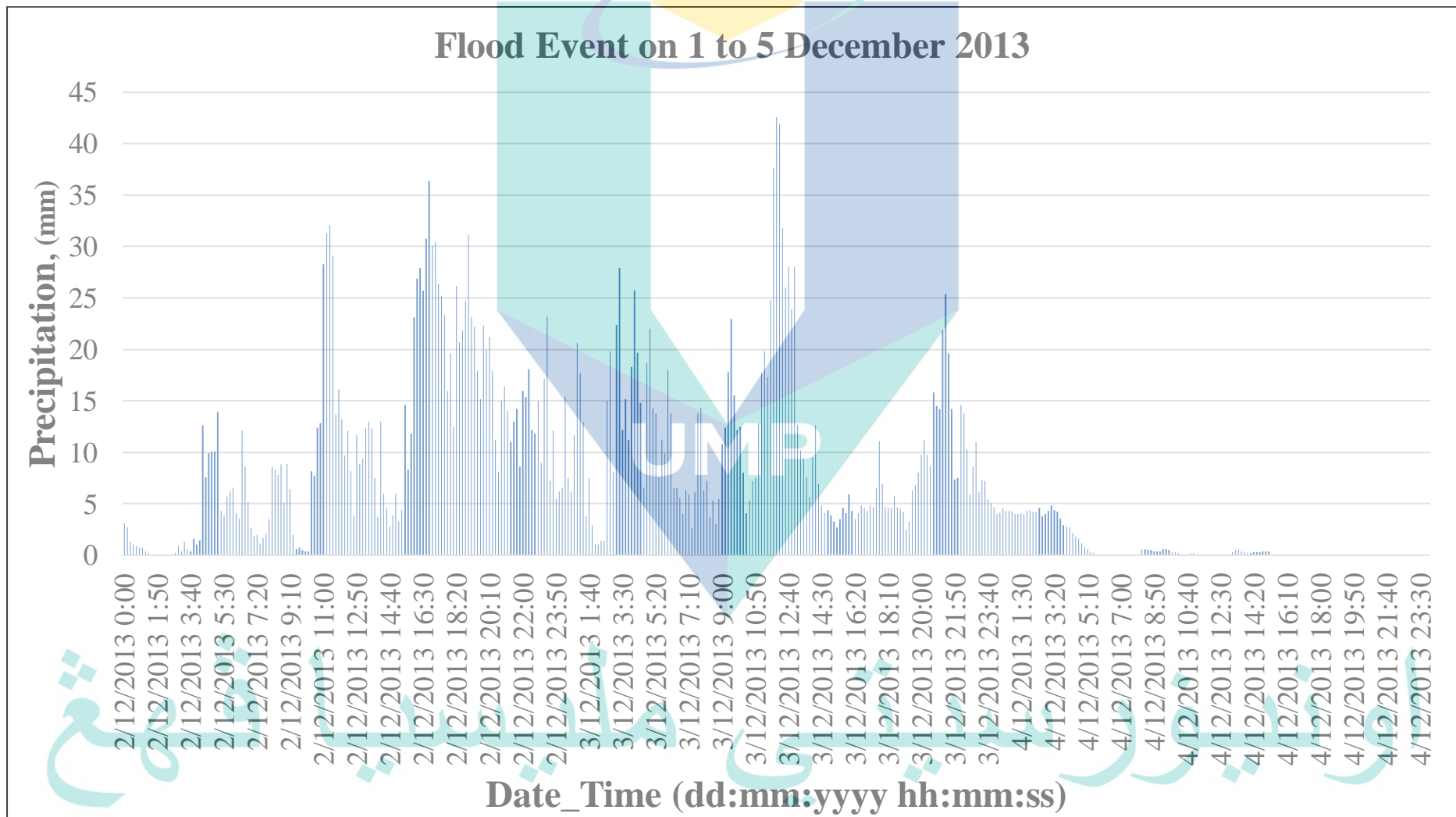


Figure 3.10 Precipitation for the event from 1st to 5th December 2013

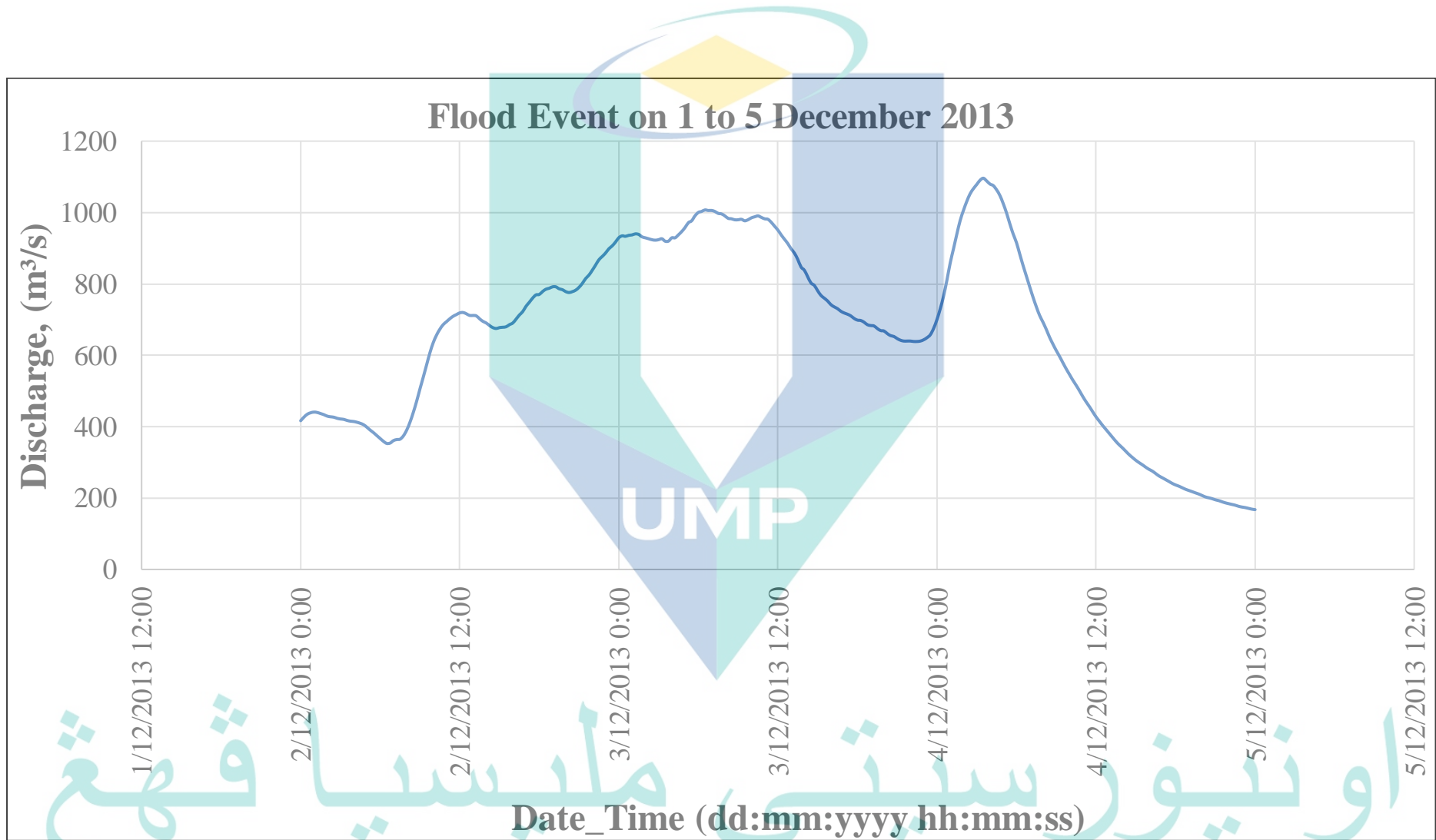


Figure 3.11 Streamflow for the event from 1st – 5th December 2013

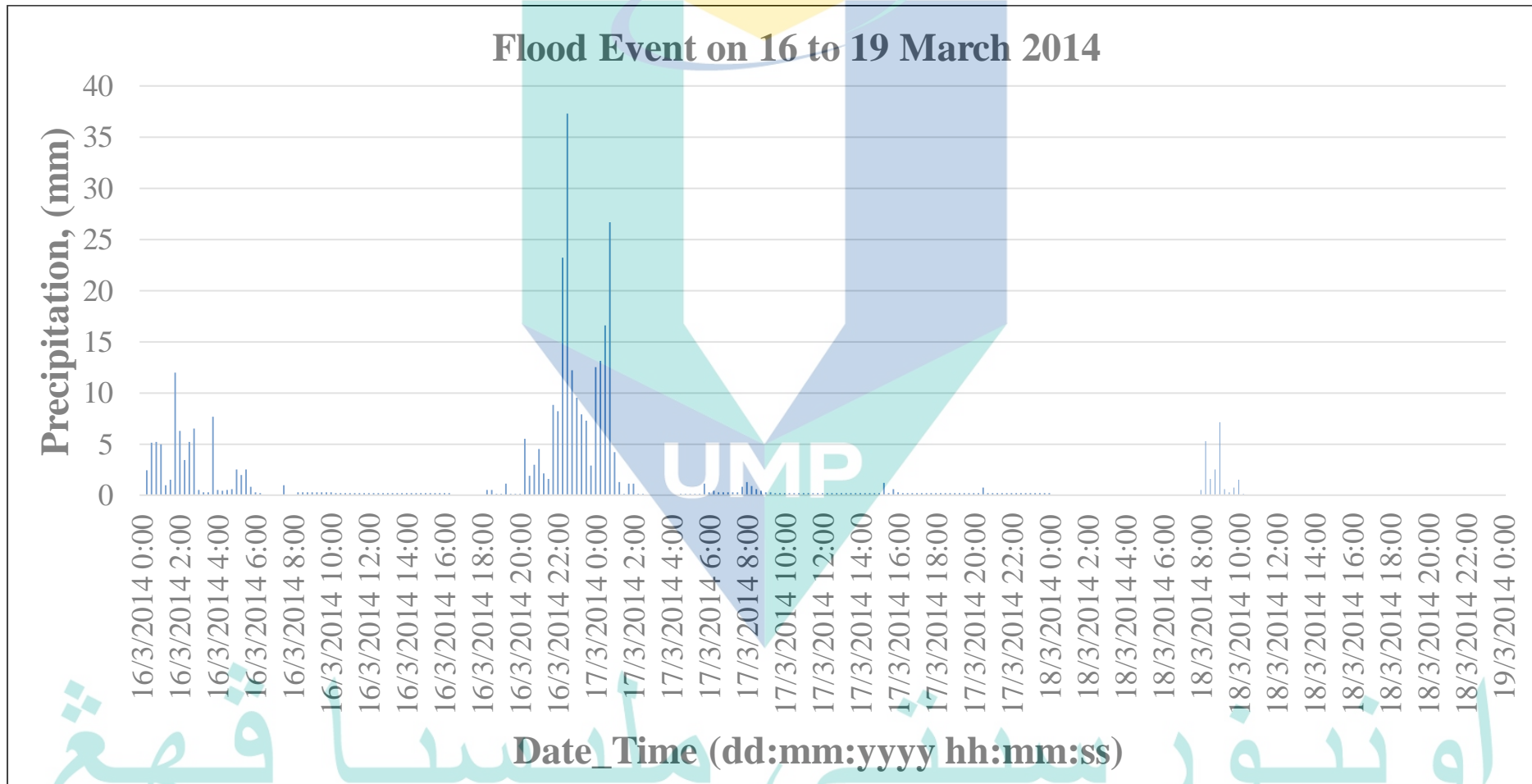


Figure 3.12 Precipitation for the event from 16th to 19th March 2014

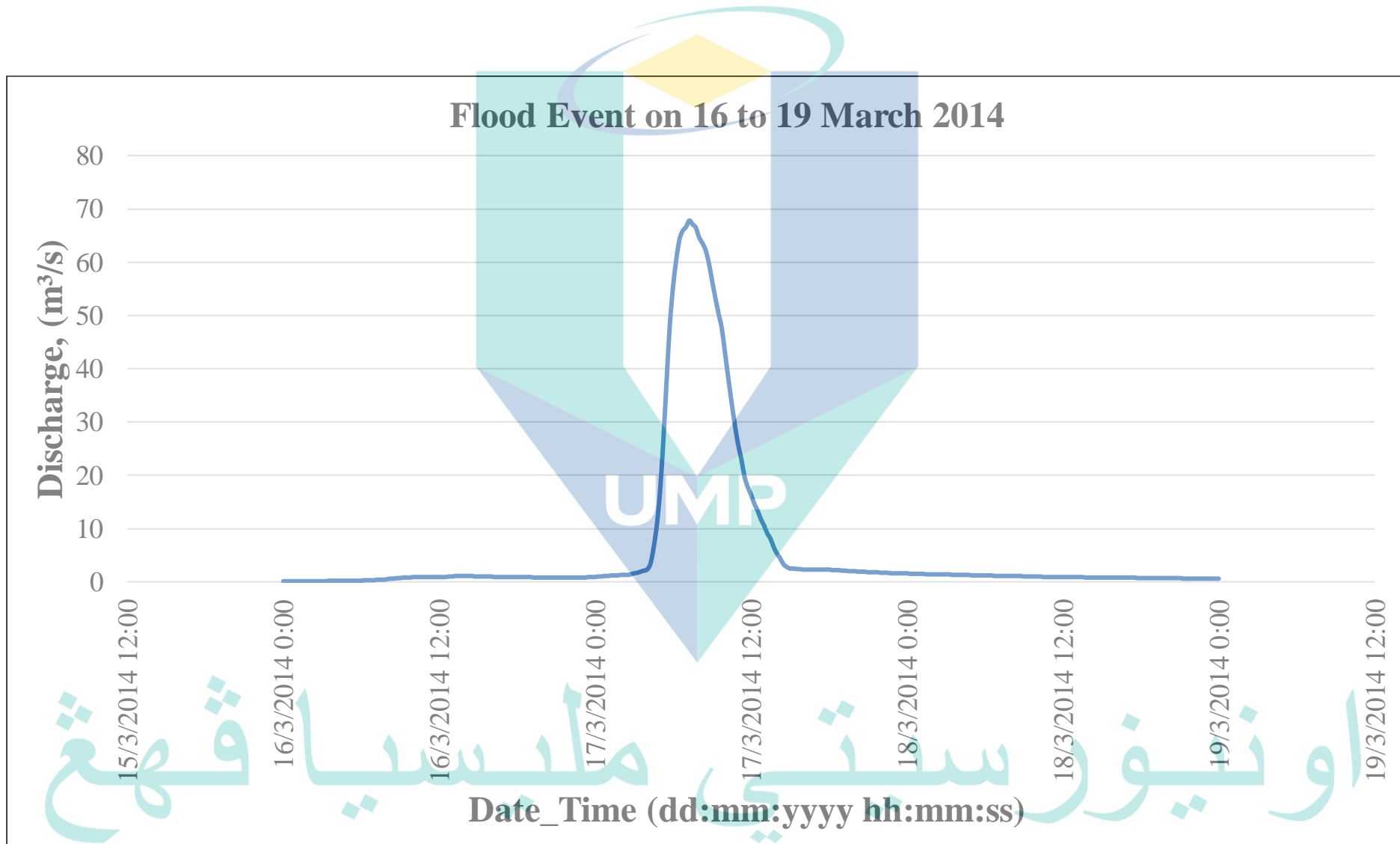


Figure 3.13 Streamflow for the event from 16th to 19th March 2014

3.3 Data Collection

For data collection, the hydrological data such as Rainfall (RF), Water Level (WL), and Streamflow (SF) stations for the year 2000 to 2016 were collected from DID. Coordinates of the hydrological stations were verified by using Global Positioning System during field observation around the basin. Besides the primary data, secondary data such as terrain topographic datasets SRTM-DEM, soil map, and land use map were retrieved from the U.S. Geological Survey website, Department of Agriculture, and the Kuantan local authority. In hydraulic modelling, river cross-section survey data is crucial, and this data was acquired from previous report of DID.

3.3.1 Hydrological Data

The hydrological data in the Kuantan River Basin is captured by three means: manual, auto logger and telemetry. For the auto logger, it can capture hourly data and the data is collected in weekly basis by DID Kuantan District personnel. The manual reading is done on daily basis while the telemetry data can be acquired from online source. Data of 15 minutes interval for the rainfall, streamflow and water level was applied and retrieved from DID.

These rainfall data were used as the primary input in the meteorologic model for the hydrological modelling. Meanwhile, the streamflow data was used as the observed discharged of flood events in the calibration and validation processes. Furthermore, the water level data was applied in the calibration and validation of water level in the hydraulic modelling.

In KRB, there are a total of eleven (11) rainfall stations, one (1) streamflow station, and three (3) water level stations. Information of all the gauging stations are described in Table 3.1 and the map is as shown in Figure 3.14. Actual coordinates of the active hydrological stations were plotted in ArcGIS 10.4 application as an input to generate rainfall distribution pattern by Thiessen Polygon method.

Table 3.1 Location of rainfall, streamflow, and water level stations in KRB

Station No	Station Name	Function	Latitude	Longitude
3631001	Kg. Pulau Manis	RF	03°39'10''	103°07'10''
3731018	JKR Gambang	RF	03°42'20''	103°07'00''
3732020	Paya Besar	RF	03°46'20''	103°16'50''
3732021	Kg. Sg. Soi	RF	03°43'50''	103°18'00''
3831001	Pasir Kemudi	RF	03°52'12''	103°11'24''
3832015	Rancangan Pam Paya Pinang	RF	03°50'30''	103°15'30''
3833002	Pejabat JPS Negeri Pahang	RF	03°48'30''	103°19'45''
3930012	Sg. Lembing P.C.C.L Mill	RF	03°55'00''	103°02'10''
3930013	Bukit Kenau	RF	03°55'12''	103°03'00''
3931013	Ldg. Nada Kolek	RF	03°54'30''	103°06'20''
3931014	Ldg. Kuala Reman	RF	03°54'00''	103°08'00''
3930401	Sg. Kuantan at Bukit Kenau	SF	03°55'55''	103°03'30''
3831401	Sg. Kuantan at Pasir Kemudi	WL	03°52'12''	103°11'24''
3930401	Sg. Kuantan at Bukit Kenau	WL	03°55'55''	103°03'30''
3832420	Kuantan Bypass	WL	03°48'19''	103°16'04''

*Note RF=Rainfall; SF=Streamflow; and WL=Water Level

UMP

اونيورسيتي ملايسيا قهغ

UNIVERSITI MALAYSIA PAHANG

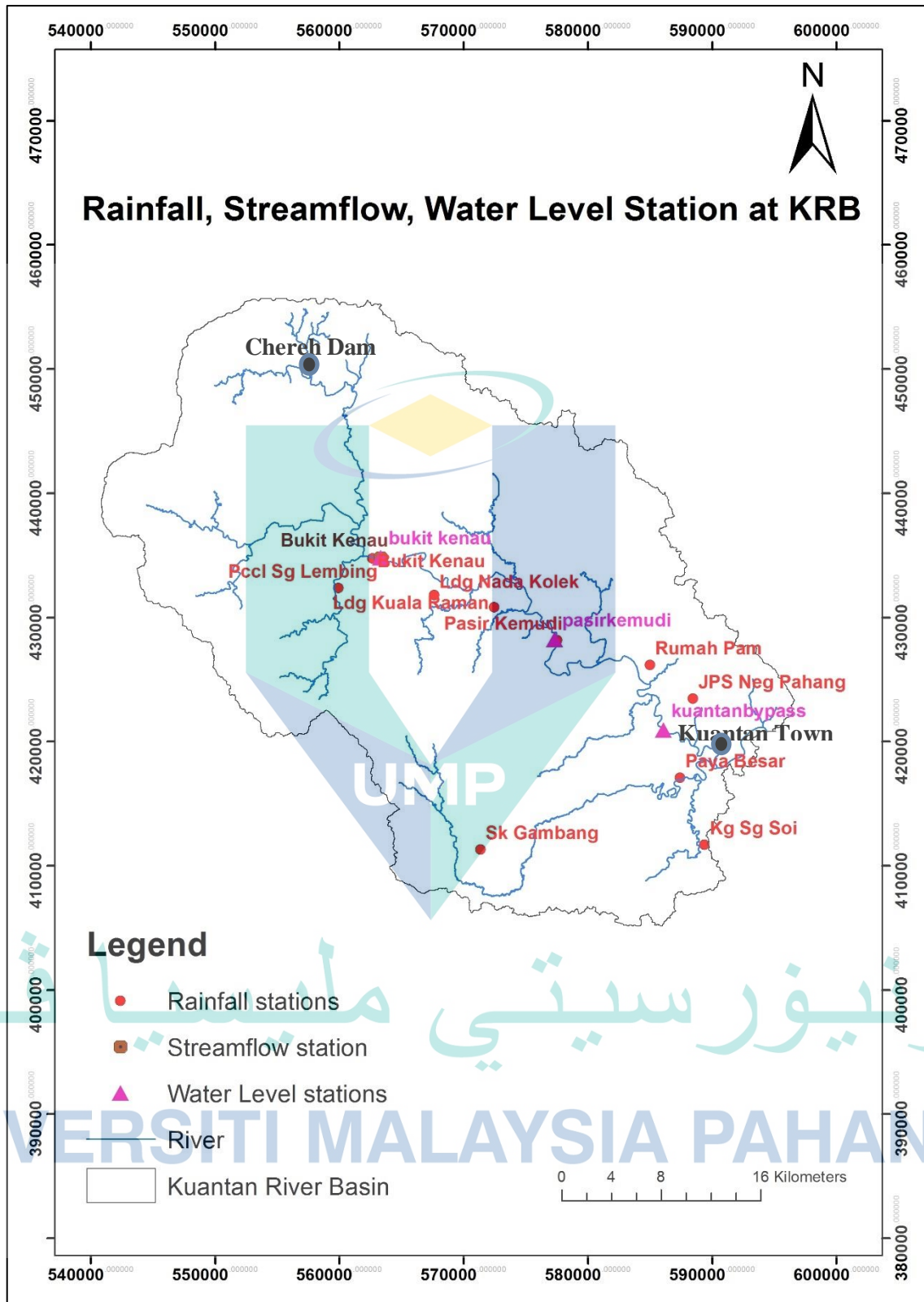


Figure 3.14 Hydrological stations within KRB

3.3.2 River Survey

River cross-section survey data which describes the profile of the river and floodplain are essential to simulate the flood propagation and inundation in hydraulic modelling. In this study, the Kuantan River cross-sectional data available covered a total reach length of 50 km. The survey data were captured at every 500 m intervals in the year 2014 in reference to the mean sea level datum projection starting at CH0 (rivermouth) to CH 68000 (upstream).

Figure 3.15 and Figure 3.16 show the location of the cross-sections surveyed points along the Kuantan River and the example of cross-sectional view at selected chainage CH 10000 and CH500 . Coordinates of each survey points were retrieved from the longitudinal survey plan which was then integrated into the GIS application and hydraulic model.



Figure 3.15 Location of the cross-sections surveyed point along the Kuantan River

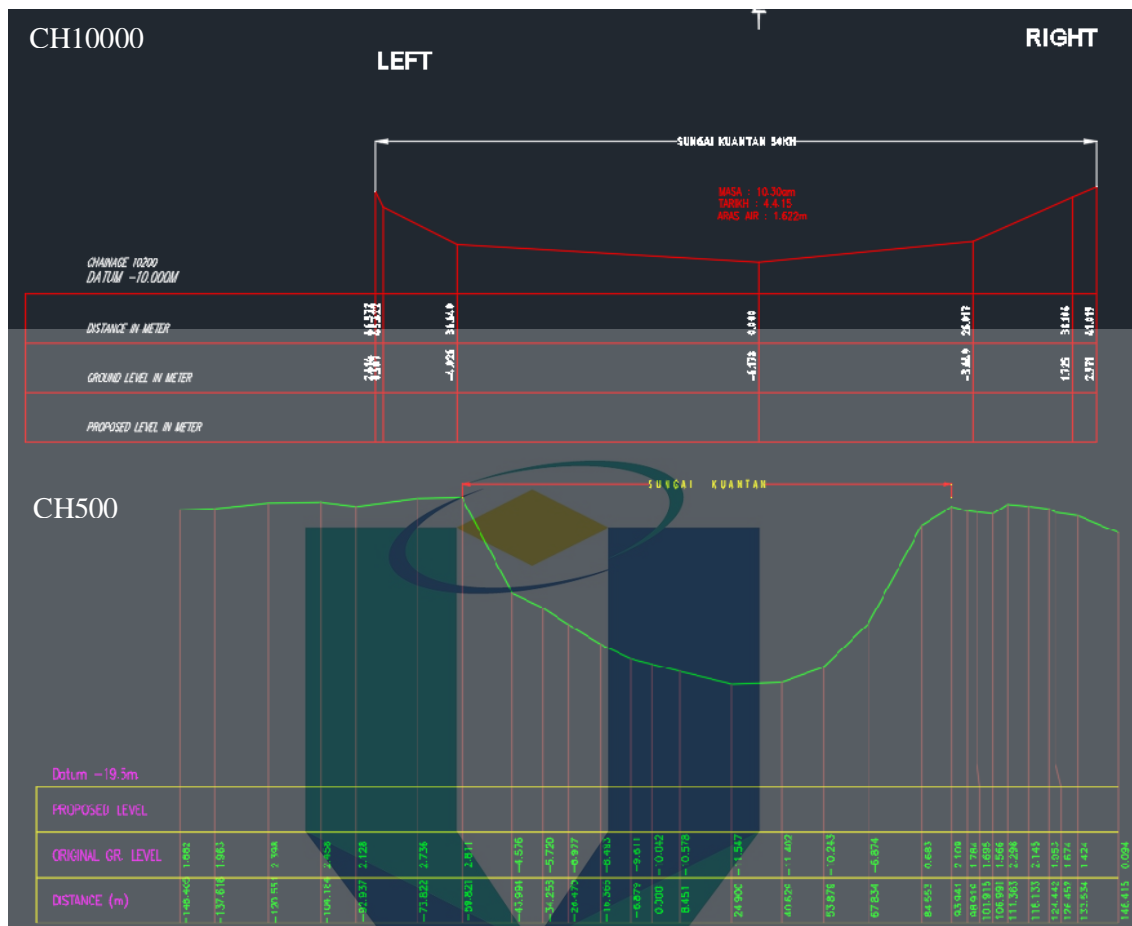


Figure 3.16 The cross-sectional view at chainage CH10000 and CH 500

3.4 ArcGIS and HEC-GeoHMS

Catchment and river network delineation of the Kuantan River were done based on the readily downloadable public domain SRTM DEM with 30-m resolution. The geographical information system used to extract the geographical information from the DEM was ArcGIS version 10.4 containing the extension of HEC-GeoHMS. All the delineation processes were performed according to the procedures provided in the HEC-GeoHMS extension guideline. Before performing the main analysis of the geographical information system, the coordinate system of the DEM was converted into the projected coordinate system, Kertau RSO Malaya (Meters) in ArcGIS. This is to ensure a consistent coordinate system for the entire analysis process to prevent error.

3.4.1 Watershed Delineation

In general, the delineation process in HEC-GeoHMS begins with pre-processing of elevation model. The flowchart of the pre-processing stages is displayed in Figure

3.17. The DEM reconditioning was performed to adjust the position of the raw DEM in accordance to the stream position of the digitized river network developed priory. River networks generated without reconditioning may not be very accurate especially when the 30-m resolution DEM are rounded off, which cause the drainage directions and the watershed boundary to be less accurate. Therefore, the reconditioning process is crucial to enhance the generation of hydrologic parameters.

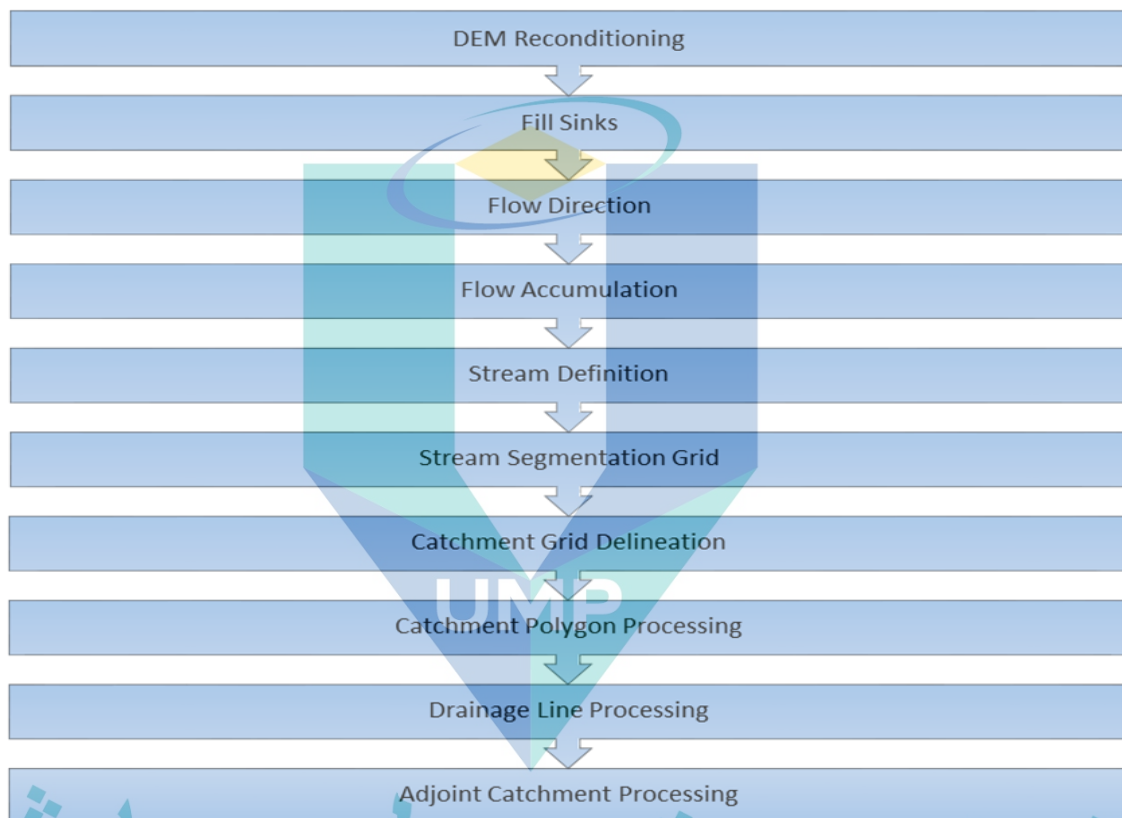


Figure 3.17 Process flow of DEM pre-processing

Sinks filling is a process to fill the depression or pits developed after reconditioning the DEM by increasing the elevation of the voids to the level of the surrounding terrain. The existence of voids in the analysis will cause disconnection between adjacent cells leading to incorrect basin delineation. Flow direction defines the direction of the steepest descent of each terrain cell. Each direction is represented by a number, which is east (1), southeast (2), south (4), southwest (8), west (16), northwest (32), north (64), and northeast (128). Flow accumulation determine the number of upstream cells draining to a given cell. The upstream drainage area at a given cell can be calculated by multiplying the flow accumulation value by the grid cell area. Based on the cell thresholds defined in the flow accumulation process, the stream definition was

performed to classify the cells belonging to the stream network. Stream segmentation divided the stream grid into segments or links which connect two successive junctions, or the division between a junction and the drainage. Catchment grid delineation was then performed to delineate the sub-basin for every stream segment. The raster image of the sub-basin were converted into polygon through the catchment polygon processing to generate the sub-catchment boundaries. For the river network, the function of drainage, line processing was applied to create the polyline representing the river networks. The ad-joint catchment processing stage was required to improve the computational performance interactively when delineating sub-basins and enhance data extraction when defining the HEC-GeoHMS project.

3.4.2 Curve Number

Curve number (CN) is one of the sensitive parameters in loss method to estimate the runoff volume during a storm event. It indicates the runoff potential of a soil-cover complex during periods when the soil is not frozen. Both factors that changes the CN value are land use/land cover and hydrologic soil group. The land use map for the years 2010 and 2013 as well as Hydrologic Soil Group (HSG) map were presented in Figure 3.18, Figure 3.19, and Figure 3.20 respectively that utilized to estimate the CN in the GIS application to be used in the runoff volume estimation.

The landuse map for the year 2010 was extracted from the previous research (Zaidi et al., 2017), whereas landuse map for the year 2013 was collected from Town and Country Planning Department (PlanMalaysia). Both landuse maps were categorized into five classes: a) Agriculture; b) Bare Soil; c) Built up; d) Forest; and e) Water. From the landuse information, it was found that the majority of the landuse is made up of forest followed by agriculture, built up area, bare soil, and water body. From the year 2010 to 2013, urbanization at the downstream region of the KRB has increased by 35.6% as referred in Table 3.3.

For the HSG data obtained from soil map, the information was provided by Department of Agriculture (DOA). There are 4 different classes of HSG namely class A, B, C, and D. The description of each classes is listed in Table 3.2. Based on the HSG map of KRB, most of the land was categorized under Class B which indicate moderate

infiltration rate. The highest runoff potential under Class D was located at the downstream region near to sea.

Both landuse and HSG data were used to estimate the CN value from based on Natural Resources Conservation Service Technical Releases 55 (SCS TR55). CN ranges from 100 to 0. The higher the number indicates the lower ability for water abstraction to soil and vice versa. The value of the CN was selected by the generation of a union table of selected CN according to the land use classification and hydrological soil group. CN map outcome was then created in ArcGIS using HEC-GeoHMS extension tool. At the final stage, weighted curve number map was generated according to sub-basins where the value of the weighted curve number was applied in the hydrological modelling which has been discussed in Section 4.2.3.

Table 3.2 Description of Hydrologic Soil Group Classification

HSG Class	Soil Type	Remarks
A	Sand, Loamy Sand	Low runoff potential and high infiltration rates even when thoroughly wetted
B	Silt loan or Loam	Moderate infiltration rate when thoroughly wetted
C	Sandy Clay Loam	Low infiltration rates when thoroughly wetted
D	Clay Loam, Silty Clay Loam, Sandy Clay, Silty Clay or Clay	High runoff potential and very low infiltration rate when thoroughly wetted

3.4.3 HEC-GeoHMS Extension

Following the basin and river network delineation processes, a HMS project database directory was setup to store all the results generated which are later used in the HEC-HMS hydrological model. In the project setup, the delineated Kuantan River Basin was automatically extracted from the entire delineated DEM cells by defining the project point at the drainage outlet. The boundary of the project areas generated was checked and confirmed to ensure the entire areas of interest were covered. From the extraction, 73 sub-basins were derived for Kuantan River Basin.

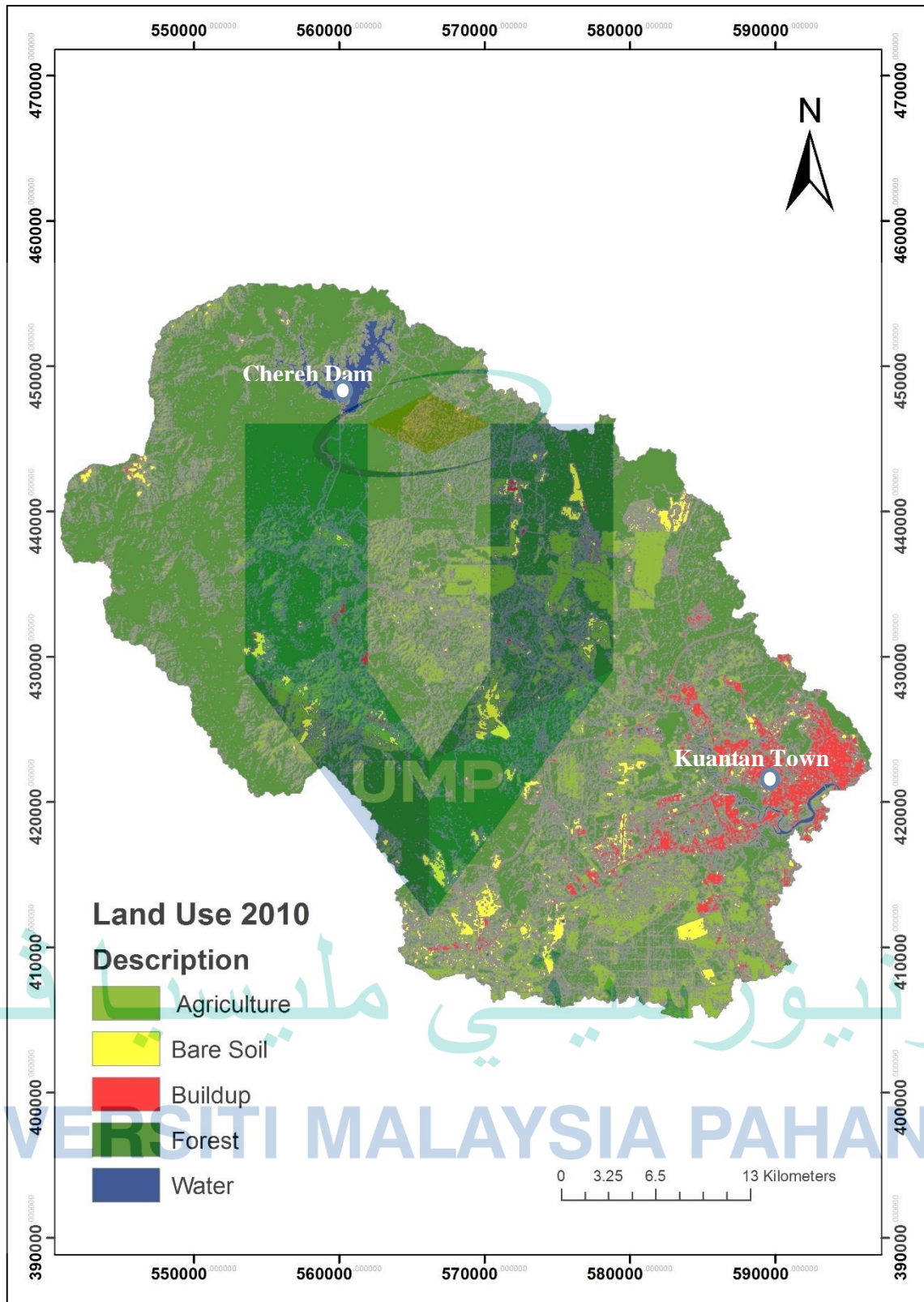


Figure 3.18 Land Use Map in 2010 for KRB

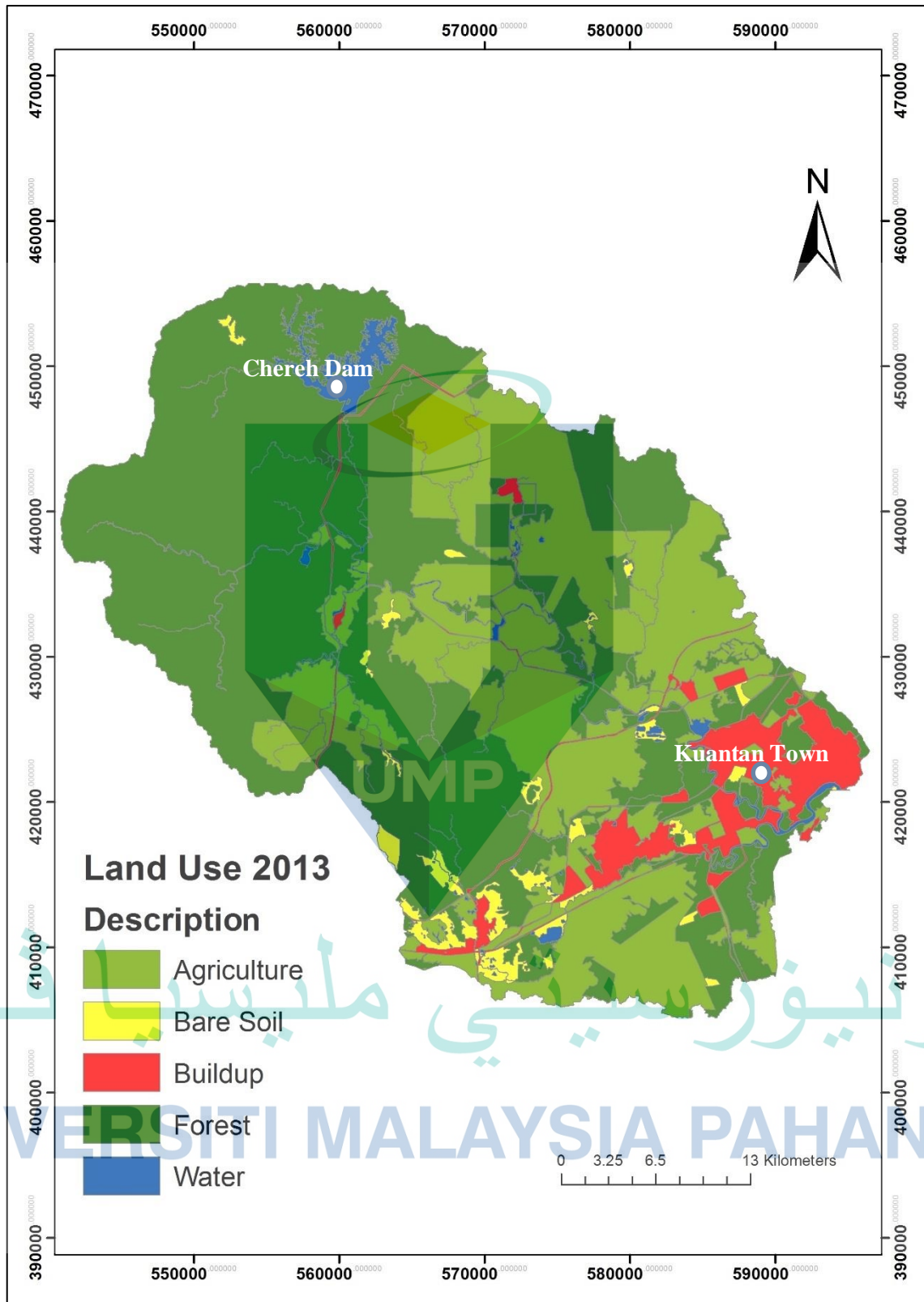


Figure 3.19 Land Use Map in 2013 for KRB

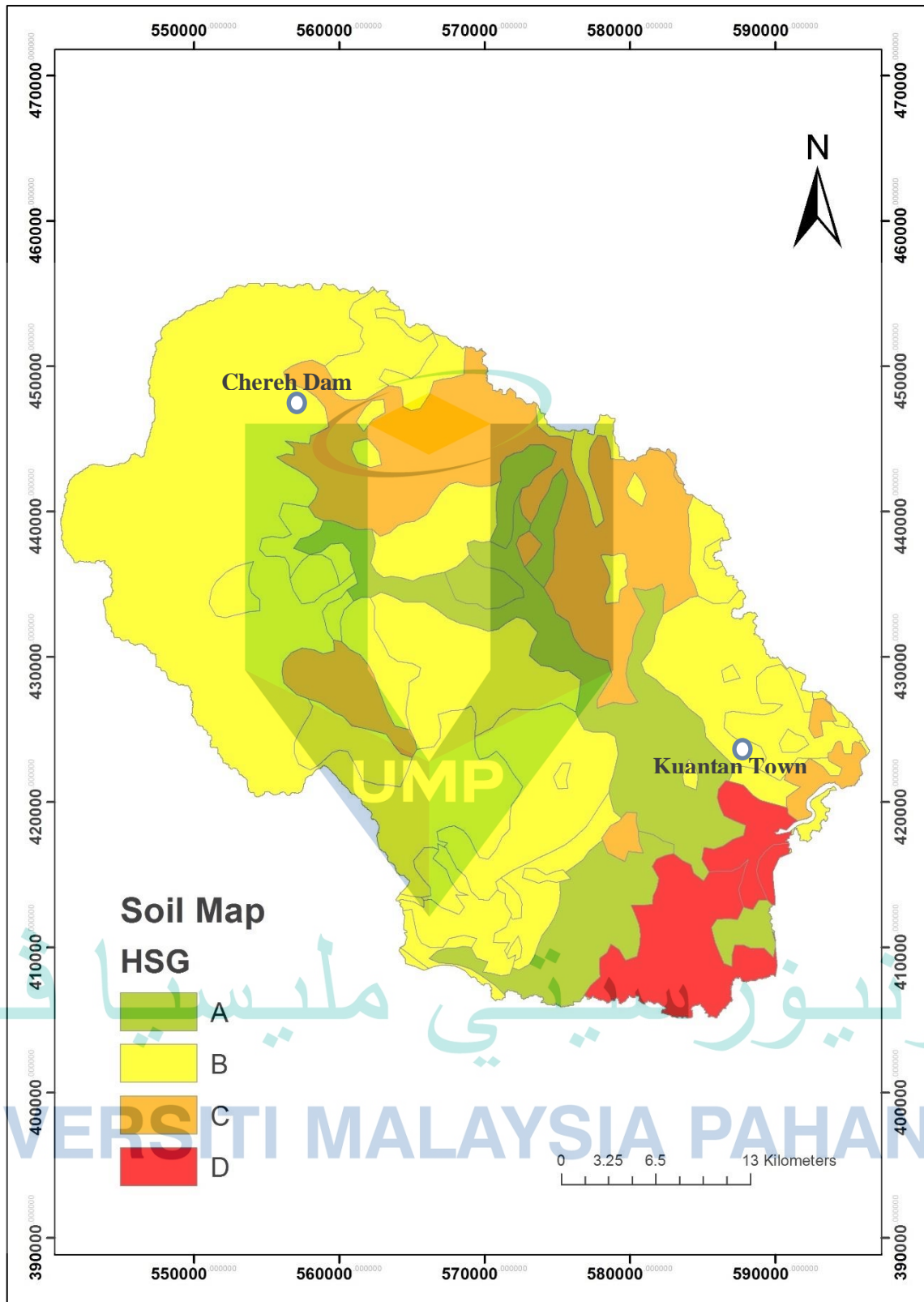


Figure 3.20 Hydrologic Soil Group (HSG) Map for KRB

3.5 Application of HEC-HMS Hydrological Modelling

In this study, the HEC-HMS version 4.1 has been chosen to perform the rainfall-runoff modelling. Rainfall-runoff modelling was carried out to estimate the flow discharge along the river in the Kuantan River Basin. HEC-HMS was used to develop rainfall-runoff models, convert excessive rainfall to channel runoff and produced flood hydrographs for the selected flood events. In the HEC-HMS modelling system, there are three main components involved namely the basin model, meteorological model and control specification.

3.5.1 Basin Model

Basin Model is the main component in HEC-HMS application. It provides the physical description of the watershed for each sub-basin and river network. In this research, the schematization of the basin model was imported from the physical and hydrologic characteristics generated through the HEC-GeoHMS in ArcGIS application which include estimated values for basin areas (km^2), CN (-), Imperviousness (%), Lag Time (mins), Baseflow (m^3/s), River Slope (m/m), Manning's n (-), Bottom Width (m), and Side Slope (-). In the Basin Model component, several methods for rainfall-runoff transformation, routing, loss, and baseflow were determined in the hydrologic parameter definition process.

For this study, the SCS unit hydrograph method was selected to estimate the discharge runoff transformed from the excess rainfalls in the form of hydrograph after considering water loss into the ground. The time of concentration representing the runoff travelling time to a junction was estimated using HEC-GeoHMS in accordance with the Natural Resources Conservation Services (NRCS) TR-55 methodology.

Hydrodynamic of river flow in the channel reach was computed using Muskingum-Cunge routing method. This routing method was applied to predict the hydrograph shape based on multiple rainfall events in different sub-catchments of the watershed. For the routing process, parameters such as channel width, side slope, Manning's n, Muskingum-Cunge shape and Kinematic Wave shape are required as the data input. Thus, river cross-section survey data is required for the parameter definition for Muskingum-Cunge routing. As the water routed along the channel, the lag time is the only parameter which affect the peak time of hydrograph in the transform method. CN

lag method was applied in this study to compute the basin lag time based on the procedures described in the NRCS National Engineering Handbook, 1972.

For the loss estimation, SCS-CN method was selected based on the land use and soil map available. Land use changes are important factors in increasing the impervious areas which subsequently increase the tendency of flooding. CN is the calibration parameter representing the land use changes in a region. It is the most sensitive parameter in the calibration process. In hydrological modelling, river base flow is one of the elements that must be considered. When there is no rainfall event, the minimum river flow is equal to the base flow. For this study, the baseflow method adopted was the monthly constant flow.

3.5.2 Meteorological Model

The Meteorological Model presents the atmospheric condition over the watershed land surface which is described by rainfall and evaporation. Specific hyetograph method was used in this study to distribute the precipitation over watershed land surface. The distribution of rainfall precipitation weight was calculated according to the nearest station for each sub-basin. No evaporation and snowmelt were considered in KRB.

There are eleven rainfall gauges considered in this study. Distribution of the rainfall precipitation was done by the Thiessen Polygon method as shown in

Figure 3.21. Thiessen Polygon method allows for areal weighting of rainfall from each gauge and it is the most widely used method to derive areal average values from point rainfall data (Satheeshkumar, Venkateswaran, & Kannan, 2017). The rainfall data selected for this study is in accordance to the flood events from 29th December 2010 to 2nd January 2011; 26th to 30th March 2011; 1st to 5th December 2013 and 16th to 19th March 2014.

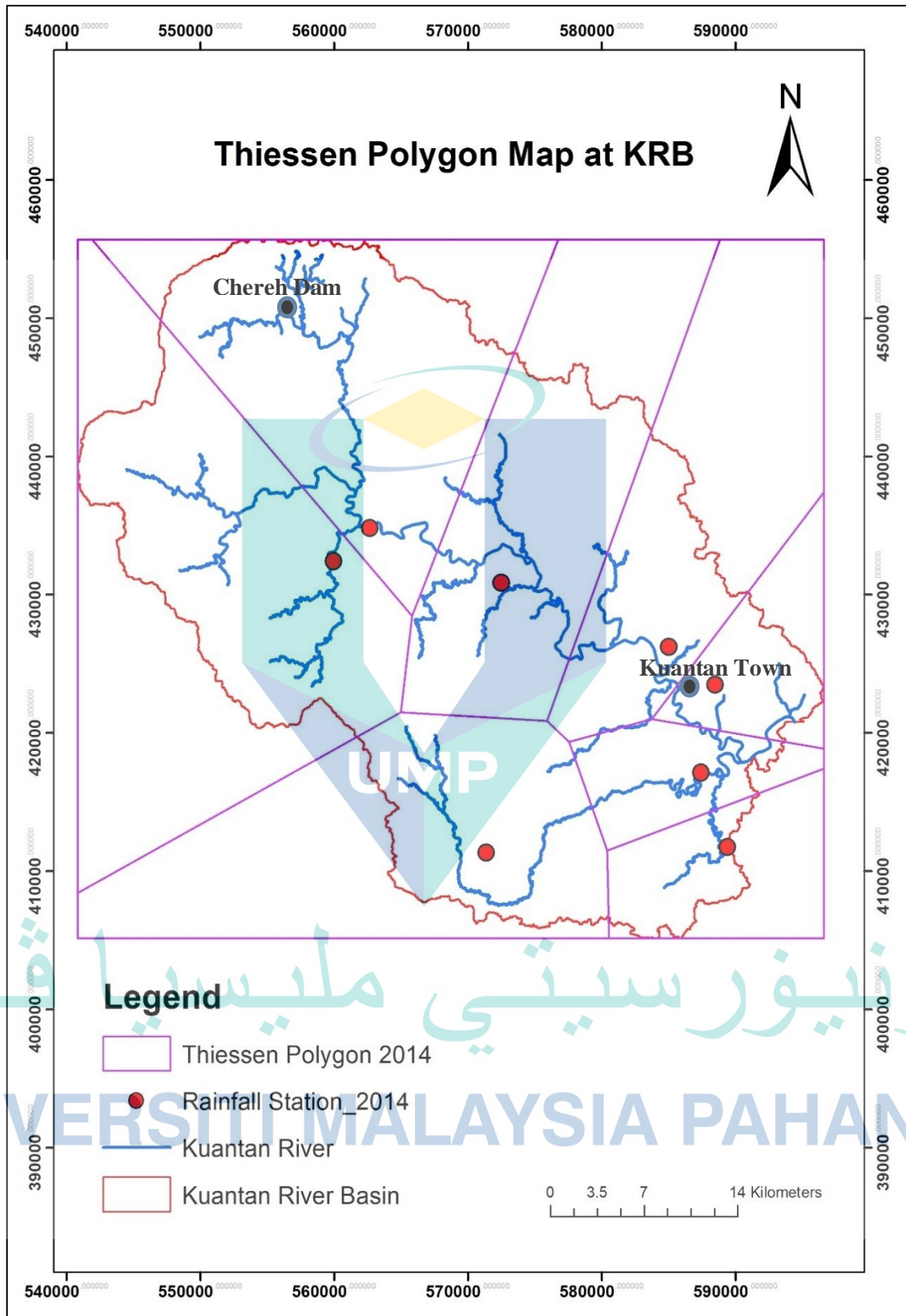


Figure 3.21 Rainfall Distribution by Thiessen Polygon Method

3.5.3 Control Specification

Control specification component was created for each flood events selected in this study. The start date, start time, end date, end time, and the time interval for the simulation period were determined in this section. It is worth noted that the date and time setup in the control specification must not exceed the rainfall time frame of the flood events provided in the meteorological model. The same condition applies streamflow simulation specified in this tool.

3.5.4 Calibration and Validation

Model calibration and validation in flood modelling is the accuracy estimation procedure to verify the validity of data input and also the acceptable data output. The simulated discharge and water level were compared to the observed data on each flood events respectively. The simulated results obtained from the hydrological model are presented in the form of hydrograph. Since in Kuantan River Basin only consist of one streamflow station namely Bukit Kenau station, the calibration and validation processes were in referenced to this station. The calibrated hydrological parameters at the Bukit Kenau station for the year 2010 and 2014 were used for validation in both year 2011 and 2013, respectively.

Physical parameters in the model such as the sub-basin area, slope, stream length, river width, side slope, and Manning's n are set as constant parameters. In the Muskingum-Cunge routing method, the river width and the channel side slope are identified from the river survey cross-sectional data. The river width and channel side slope applied in this study ranges between 50 m to 300 m, and 0.1 to 1, respectively.

3.6 Application of HEC-RAS Hydraulic Modelling

In this study, the HEC-RAS version 5.0.3 has been chosen to perform hydraulic modelling. Hydraulic modelling was carried out to simulate the water level within the river channel and the flood depth on floodplain in Kuantan River Basin. HEC-RAS was used for flood modelling to estimate the flood depth along the Kuantan River. In the HEC-RAS modelling system, there are three main data such as geometric data, boundary condition data, and flow simulation data.

3.6.1 Hydraulic Data Input

In hydraulic modelling, the river survey cross-sectional data was adopted to represent the 1D river channel model. These survey data were transferred into geometric data editor manually in HEC-RAS model. The model network projection system was standardized into RSO Kertau Malaysia coordinate system for the 1D model. Boundary condition data (initial inflow) obtained from the simulated hydrographs through the hydrological modelling were assigned at all the confluences along Sg. Kuantan in this 1D modelling. There were total of eleven (11) confluences or junctions transferring water flows into Sg. Kuantan. The boundary conditions were set at these eleven (11) junctions as Lateral Inflow Hydrographs and the outlet was set as the Stage Hydrograph boundary type.

In 2D modelling, the basic data used was the generated terrain satellite data from SRTM-DEM in floodplain modelling. The adopted grid size of the satellite image was 30m as the original grid size. For the coordinate system, the projection used was the same as in the 1D model. After the overlaying of terrain data, the lateral link to connect 1D model into 2D model (active area) was created to generate the potential floodplain area. The lateral link acts as a weir bridge to allow the overspilling water from the 1D model into 2D model and return back into the channel model.

After 1D-2D modelling, the results of 1D model were compared with the observed data recorded at the water level stations. There are total of three (3) WL stations within KRB, however only 2 stations contained complete data. As a result, these two stations namely Bukit Kenau station and Kuantan ByPass station were utilized for the calibration and validation purpose. The sensitive parameters including the manning roughness of channel and floodplain were calibrated in year 2010 to be used in year 2011 and 2013 for validation purpose. Note that for hydraulic modelling, the flood simulation for the year 2014 was not performed due to incompleteness of water level observation data.

Finally, total of three (3) flood events to generate FIMs. However, only one event on 1st to 5th December 2013 can be compared with the observed data obtained from flood report of DID Pahang. On the other hand, the other flood events will be omitted for comparison due to no flood occurrence within KRB or along Kuantan River.

3.6.2 Hydraulic Model Run

3.6.2.1 1D Steady and Unsteady Flow Simulation

The 1D steady flow was simulated to ensure good conveyance along the cross-section. At this stage, sensitive parameters such as the cross section spacing, computational time step, and Manning's n value are crucial and must be defined accordingly. If the cross sections spacing is too large, it can cause numerical diffusion and model instability. On the other hand, if the spacing is too small it can cause overestimation and instability on the rising side of the flood wave. The calculated cross section spacing for the research model at upstream is 375 m whereas spacing at downstream is 750 m using Samuels Equation (Ridolfi et al., 2014). Thus, the spacing in the model in HEC-RAS 500 m which is within the range of the calculated spacing.

Selection of the computational time step is significant to the model stability. Large time step can cause numerical diffusion (attenuation of the peak) and model instability. Conversely, small time step can lead to model instability as well as lengthen computation times. As a result, stability and accuracy can be achieved by selecting a time step that satisfies the condition that the Courant number is not more than 1 (Brunner, 2014). The calculated time step used in this HEC-RAS modelling was 50 second.

Manning's n value is another parameter affecting the accuracy of the model. If the values are too low, they can cause drop in water level, rise in velocities, and create supercritical flows especially in steep streams. Oppositely, higher Manning's n values increase water level and induce hydrograph attenuation as the water flows downstream (Brunner, 2014). Roughness values for floodplains are different from values for channels. Therefore, the Manning's roughness for this research was determined according to the default value in HEC RAS manual (USAC, 2010).

After the pre-defined hydraulic parameters have been setup, the 1D steady flow simulation was performed to monitor the conveyance of the model. Initial boundary condition and minimum flow at every junction was defined prior to the simulation run. If errors occurred during the simulation process, the hydraulic parameters were adjusted by trial and error until a stable model was obtained. The adjusted hydraulic parameters in the steady flow process were then applied in the unsteady flow simulation. Water level

results simulated for the unsteady flow were compared with the observed water levels near the downstream region at the (Kuantan Bypass station).

In the 1D unsteady flow simulation, the Manning's roughness of channel and floodplain were calibrated to fit the simulated curve against the observed. Different flood events were tested using the calibrated roughness values validated the correctness of the model simulation setup and calibrated parameters. The model accuracy was further confirmed by statistical error analysis such as Nash–Sutcliffe model efficiency coefficient (NSE) and Root Mean Square Error (RMSE).

3.6.2.2 1D-2D Modelling Execution

Following the 1D modelling, excess or overtopping flow from the river was analyzed in 2D modelling showing spatial flow extension. In the 2D modelling, basin terrain information is the most crucial because the flood inundation areas can only be generated with the combination of the water surface elevation from HEC-RAS and the terrain elevation from DEM. Figure 3.22 shows the elevation variation generated for KRB using the 30-m spatial resolution of Shuttle Radar Topography Mission (SRTM) DEM. From the terrain map, it is noted that the vertical resolution of DEM is too coarse to analyse the flood inundation areas. Therefore, detailed surveying at the floodplain areas along the channel are required to achieved reliable forecasts of the flood inundation extends.

The minimum elevation detected from the DEM of KRB shows a zero value whereas the elevation of the observed cross-sectional data collected from DID Malaysia contains value of below zero at many locations at downstream region. This means that the terrain generated by the DEM did not represent the elevations well within the channel. Thus, 1D model with updated river cross sections were linked into 2D modelling for better accuracy result.

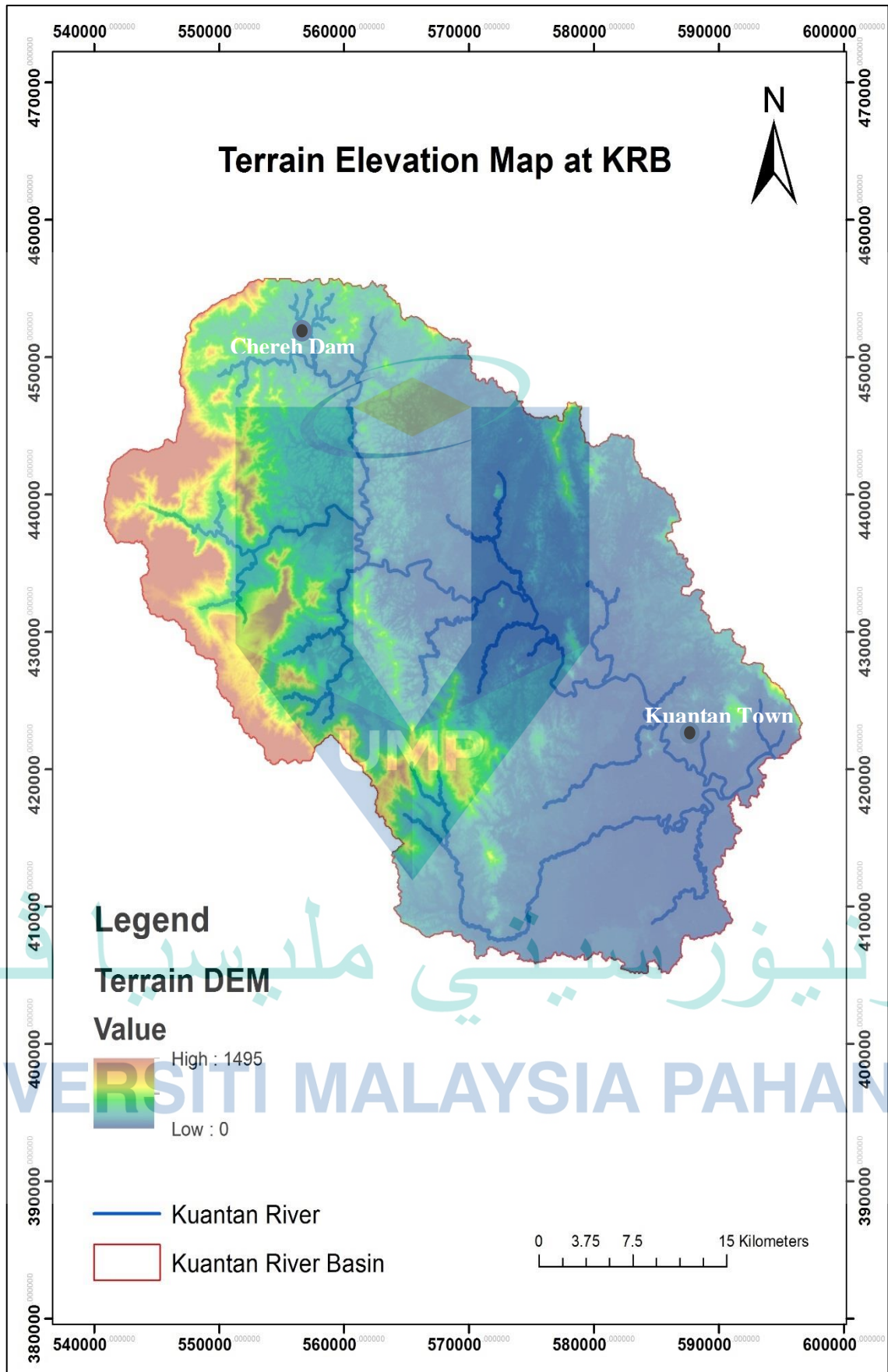


Figure 3.22 Terrain created based on the SRTM DEM for KRB

For the linkage between 1D-2D modelling, HEC RAS 5.0.3 was used to the linkage between 1D-2D model where an active boundary was defined within the terrain data to be linked with the 1D model. The lateral links were created by importing both left and right bank line to represent the weir bridge to allow over-spilling water from 1D model flows into 2D model and return into 1D model. This simulation was conducted follow the three event dates in year 2010, 2011, and 2013 to generate the FIM where the flood extent and flood depth will be justified with available observed data.

3.6.3 Flood Inundation Map Based on Historical Flood Events

The results of FIM were presented in term of the flood area and flood depth. According to flood map collected from DID, there are 3 classes of flood depth to differentiate the flood categories which are a) less than 0.5 m; b) 0.5 m to 1.2 m; and c) more than 1.2 m. In HEC-RAS, RAS Mapper is a platform to view and animate the flood data results in term of flood depth, flood velocity and flood route. Justification of the simulated FIM was done by comparing with the observed flood data obtained from the historical flood report provided by DID for the year 2013. The flood extent areas (km²) were discussed as well as the flood depth in term meter (m) height. Fitting of the flood extent against the observed information has been conducted by calibrating the Manning's n roughness of the floodplain based on landuse type. However, the Manning's roughness was not calibrated this study, and default value of 0.06 was adopted to indicate the floodplain area filled with light brush and trees, cleared land with tree stumps with a heavy growth of sprouts.

3.7 Flood Inundation Map Based on Landuse Changes Impact

Based on the landuse maps for year 2010 and 2013, different types of land cover were assessed to observe the significant changes on landuse within these 3 years duration. Table 3.3 shows the landuse changes from year 2010 to year 2013. From the examination of the five landuse classes, it was found that the water (53.8%) and built up area (35.6%) have increased the most over the three years period. The built up areas mainly focused at downstream of KRB.

Urbanization increased the runoff volume in the basin due to the increment in the imperviousness of the land surfaces. Urban area consists of buildings and roads which fully covered with concrete or tar materials. These types of material reduce the infiltration

rate of the rainfall and the storage capacity of the existing drains causing the water fully occupied and over-spilled causes flash flood. The urban area also caused the water to flow faster due the reduction in the land surface resistance. As a result, the peak discharge eventually increased in urban area.

To compare the FIM based on the landuse for year 2010 and 2013, two sets of discharge output were simulated in for the selected flood event in the year 2013. The simulations were carried out with varies landuse imperviousness while maintaining the other hydrological parameters. The flood event in year 2013 was selected because it was the only result which can be justified with the observed data obtained from DID Pahang. The flood area (km²) and flood depth (m) were compared and discussed in detail between both generated FIM for 2010 landuse and 2013 landuse condition.

Table 3.3 The Landuse changes between year 2010 and 2013

Landuse Type	Year 2010 (km ²)	Year 2013 (km ²)	Differences (%)
Agriculture	466.18	475.96	2.1
Bare Soil	73.35	57.05	-22.2
Buildup	96.17	130.4	35.6
Forest	973.11	933.99	-4.0
Water	21.19	32.60	53.8

3.8 Model Performance Evaluation

The accuracy of the hydrological and hydraulic models in this study was evaluated by statistical error analysis. This evaluation is important to measure the level of accuracy of the models. There are many different model efficiency methods available presented in (Ibarra et al., 2016; Pachepsky, Martinez, Pan, Wagener, & Nicholson, 2016; Sulaiman, El-Shafie, Karim, & Basri, 2011). In this study, the evaluation was done by adopting the Nash-Sutcliffe Efficiency (NSE) and Root Mean Square Error (RMSE).

The Nash–Sutcliffe Efficiency (NSE) is frequently applied in hydrologic and hydraulic simulation to assess the model performance. The NSE is a standard statistical which determines the relative magnitude of the residual variance compared to the variation of the measured data as shown in Equation 3.1:

$$NSE = 1 - \frac{\sum_{i=1}^n (O_i - P_i)^2}{\sum_{i=1}^n (O_i - \bar{O})^2} \quad 3.1$$

where O_i is the i th ordinate of the observed discharge or stage-hydrograph; P_i is the i th ordinate of the estimated discharge or stage-hydrograph; \bar{O} is the mean of the observed discharge or stage-hydrograph ordinates; and n is the total number of discharge or stage-hydrograph ordinates to be simulated. The range of NSE lies between 1.0 (perfect fit) and $-\infty$. In general, model simulation can be justified as satisfactory if $NSE > 0.50$ (Zarrineh, Griensven, Sennikovs, Bekere, & Plunge, 2015). It indicates how well the plot of the observed value versus the simulated value fits a 1:1 line and ranges from $-\infty$ to 1, where higher values indicating better agreement.

The Root Mean Square Error (RMSE) also used in model accuracy assessment that computed as shown in Equation 3.2:

$$RMSE = \sqrt{\frac{\sum_{i=1}^n (O_i - P_i)^2}{n}} \quad 3.2$$

There are many research studies on flood modelling which applied RMSE as the statistic error measurement. The model is considered as high in accuracy if the RMSE is near to zero (El-Shafie, Jaafer, & Seyed, 2011; Ng, Gisen, & Akbari, 2018).

اونيور سيئي ملايسيا فهغ

UNIVERSITI MALAYSIA PAHANG

CHAPTER 4

RESULTS AND DISCUSSION

4.1 Introduction

The river basin and river network in the Kuantan River Basin have been successfully delineated through ArcGIS version 10.4 application integrated with the HEC-GeoHMS extension. Both the physical and hydrologic characteristics generated from the GIS application were utilized in the HEC-HMS model. Calibrated and validated processes were performed and analyzed accordingly in hydrological modelling. The calibrated hydrological parameters such as CN (-) and lag time (min) for the year 2010 and 2014 were adopted to validate the model results of the year 2011 and 2013 respectively. The simulated results of the hydrological modelling were presented in the form of streamflow hydrographs in each selected flood events which were utilized as input in the HEC-RAS hydraulic model. Vertical water level variations have been calibrated and validated in the 1D-2D model where the simulated water level was compared to observed data as well as the flood extent was generated for the flood event considered in this study. The results of Flood Inundation Map for the Kuantan River Basin such as the flood area and flood depth was justified with available flood data. Only the result in year 2013 can be compared to the observed data where the observed flood data was obtained from DID Pahang. Lastly, two flood inundation maps in flood event year 2013 were generated based on two different sets of boundary conditions adopted with varies landuse type to discuss on landuse impact towards flood result. This chapter presents the findings obtained in this research in reference to the study objectives.

4.2 Watershed and River Network Delineation

Based on the elevation data and stream generation processes, the watershed and sub-basins of the Kuantan River Basin were successfully delineated using HEC-GeoHMS extension in ArcGIS application. There was a total of seventy-three (73) sub-basins and river networks including the mainstream and tributaries extracted from the SRTM-DEM. Physical characteristics of the entire catchment, sub-basins and river networks were also extracted and compiled accordingly in pre-processing stage by ArcGIS 10.4 as shown Figure 4.1 to Figure 4.5.

DEM reconditioning and fill sink processes have been performed using ArcGIS and HECGeoHMS extension tools to refine the raw SRTM-DEM into an enhanced and accurate DEM for the further hydrological preprocessing. Reconditioning was done by overlaying the digitized river network to the DEM to ensure the coordinate position are well-aligned. Fill sink on the other hand was used to fill any possible empty cells in the DEM. From the reconditioning and fill sink results as display in Figure 4.1 and Figure 4.2 respectively. The overall enhanced elevation data within Kuantan River Basin was found to ranges from 0 m (low-laying flat downstream region) to 1495 m (mountainous upstream region).

4.2.1 Delineation of Kuantan River Network

Flow direction (Figure 4.3) defined the direction of the steepest descent of each terrain cell in total eight (8) classes: east (1), southeast (2), south (4), southwest (8), west (16), northwest (32), north (64), and northeast (128). It is used to determine the number of upstream cells draining to specified cell in flow accumulation process (Figure 4.4) and then the stream network generation within Kuantan River Basin. Figure 4.5 indicates a total of 73 numbers of both delineated rivers networks and river sub-basins. The delineated river was overlaid with the actual river network for comparison. Almost 80% of the river was matched satisfactorily, while a few stretches of river such as Sungai Belat and those at the downstream region were altered to improve the river alignment. The factor affecting the misalignment in river network generated might be due to urbanization and river sedimentation issues.

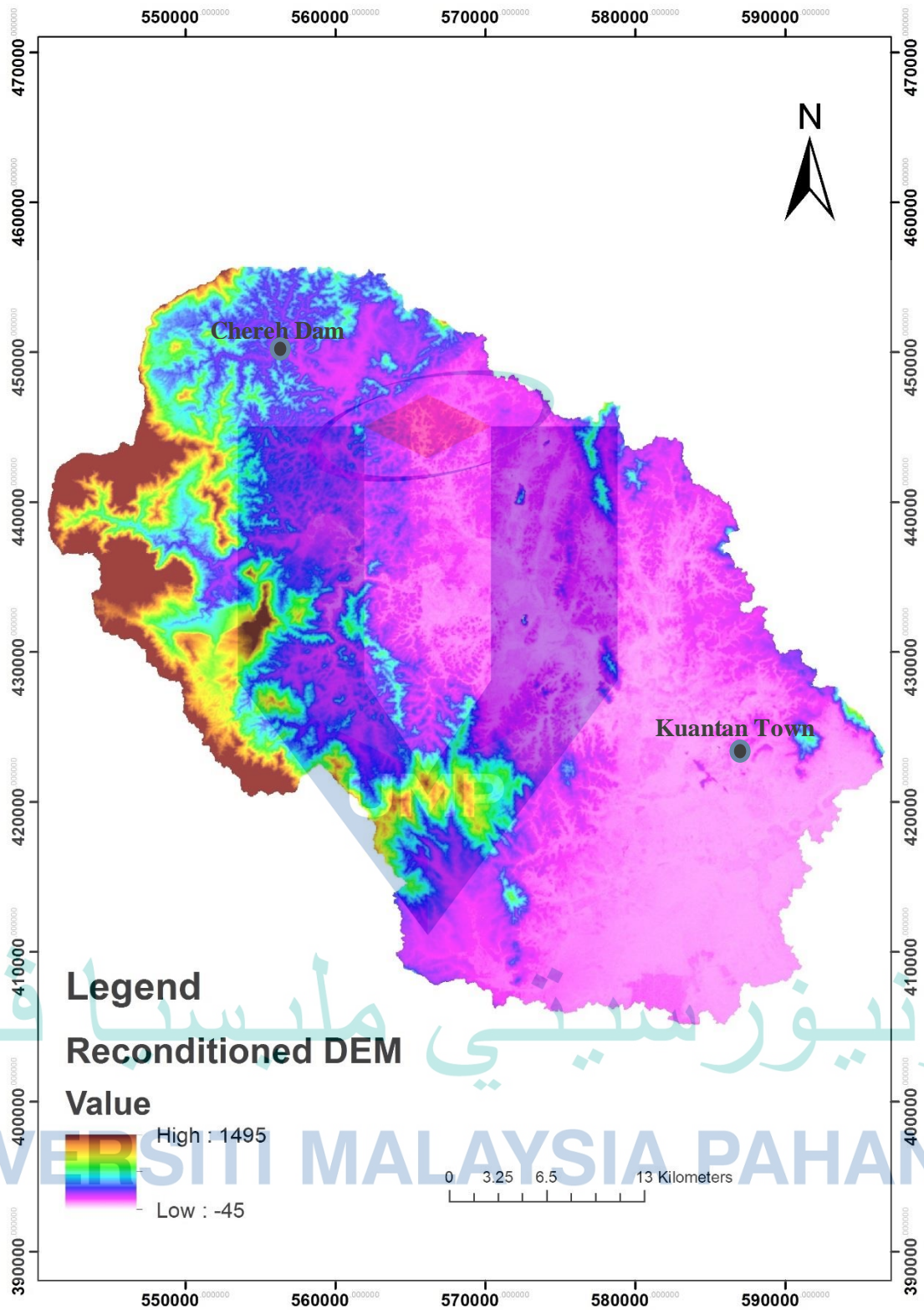


Figure 4.1 Reconditioned DEM for KRB

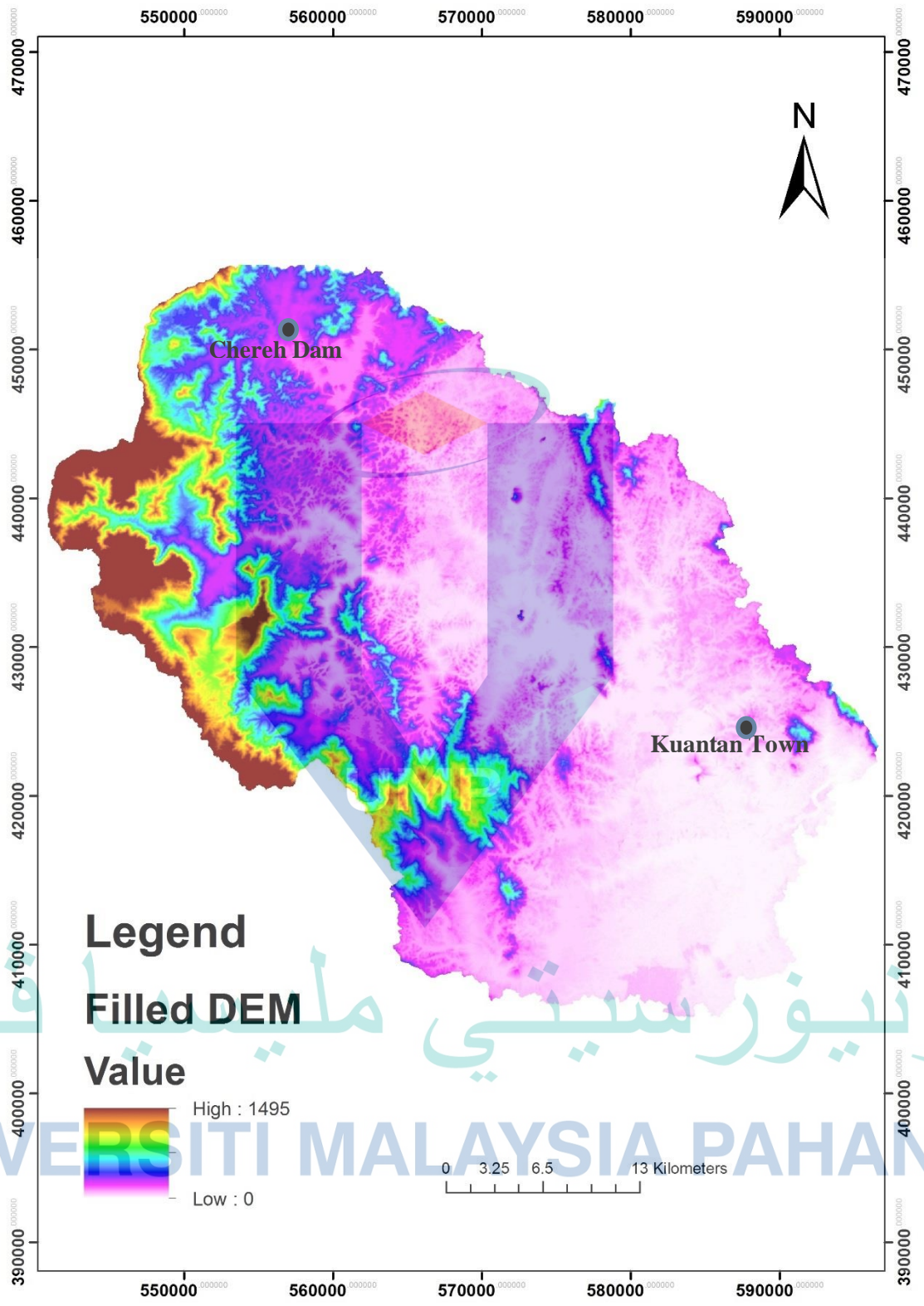


Figure 4.2 Filled DEM for KRB

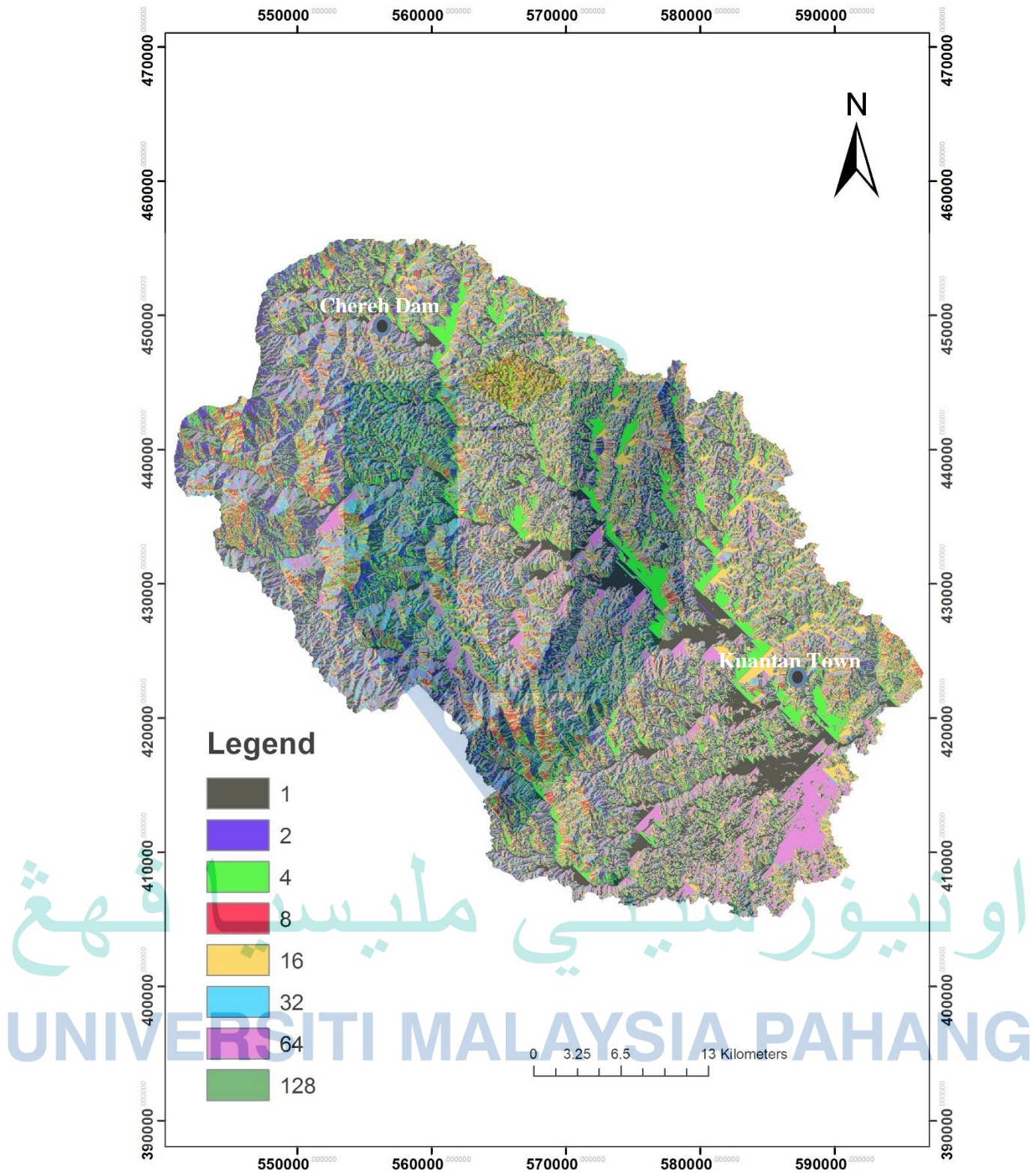


Figure 4.3 Flow Direction DEM for KRB

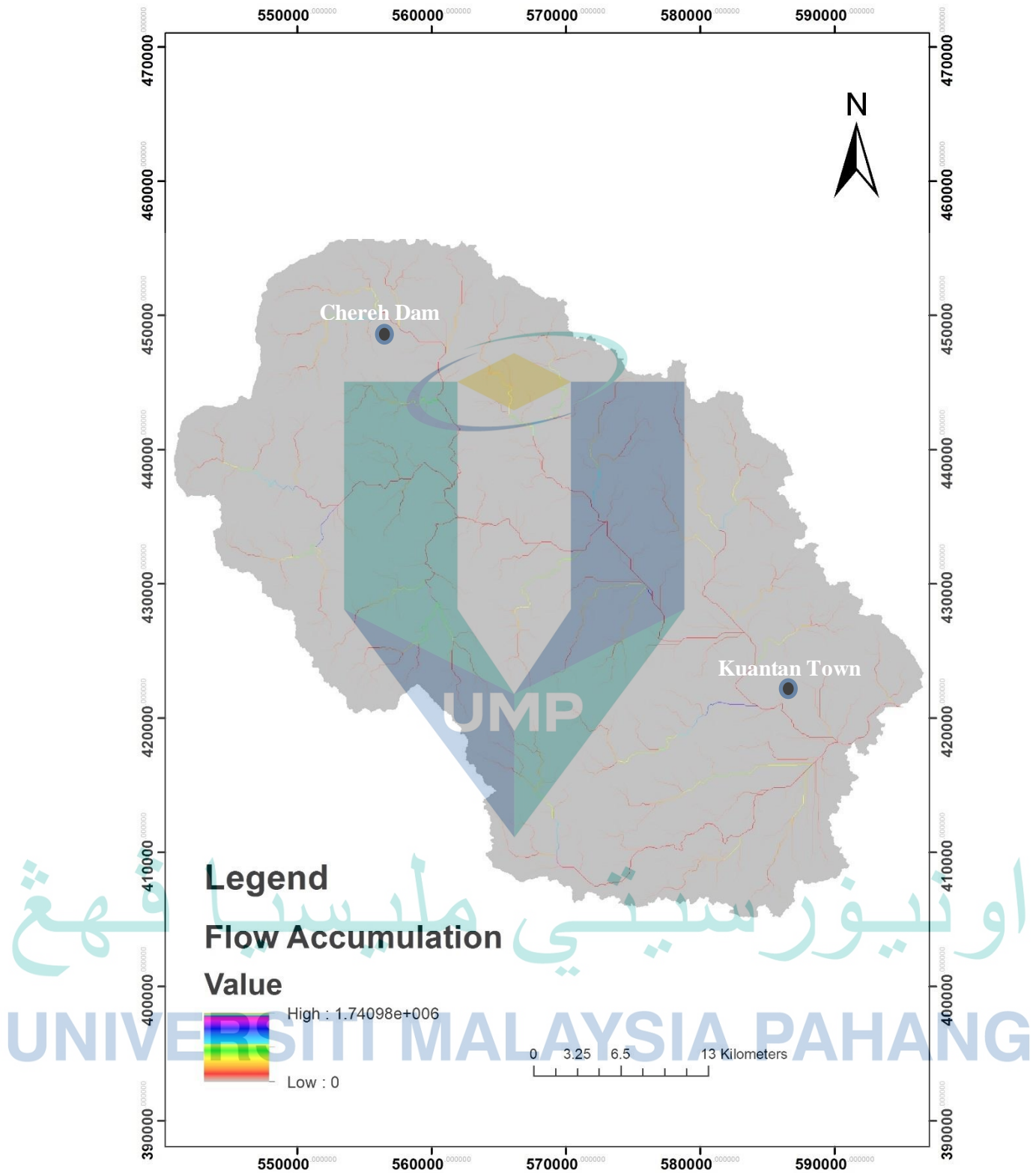


Figure 4.4 Flow Accumulation DEM for KRB

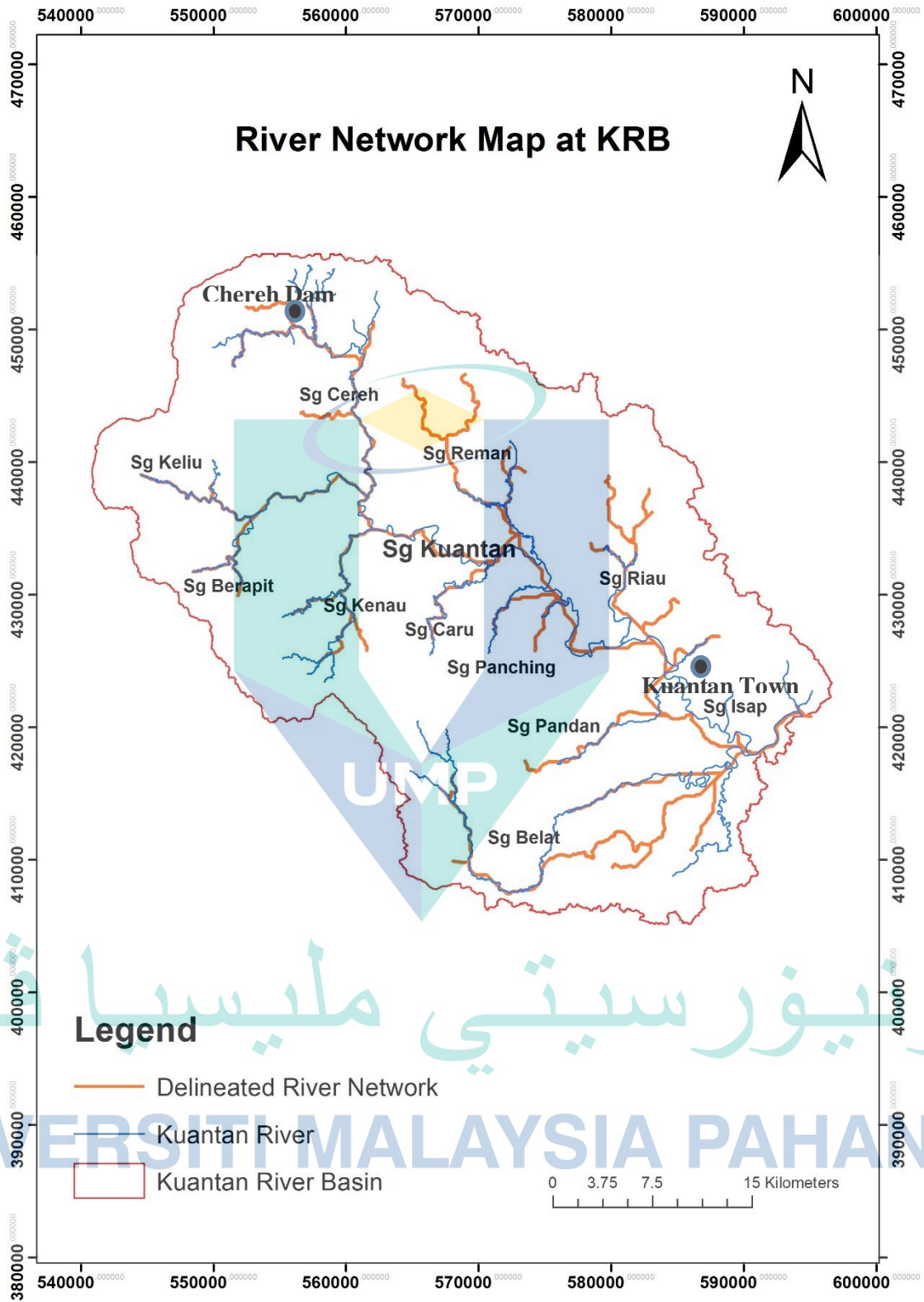


Figure 4.5 Delineated river network in the Kuantan River Basin

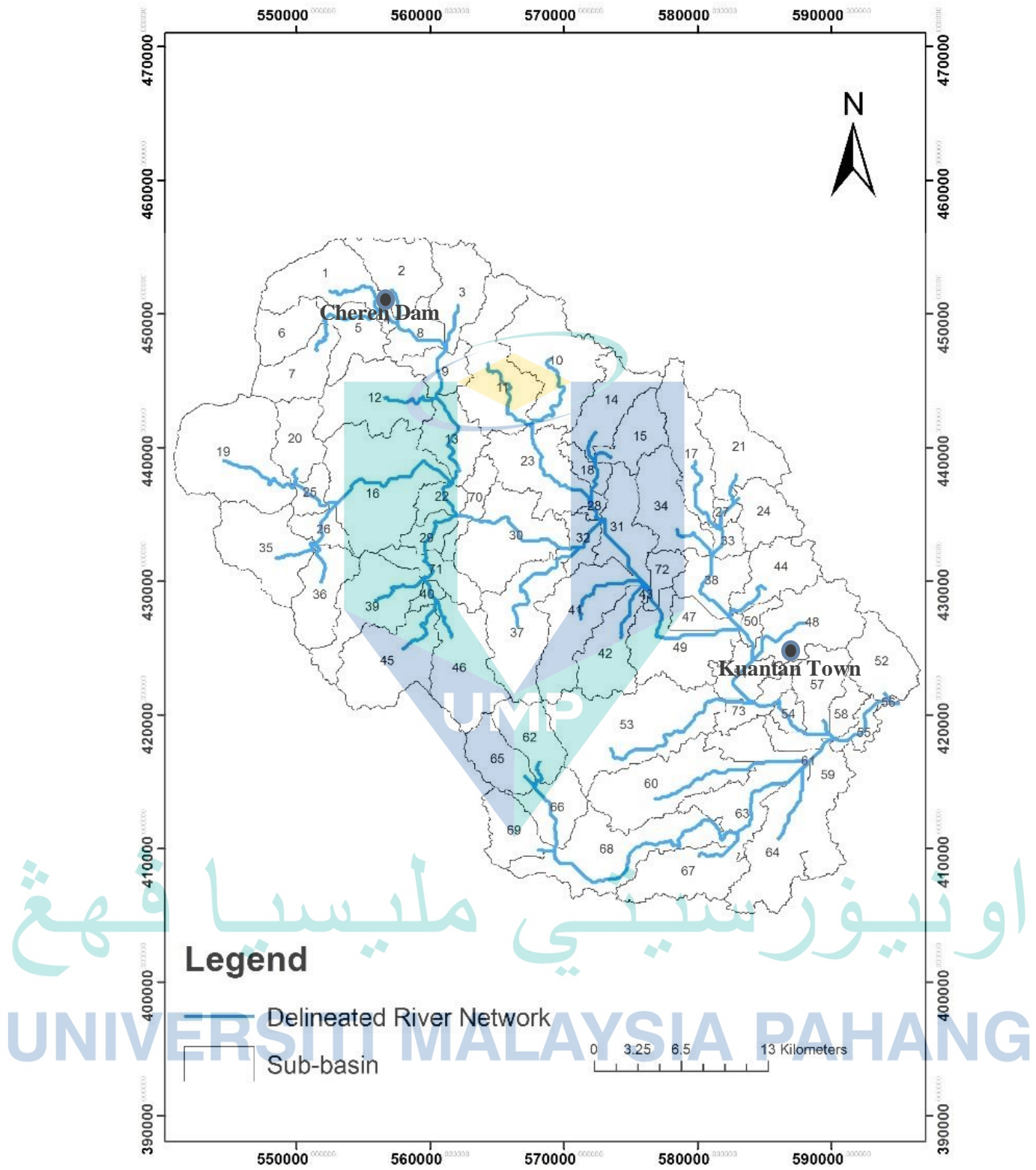
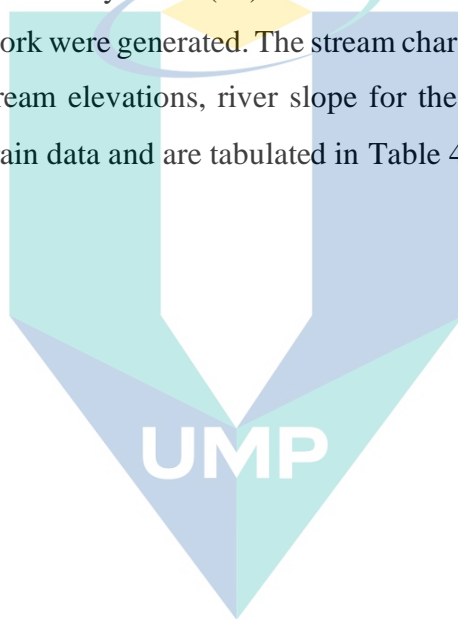


Figure 4.6 Delineated sub-basins and river network

4.2.1 Generation of Kuantan River Basin

Watershed of the Kuantan River Basin delineated from the 30 m resolution DEM covered a total area of 1652 km² as shown in Figure 4.6 slightly larger compared to Zaidi et al. (2014) who reported the catchment area of 1630 km². This difference might be due to the different year of DEM information and also the future development occurred within KRB. On the other hand, the delineated total perimeter of Kuantan River Basin was found to be 302 km. The physical characteristics such as basin area, basin slope, and the upper and lower boundary of each sub-basin in the watershed are presented in Table 4.1. From the analysis, a total of seventy-three (73) sub-basins were delineated along with (73) reaches in stream network were generated. The stream characteristics such as river length, upstream and downstream elevations, river slope for the river in each sub-basin were extracted from the terrain data and are tabulated in Table 4.2.



اونيورسيتي ملايسيا قهغ

UNIVERSITI MALAYSIA PAHANG

Table 4.1 The characteristics of the main basin and sub-basins as stated above in the paragraph

Basin No.	Basin ID	Basin Slope	Basin Perimeter (km)	Basin Area (km ²)
1	W700	28.20	36.53	30.12
2	W710	18.13	33.27	25.30
3	W720	18.39	34.07	23.98
4	W730	9.98	8.99	2.24
5	W740	26.83	32.84	18.24
6	W750	28.66	24.58	16.78
7	W760	32.97	29.33	20.75
8	W770	16.45	22.86	12.83
9	W780	19.67	27.17	13.12
10	W790	10.65	56.80	47.48
11	W800	17.99	57.30	43.86
12	W810	26.36	46.02	37.41
13	W820	15.28	29.88	20.45
14	W830	10.35	42.45	24.11
15	W840	13.40	30.43	17.57
16	W850	26.35	53.85	61.18
17	W860	17.65	43.37	28.35
18	W870	5.56	22.12	7.12
19	W880	46.97	43.68	56.99
20	W890	29.49	27.35	18.77
21	W900	11.88	40.66	30.90
22	W910	14.24	17.68	8.34
23	W920	7.37	46.33	33.34
24	W930	10.89	28.83	17.84
25	W940	31.19	18.36	7.69
26	W950	22.38	21.44	8.99
27	W960	7.62	10.78	3.42
28	W970	3.24	11.58	2.50
29	W1450	24.01	17.37	8.13
30	W1400	11.97	46.76	41.59
31	W1000	7.57	40.42	23.57
32	W1010	3.69	26.18	9.04
33	W1020	5.92	16.51	5.80
34	W1030	9.37	38.32	27.56
35	W1040	24.58	39.06	36.16
36	W1050	21.64	32.71	24.33
37	W1060	20.60	51.81	41.39
38	W1070	6.27	29.88	19.15
39	W1080	28.60	46.33	33.31
40	W1090	16.46	12.20	3.42
41	W1100	12.79	48.86	38.90
42	W1110	14.43	37.33	25.18
43	W1120	6.63	4.74	0.49
44	W1130	7.35	36.23	21.91
45	W1140	28.85	43.56	39.45
46	W1150	23.82	41.34	37.19
47	W1160	8.04	19.28	9.00
48	W1170	8.76	42.45	35.04
49	W1500	6.79	48.73	34.08

50	W1190	4.36	18.61	5.18
51	W1200	3.88	30.19	14.14
52	W1210	13.62	29.88	23.28
53	W1220	13.50	67.09	66.33
54	W1550	2.06	18.98	5.90
55	W1240	3.99	25.81	6.98
56	W1250	2.50	6.41	0.62
57	W1260	7.35	28.59	19.33
58	W1270	3.12	37.03	13.86
59	W1280	1.81	67.65	36.58
60	W1290	5.13	62.59	44.09
61	W1300	0.81	0.12	0.00
62	W1310	23.77	27.35	20.27
63	W1320	1.56	47.13	24.39
64	W1330	2.17	48.86	37.32
65	W1340	23.74	24.95	17.97
66	W1350	8.74	28.83	18.37
67	W1360	2.60	43.87	29.94
68	W1370	5.70	70.23	50.82
69	W1380	12.15	28.03	18.15
70	W1410	21.75	29.14	10.90
71	W1460	31.51	30.00	14.33
72	W1510	8.01	18.79	7.92
73	W1560	3.86	30.50	11.03

UMP

اونيورسيتي ملايسيا قهق

UNIVERSITI MALAYSIA PAHANG

Table 4.2 The Characteristics of the River Network for KRB

River No.	River ID	River Slope	River Length (km)	Longest Flow Path (km)	Centroidal Longest Flow Path (km)
1	R10	0.0069	6.19	7.18	12.95
2	R50	0.0055	3.08	5.04	9.88
3	R80	0.0177	3.97	5.19	12.52
4	R40	0.0139	1.95	0.96	2.43
5	R20	0.0050	5.00	4.42	9.67
6	R30	0.0064	0.31	3.57	7.62
7	R60	0.0083	3.51	6.26	11.20
8	R70	0.0141	4.80	3.20	6.41
9	R90	0.0027	4.14	2.48	6.50
10	R120	0.0010	9.03	8.95	18.05
11	R110	0.0030	8.65	7.16	17.86
12	R100	0.0038	5.31	5.83	14.45
13	R160	0.0017	8.64	4.83	9.69
14	R130	0.0021	2.81	5.60	12.42
15	R140	0.0061	1.98	4.74	9.35
16	R180	0.0056	11.61	7.52	16.84
17	R260	0.0036	6.74	8.21	15.93
18	R230	0.0003	3.81	3.97	7.77
19	R170	0.0178	7.87	7.22	15.12
20	R150	0.0260	1.73	4.25	8.71
21	R190	0.0069	2.51	4.72	10.99
22	R240	0.0009	3.21	1.99	5.04
23	R220	0.0007	8.51	5.64	12.18
24	R200	0.0053	0.63	3.11	7.01
25	R210	0.0033	4.25	2.64	6.39
26	R280	0.0073	3.98	2.25	5.57
27	R270	0.0023	2.66	1.77	4.02
28	R250	0.0018	1.68	1.45	3.12
29	R370	0.0025	7.13	5.21	12.59
30	R290	0.0007	3.06	2.37	5.63
31	R320	0.0056	2.79	1.50	4.26
32	R310	0.0012	4.22	6.10	11.73
33	R330	0.0256	4.25	5.33	13.52
34	R350	0.0499	3.87	4.82	10.73
35	R430	0.0036	10.71	10.67	17.71
36	R400	0.0003	6.21	4.66	8.94
37	R390	0.0072	5.13	5.71	14.41
38	R380	0.0391	2.03	1.51	3.65
39	R420	0.0012	7.42	7.73	15.85
40	R460	0.0012	4.87	6.19	11.15
41	R360	0.0248	0.83	0.18	1.13
42	R410	0.0030	4.71	6.50	10.83
43	R480	0.0096	6.05	7.46	14.98
44	R450	0.0072	3.59	6.55	11.96
45	R440	0.0272	1.32	3.35	7.24
46	R500	0.0008	6.27	6.42	12.34
47	R490	0.0019	2.68	3.55	7.15
48	R520	0.0045	4.59	3.40	7.13
49	R510	0.0262	0.81	3.71	8.52

50	R580	0.0023	14.95	16.72	23.83
51	R570	0.0010	6.27	3.53	6.96
52	R530	0.0085	0.83	0.92	2.23
53	R550	0.0268	1.33	4.23	9.55
54	R560	0.0013	0.52	0.21	7.54
55	R600	0.0012	2.72	1.71	12.89
56	R630	0.0012	13.14	11.54	20.43
57	R590	0.0020	0.03	0.02	0.02
58	R620	0.0057	2.82	5.27	10.47
59	R640	0.0003	8.96	6.91	13.46
60	R650	0.0019	6.90	7.69	14.97
61	R610	0.0530	1.39	4.59	8.57
62	R670	0.0023	5.69	3.63	8.53
63	R680	0.0005	4.44	6.98	13.30
64	R690	0.0012	20.63	12.19	24.40
65	R660	0.0071	1.41	5.22	9.79
66	R300	0.0008	9.70	5.17	14.19
67	R1420	0.0052	1.34	1.23	6.51
68	R340	0.0588	4.59	3.07	6.10
69	R1470	0.0054	3.14	2.46	7.63
70	R470	0.0001	9.08	6.56	11.57
71	R1520	0.0143	1.35	2.77	6.77
72	R540	0.0004	5.43	3.93	6.82
73	R1570	0.0011	2.14	1.55	6.29

4.2.2 Generating Curve Number

The range of the adjusted curve number after calibration was identified from 18 to 100 as shown in Figure 4.7 and Figure 4.8 in the year 2010 and 2013 respectively. Higher curve number indicates the lower ability for water abstraction to soil and vice versa. Based on both adjusted CN maps, higher runoff was found to occur in densely developed areas. This is because in buildup region, the land covers are mainly paved roads and concretes where almost no infiltration allowed. The CN obtained for the downstream region ranges from 70 to 100. On the other hand, the low runoff potential and high infiltration rates with lower CN values were distributed at the floodplain surroundings the rivers (green patches with CN number from 18 to 30). This adjustment was made through the conversion from $CN_{0.2}$ to $CN_{0.05}$ which is capable to provide a reasonable indication for flood runoff simulation in tropical region such as KRB refer in Section 2.6.2.3. The weighted CN values for each sub-basin were being used for hydrological modelling.

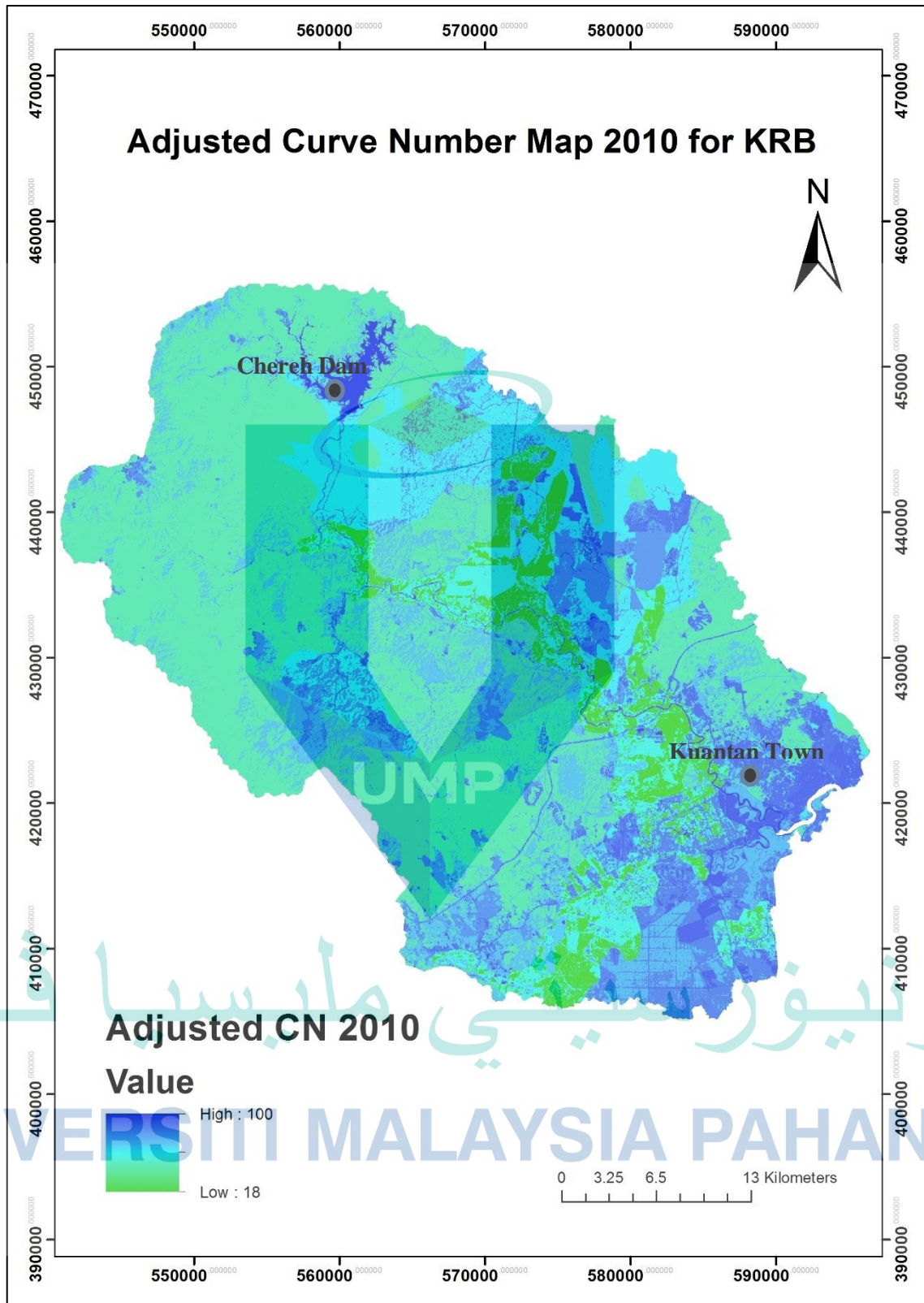


Figure 4.7 The adjusted curve number map of the year 2010 at KRB

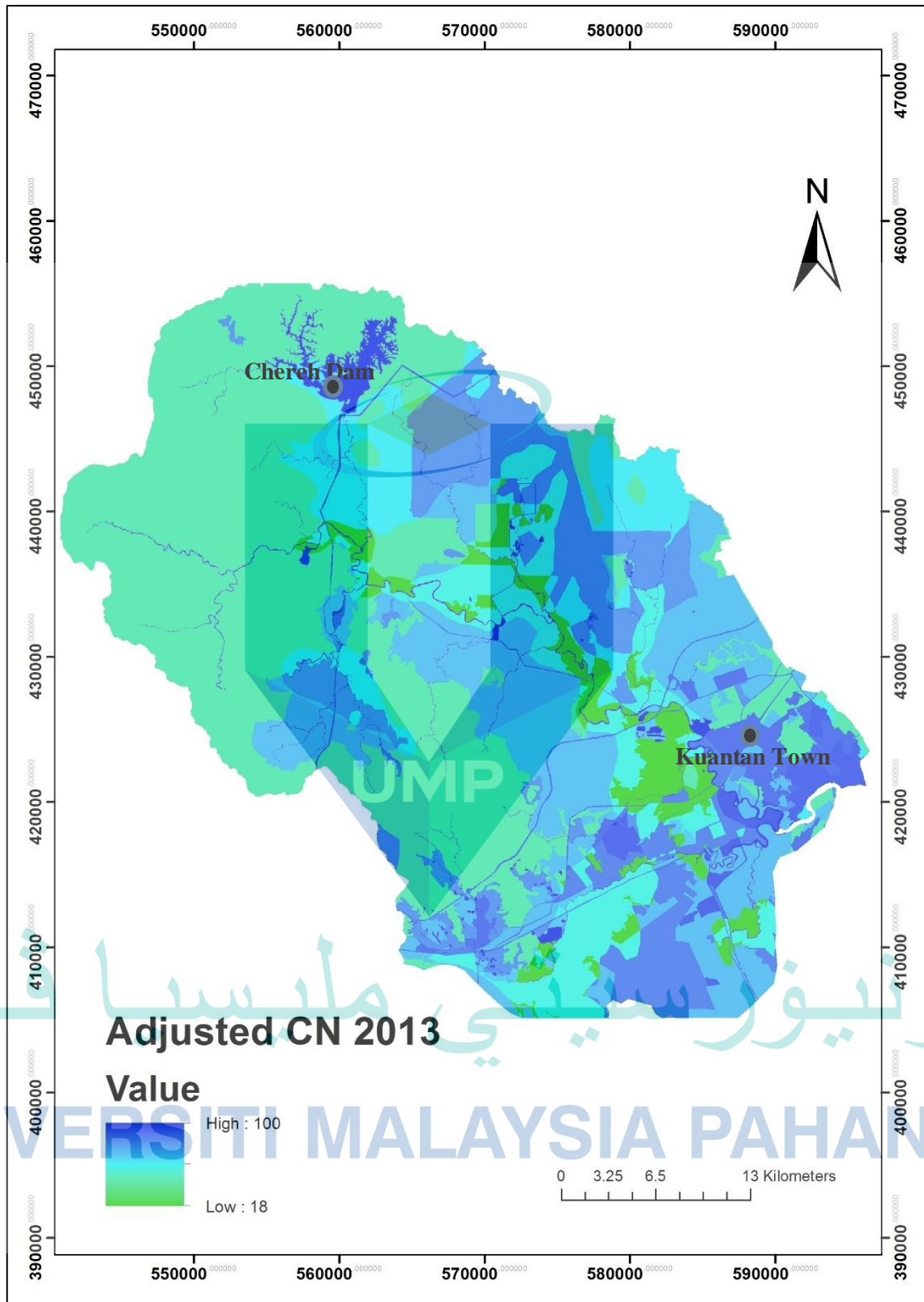


Figure 4.8 The adjusted curve number map of the year 2013 at KRB

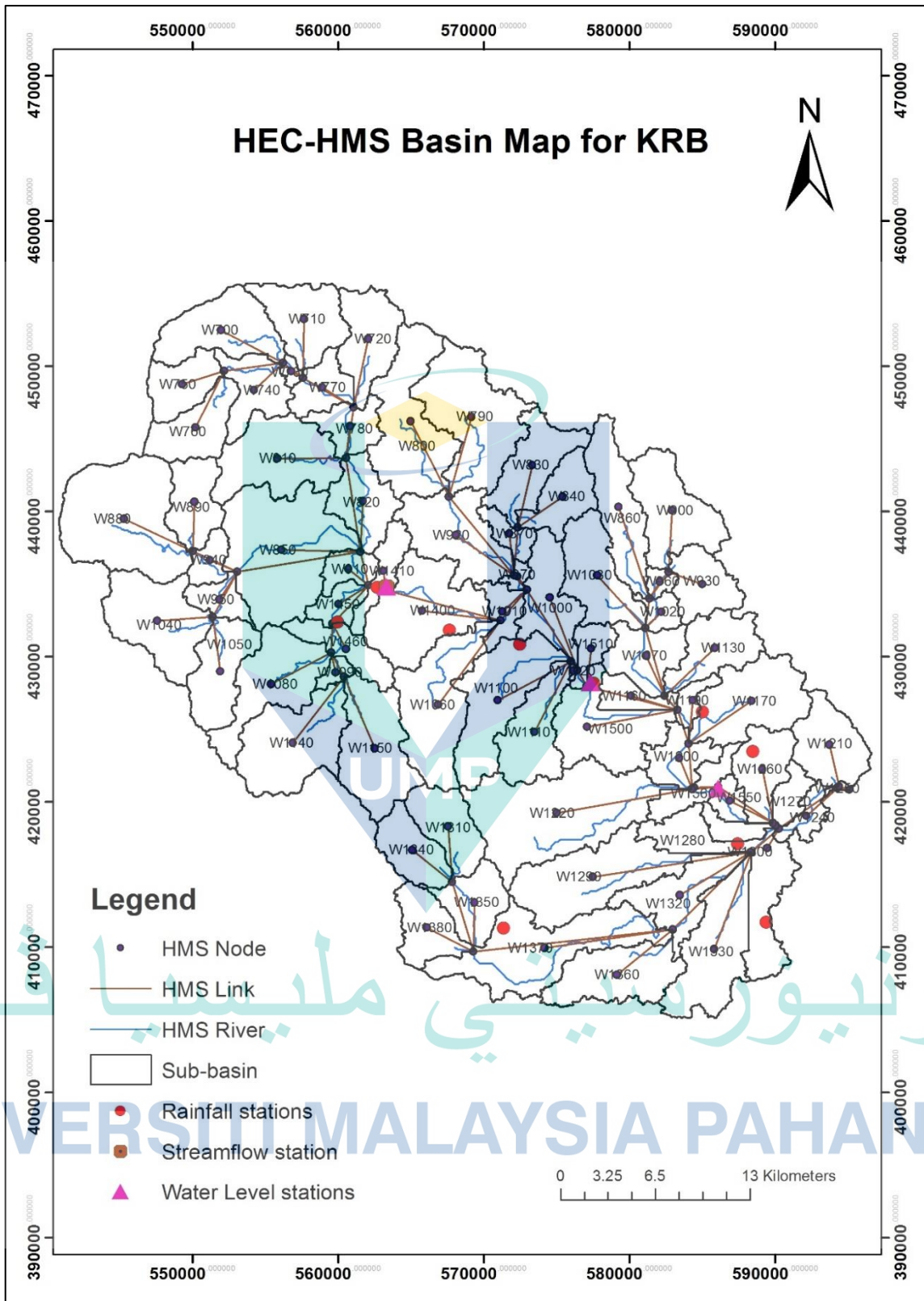


Figure 4.9 Basin Model Component in HECHMS

4.2.3 Generating Basin Model Components for Hydrologic Modelling

The estimated physical hydrologic parameters, the curve number map, and the rain distribution pattern by Thiessen Polygon have been used in model schematization and generation of HEC-HMS file. The basin schematics, legend, coordinates, background map, and both the physical and hydrologic parameters were compiled and exported to the HEC-HMS for rainfall runoff modelling as shown in Figure 4.9. The HMS nodes represented the hydrological basins information of each sub-catchment whereas HMS links indicated the river details of HMS river in KRB.

4.3 HEC-HMS Rainfall-Runoff Modelling

In HEC-GeoHMS, the background basin map and HEC-HMS basin model components were generated. The information and results produced in GIS were imported into HEC-HMS model. Meteorological data namely the analyzed rainfall and streamflow data were also imported into the HEC-HMS model as part of the input for rainfall-runoff modelling.

4.3.1 HEC-HMS Model Simulation

The physically measurable parameters for example sub-basin area, river slope, river length, river width, river side slope, and Manning's roughness were assigned as the constant parameters. Meanwhile, the conceptual parameters in the SCS CN loss method, SCS unit hydrograph transform method and the constant monthly baseflow method were adjusted iteratively to obtained best fitting of the simulated result to the observed. The calibrated parameter of HEC-HMS model was presented in Appendix C4. Hydrologic parameters such as CN, initial abstraction, and lag time were the sensitive parameters to be adjusted.

In the hydrological modelling aspect, the CN value is calculated as an average per basin while Manning's n coefficient is a constant value for natural channels. The CN is the most sensitive hydrologic parameters among the rest which characterize the runoff properties for a soil and ground cover. When CN value decreases, the peak discharge and runoff volume also decreases. A higher CN values indicate most of the rainfall to appear as runoff, with minimal losses whereas a lower CN values correspond to an increased ability of the soil to retain rainfall and produce much less runoff. As Kuantan is covered

with agriculture and forest land use up to 90 % as referred to the land use map provided by DOA, thus the CN value must be low to percolate the rainfall.

Another parameter which affect the runoff volume in the loss method is the initial abstraction. In a tropical region such as Kuantan, the initial abstraction can be neglected and assumed to be zero due to the antecedent or previous heavy rainfall that has fully filled the soil storage (fully saturated). Thus, the volume of surface runoff generated is directly equal to the volume of rainfall. The I_a/S , coefficient of both 0.2 and 0.05 were tested to evaluate the performance of discharge hydrograph simulated. It was found that coefficient of 0.05 perform better than 0.2 as supported by (Akbari et al., 2016)

For the rainfall runoff transformation model, the lag time parameter was estimated from the physical catchment characteristics using GIS tools. The lag time calculated using Kirpich method refer to Hilbert (2015) was optimized in reference to the adjusted CN value to fit the simulated hydrograph with the observed. The discharge time to peak can be improved with the adjustment of the lag time in the transformation model. Sensitivity analysis indicated that lag time depends on initial abstraction, the intensity of rainfall, and percent impervious area. While keeping all the hydrologic parameters constant, lag times were defined as the auto estimated value in the events on 2010 and 2011 as well as increased 30 % more in the events on 2013 and 2014. The high intensity of rainfall in the year 2013 caused the early generation of surface runoff occurred which could be attributed to fast soil wetting. This has led to overestimating of peak discharge. Thus, the lag time was increased so that the peak discharge and the time to peak are near to the observed data.

The baseflow method adopted in this study was the monthly constant approach. Baseflow values were calibrated by comparing the simulated flow with the observed flow level before the rising limb in the hydrograph. In the KRB, there is only one streamflow station available which is the Bukit Kenau Station. The simulated flood hydrographs obtained at the Bukit Kenau junction in HEC-HMS were compared to the observed data for all the flood events selected in the study.

The flood event from 29th December 2010 to 2nd January 2011 were simulated as the calibration dataset. After several adjustment and trial and error of the calibration parameters, the best simulated result of the hydrograph obtained is presented in Figure

4.10. Table 4.3 listed the values of the calibration parameters used in the calibration. From the hydrograph, the simulated streamflow pattern showed four (4) peak discharges in the entire event while the observed indicated three (3) peak discharges in this flood event. The first peak which occur on 30th December 2010 showed that the simulation has underestimated the streamflow by 60 m³/s. At the end of 31st December 2010, a peak discharge was simulated in hydrological model while no sign of peak was observed from the gauging data. For the other two peaks in the month of January 2011, the simulation overestimated the peak discharge by 53.5 m³/s on the 1st January 2011 and more on the 2nd January 2011 by 200 m³/s. It is also observed that the peak occurred latter one hour compared to the observed peak.

In addition, the Nash-Sutcliffe model efficiency coefficient, NSE of this hydrograph obtained was 0.752 and the Root Mean Square Error, RMSE was 64.8 m³/s. Since the NSE is more than 0.5, the model is considered good in calibration. However, the model underestimated at the first peak of the discharge and overestimated the subsequent 3 peaks with an average difference of 64.8 m³/s. The overestimation of the simulated result might be due to the insufficient rainfall stations available near the Bukit Kenau streamflow station which subsequently affect volume of rainfall distribution. This error might be reduced by reducing by introduce the initial loss abstraction in runoff volume model estimation to reduce the runoff volume via infiltration loss.

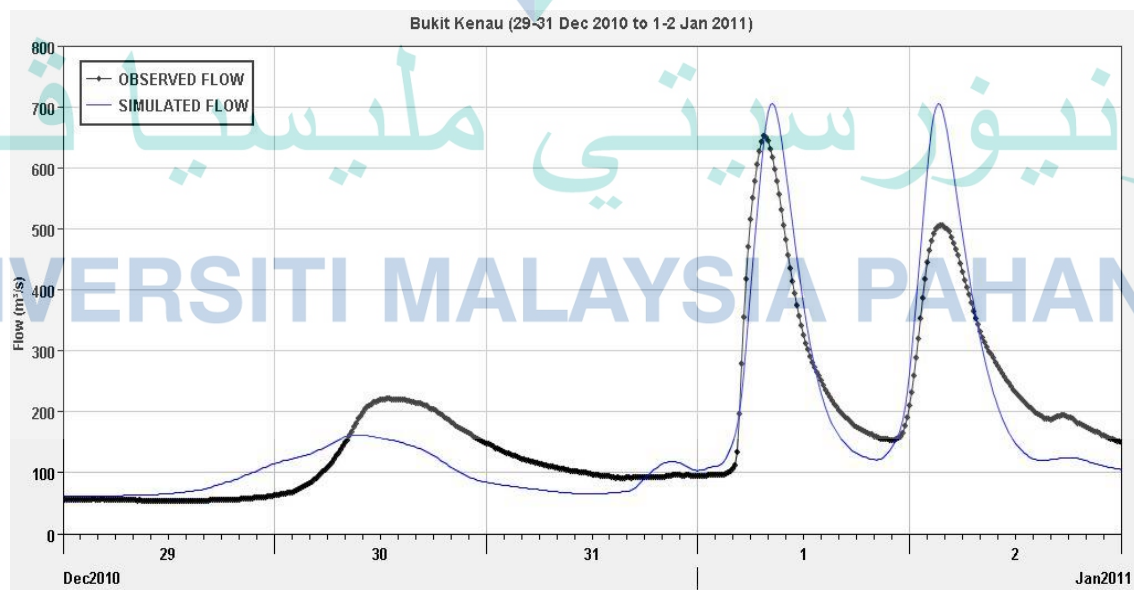
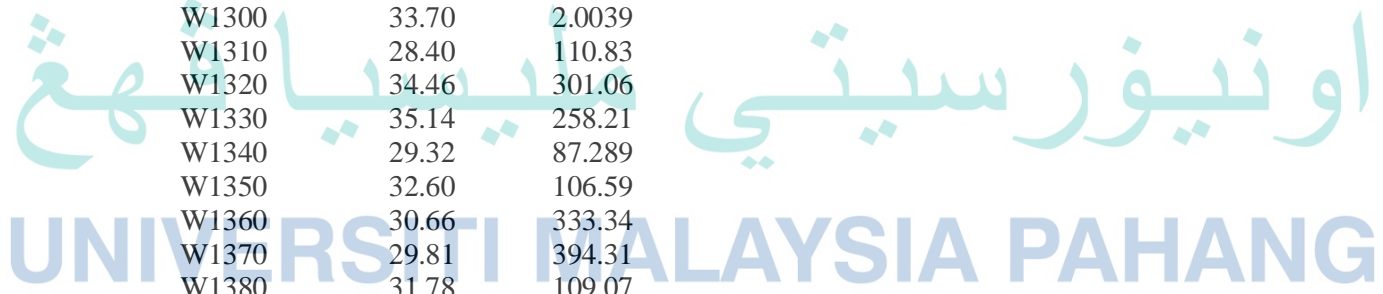


Figure 4.10 The simulated vs observed data on 29th December 2010 to 2nd January 2011 at Bukit Kenau Station

Table 4.3 The calibration parameters used in the calibration on 29th December 2010 to 2nd January 2011

Subbasin	CN	Lag Time (min)			
W1000	27.91	237.32	W740	28.27	98.988
W1010	25.90	211.39	W750	28.40	78.298
W1020	26.50	127.05	W760	27.92	103.45
W1030	33.56	120.89	W770	33.69	55.503
W1040	27.90	139.47	W780	30.94	66.671
W1050	27.98	122.8	W790	31.85	188.92
W1060	29.21	169.22	W800	30.84	157.97
W1070	27.96	197.55	W810	28.72	132.52
W1080	30.20	111.65	W820	31.00	103.54
W1090	34.02	34.215	W830	28.57	189.72
W1100	30.06	182.48	W840	28.25	136.54
W1110	29.50	136.17	W850	28.44	153.48
W1120	27.56	37.969	W860	32.26	127.8
W1130	29.64	184	W870	26.84	205.87
W1140	30.44	112.3	W880	28.57	104.26
W1150	30.37	103.84	W890	28.17	87.534
W1160	29.28	131.54	W900	32.29	115.44
W1170	30.96	166.7	W910	27.60	85.345
W1190	31.40	146.64	W920	28.83	216.72
W1200	26.63	234.02	W930	29.56	107.57
W1210	35.00	66.603	W940	27.96	67.672
W1220	29.42	260.22	W950	28.01	71.313
W1240	35.54	98.37	W960	31.63	68.454
W1250	36.45	44.723	W970	24.36	160.53
W1260	35.09	98.351			
W1270	35.82	114.7			
W1280	33.14	309.51			
W1290	31.10	321.83			
W1300	33.70	2.0039			
W1310	28.40	110.83			
W1320	34.46	301.06			
W1330	35.14	258.21			
W1340	29.32	87.289			
W1350	32.60	106.59			
W1360	30.66	333.34			
W1370	29.81	394.31			
W1380	31.78	109.07			
W1400	29.18	186.24			
W1410	29.43	72.514			
W1450	30.26	61			
W1460	29.92	65.583			
W1500	28.27	227.16			
W1510	32.84	90.405			
W1550	36.21	124.1			
W1560	29.40	167.95			
W700	28.86	115.91			
W710	28.32	121.9			
W720	32.28	103.01			
W730	32.07	38.38			



Values of the calibrated parameters adjusted for the 29th December 2010 to 2nd January 2011 flood event were remained and used in the flood event in 26th to 30th March 2011 for validation. The validated flood hydrograph was simulated as presented in Figure 4.11. The observed streamflow pattern showed four (4) peak discharges in the entire event while the simulated indicated five (5) peak discharges in this flood event. The first peak showed that the simulation overestimated the discharge by 51.5 m³/s on 27th March 2011. However, a peak discharge was simulated in hydrological model while no sign of peak was observed from the gauging data on 28th March 2011. The third simulated peak discharges were slightly underestimated compared to the observed data from the gauging data at the end of 28th March 2011. In addition, the two (2) more simulated peaks on 29th and 30th March 2011 were also underestimated than the observed peak discharge by 9.7 m³/s and 4.6 m³/s respectively. It is observed that the peak occurred on the same period as the observed peak. The NSE of the flood hydrograph obtained was 0.589 with RMSE of 35.1 m³/s. This indicates equally overestimation and underestimation of discharge data with a small difference between the simulated and observed data.

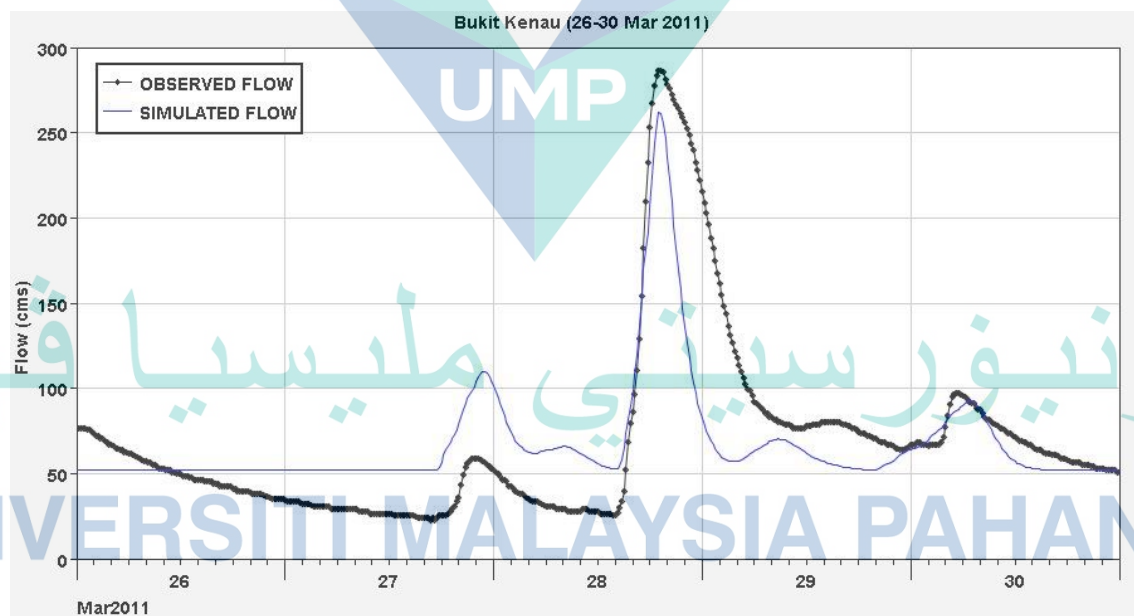


Figure 4.11 The simulated vs observed flood hydrograph on 26th to 30th March 2011 at Bukit Kenau Station

On 16th to 19th March 2014 flood event, the hydrological parameters were calibrated. The observed streamflow pattern showed one (1) peak discharge in the entire event while the simulated indicated two (2) peak discharges in this flood event in Figure 4.12. The first peak showed that the simulation overestimated the discharge by 20.5 m³/s on 16th March 2014 where the observed data is around 2.0 m³/s. The second simulated peak discharges were slightly underestimated compared to the observed data from the gauging data at the quarter of 17th March 2014 at 56.8 m³/s and 67.8 m³/s respectively. It is observed that the peak occurred on the same period as the observed peak. The NSE of the flood hydrograph was 0.540 and the RMSE was 10.7 m³/s. There were equally overestimated and underestimated discharge data which have a small difference between the simulated and observed data. Table 4.4 presents the calibrated parameters in HEC-HMS.

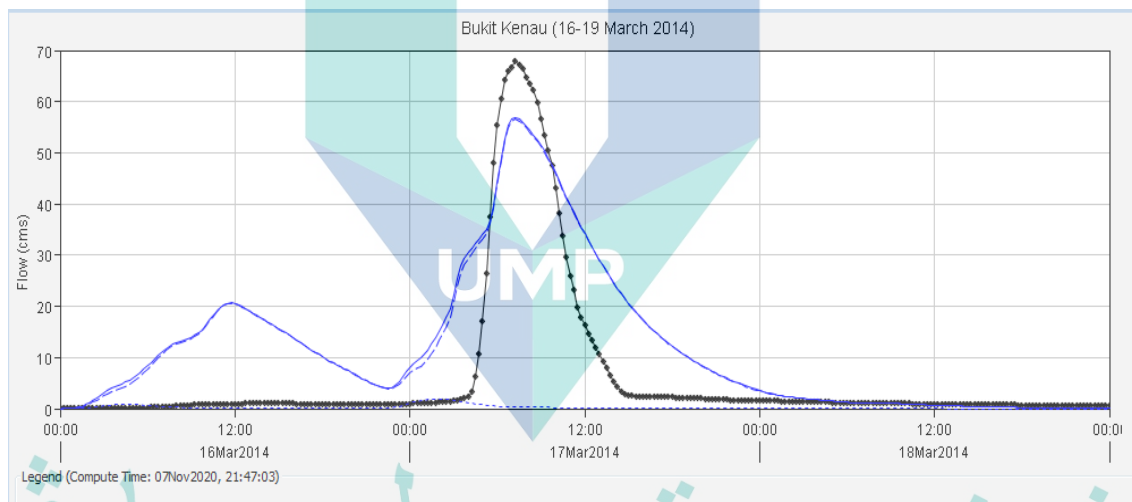


Figure 4.12 The simulated vs observed flood hydrograph on 16th to 19th March 2014 at Bukit Kenau Station

Table 4.4 The calibration parameters used in the calibration on 16th to 19th March 2014

Subbasin	CN	Lag Time (min)			
W1000	19.47	436.17	W740	17.64	219.21
W1010	21.49	274.23	W750	17.47	177.80
W1020	22.48	158.01	W760	17.46	225.91
W1030	24.28	235.47	W770	24.02	112.58
W1040	17.46	303.99	W780	21.07	138.32
W1050	17.56	267.12	W790	24.06	319.36
W1060	19.41	349.08	W800	21.61	309.30
W1070	21.33	309.03	W810	18.66	279.72
W1080	19.54	248.36	W820	20.59	225.54
W1090	24.09	71.35	W830	22.07	292.02
W1100	21.11	349.02	W840	21.03	225.24
W1110	22.44	219.30	W850	17.58	346.54
W1120	13.54	112.07	W860	21.97	275.60
W1130	22.93	285.93	W870	18.66	370.54
W1140	21.28	218.82	W880	17.50	239.69
W1150	20.28	219.78	W890	17.41	196.06
W1160	20.26	253.80	W900	22.36	240.82
W1170	22.62	300.09	W910	17.29	183.97
W1190	21.93	293.18	W920	19.61	425.50
W1200	13.90	619.50	W930	23.45	157.58
W1210	25.16	137.31	W940	17.74	144.85
W1220	19.85	526.40	W950	17.77	152.76
W1240	23.35	261.51	W960	24.50	108.21
W1250	24.09	124.66	W970	17.63	255.65
W1260	25.61	194.40			
W1270	25.61	246.89			
W1280	22.58	686.57			
W1290	23.11	559.31			
W1300	23.70	4.20			
W1310	17.53	250.46			
W1320	23.94	667.54			
W1330	23.20	665.17			
W1340	20.00	172.91			
W1350	22.32	229.95			
W1360	23.80	519.22			
W1370	20.68	767.13			
W1380	22.52	213.75			
W1400	20.31	354.71			
W1410	16.85	189.58			
W1450	21.61	113.48			
W1460	19.70	140.36			
W1500	19.06	445.72			
W1510	21.68	211.91			
W1550	26.45	252.77			
W1560	17.55	412.77			
W700	17.82	265.98			
W710	18.66	248.70			
W720	22.44	213.12			
W730	21.86	82.15			

Values of the calibrated parameters adjusted for the 16th to 19th March 2014 flood event were remained and used in 1st to 5th December 2013 flood event in for validation. The validated flood hydrograph was simulated as presented in Figure 4.12. The simulated streamflow pattern showed five (5) peak discharges in the entire event while the observed indicated eight (8) peak discharges in this flood event. The first peak which occurred on 1st December 2013 showed that the simulation underestimated the discharge by 126.1 m³/s. On 2nd December 2013, there are two (2) simulated peak discharges which were underestimated compared to the three (3) observed data from the gauging data. In addition, the third simulated peaks on 3rd January 2011 was slightly overestimated than the observed peak discharge by 288.3 m³/s. The last peak discharge was simulated higher compared to the observed data by 550.9 m³/s. It is observed that the peak occurred on the same period as the observed peak.

This flood hydrograph has the NSE of 0.682 and the Root Mean Square Error, RMSE of 172.8 m³/s. There were overestimated discharge data which occurred on the last two (2) peak due to significant flooding on that date due to continuous rainfall event. The erroneous of the gauging instrument may affect the accuracy of data collection especially during flooding. Overall, the simulated hydrograph has NSE more than 0.5 which is consider acceptable condition. However, the highly overestimated flows at the peak discharge might be due to the poor rainfall distribution data and the initial abstraction as infiltration in soil to reduce the runoff volume and runoff discharge of the flood event. The error could be solved by increase the initial abstraction of the event to reduce the runoff volume of the flood. The sufficient rainfall data also became a factor of model accuracy.

All in all, the model calibration was carried out at the streamflow station junction (Bukit Kenau 3930401) which is the only discharge gauge in KRB. The summary table on model prediction as presented in Table 4.5.

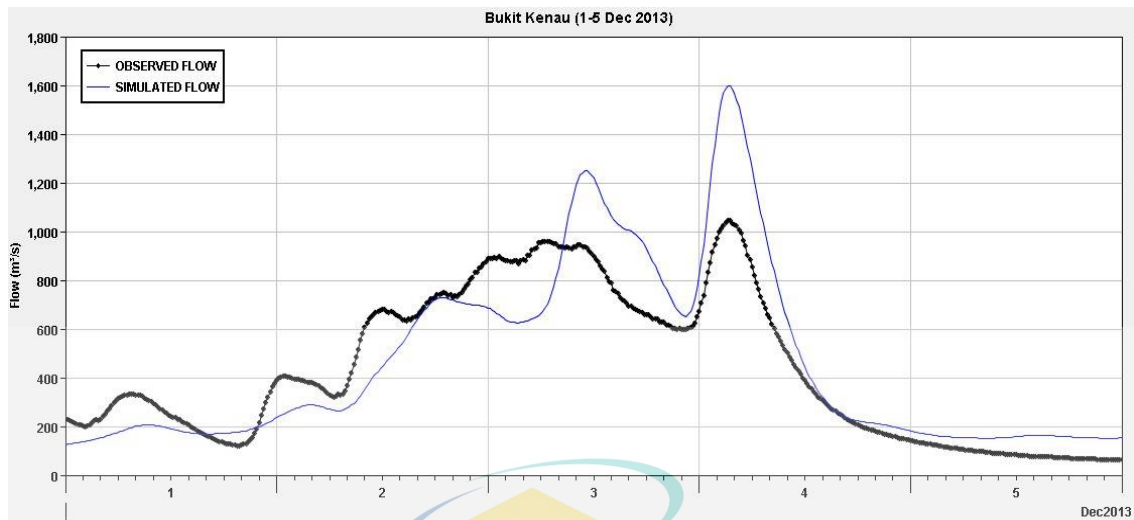


Figure 4.13 The simulated vs observed flood hydrograph on 1st to 5th December 2013 at Bukit Kenau Station

Table 4.5 Summary of model prediction on discharge

Accuracy	Bukit Kenau Station				Average
	2010	2011	2013	2014	
NSE	0.752	0.589	0.682	0.540	0.641
RMSE	64.8	35.1	172.8	10.7	70.9

In general, the model result was acceptable with average NSE of 0.641 which is higher than 0.5. However, the RMSE value of 70.9 is consider a little on the high side indicating room for improvement in the accuracy. The high RMSE value may be due to scarce rainfall distribution and assumption of model parameterization.

4.4 Hydraulic Modelling

4.4.1 1D-2D Unsteady Simulation

In 1D unsteady flow simulation, the water level data was the main parameter to be calibrated and validated with the observed data from DID at Bukit Kenau and Kuantan bypass stations according to selected flood events. The flood event in 2010 was selected as the calibration date to perform the Manning's n optimization. The initial Manning's roughness of the model was set at 0.030 for every cross-section. The finalized Manning's n value to represent the cross-section was found to be 0.050 at node (68000 – 25000) for the upstream cross-section and 0.030 at node (24800 – 0) for the downstream cross-section. The characteristic of the channel surface based on the Manning's roughness coefficient is as below as shown in Appendix B:

- a. Initial Manning's n value (0.030)

Major Stream with top width at flood stage more than 40m. The n-value is less than that for minor streams of similar description because banks offer less effective resistance with clean, straight, full stage, no rifts, or deep pools

- b. Calibrated Manning's n value (0.050 at upstream and 0.030 at downstream)

Major Stream with the same description as above because the range of n value is (0.025 -0.060) with more stone in the upstream region.

In the flood event of year 2010, the water level results were obtained at both Bukit Kenau and Kuantan Bypass stations.

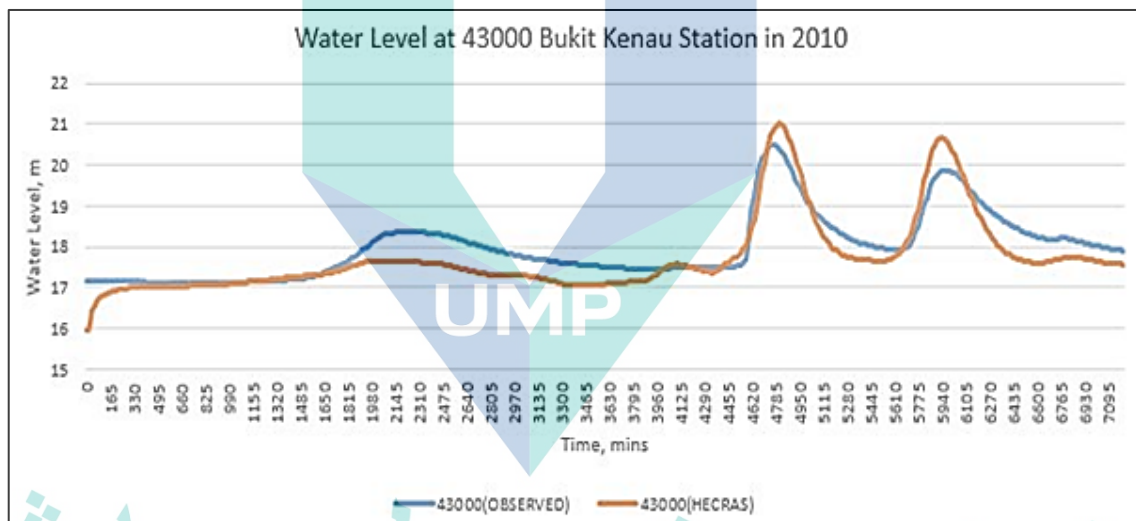


Figure 4.14 The simulated vs observed stage hydrograph on 29th December 2010 to 2nd January 2011 at Bukit Kenau Station

The calibrated Manning's n coefficient was fixed for 2010 flood event. Figure 4.14 has shown that the simulated stage hydrograph which has been fitted with the observed stage hydrograph at the upstream of Bukit Kenau station. The NSE obtained for this simulation is 0.6988, and RMSE of 0.4336 m. Overall, the result of the simulated stage hydrograph is acceptable result because it has NSE is more than 0.5 however RMSE more than 0.1 m.

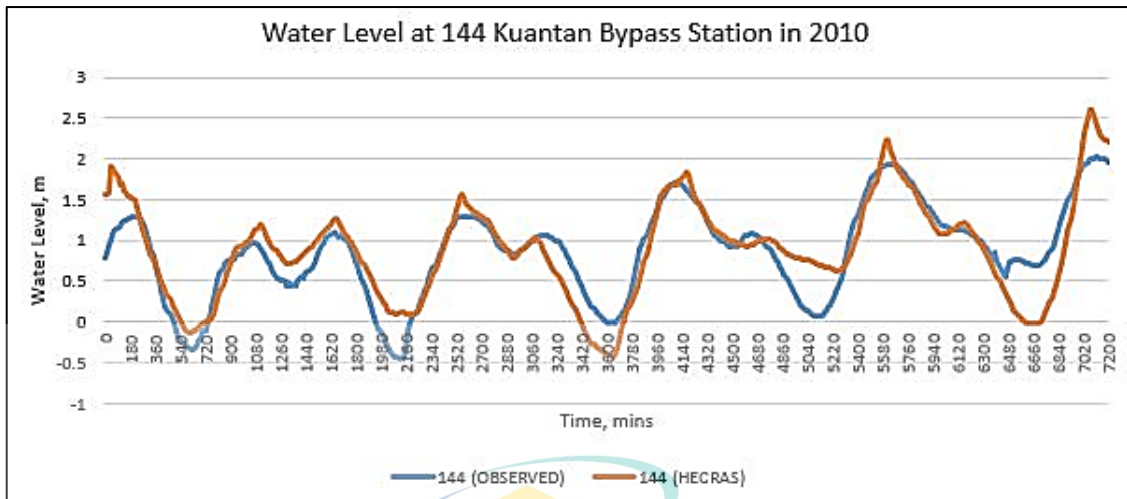


Figure 4.15 The simulated vs observed stage hydrograph on 29th December 2010 to 2nd January 2011 at Kuantan Bypass station

Figure 4.15 shows that the simulated stage hydrograph on 29th December 2010 to 2nd January 2011. It shows that the result fairly fitted with the observed stage hydrograph especially at low water section. For this simulation, the NSE obtained was 0.7140, and RMSE of 0.3012 m. Based on the error analysis, the simulated stage hydrograph is acceptable result.

For the flood event in the year 2011 and 2013, they were used for validation purpose adopting the same hydraulic parameters as 2010. The result for both flood events are presented in the Figure 4.16 to Figure 4.19.

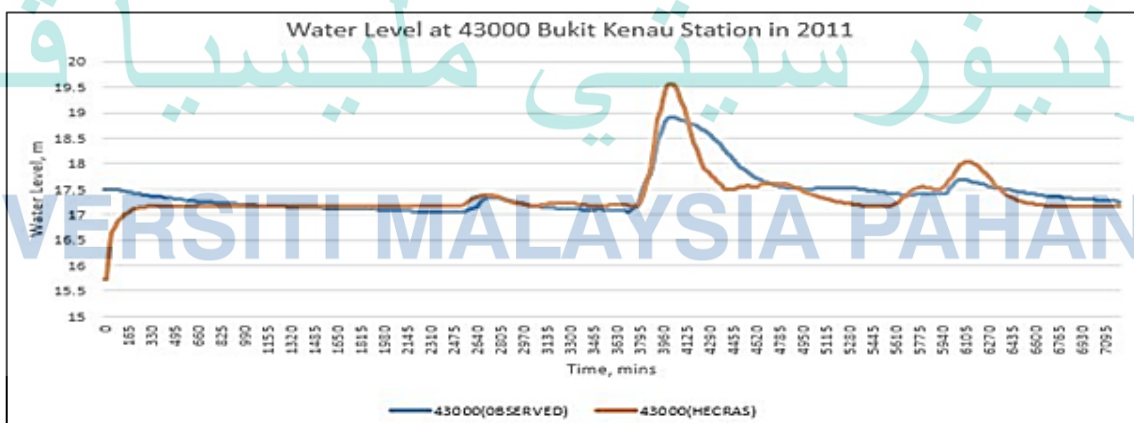


Figure 4.16 The simulated vs observed stage hydrograph on 26th to 30th March 2011 at Bukit Kenau Station

For validation process, Figure 4.16 shows the simulated result is acceptable with obtained NSE of 0.5458 and RMSE of 0.2734. This graph presented the simulated and

observed water level at Bukit Kenau station where overestimation at peak water level. This might be caused by changes of Manning roughness of channel and floodplain due to land use effect

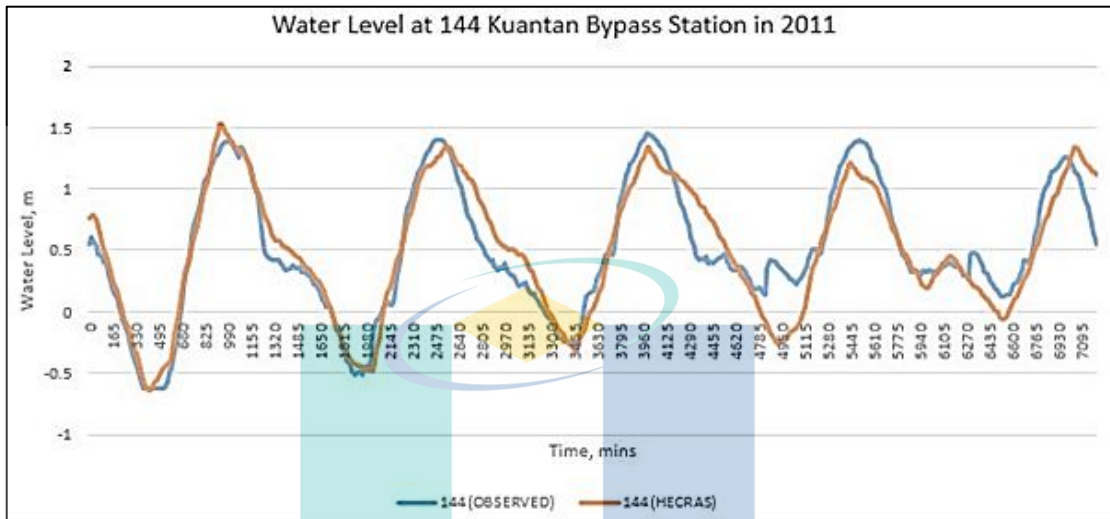


Figure 4.17 The simulated vs observed stage hydrograph on 26th to 30th March 2011 at Kuantan Bypass Station

Figure 4.17 shows on the simulated stage hydrograph on 26th to 30th March 2011 which was fitted well with the observed stage hydrograph and the result at downstream is tidal influence effect. The obtained NSE is 0.8697 with RMSE of 0.1909 m. Overall, the result is acceptable because NSE near to 1 while RMSE is still consider high.

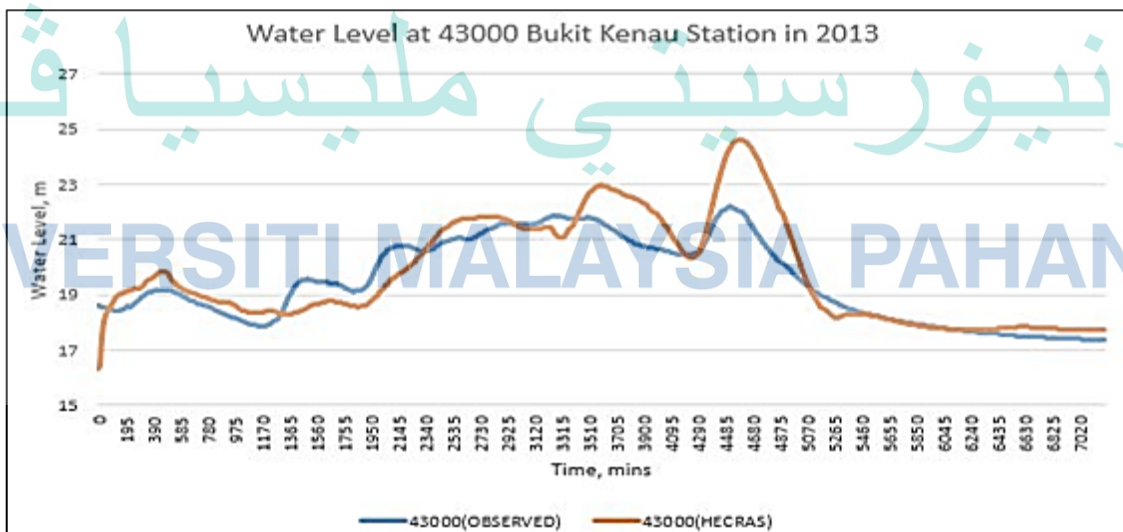


Figure 4.18 The simulated vs observed stage hydrograph on 1st to 5th December 2013 at Bukit Kenau Station

On 1st to 5th December 2013 flood event, the result in Figure 4.18 shows that the simulated stage hydrograph is moderately overestimated compare with the observed stage hydrograph at upstream Bukit Kenau station. The obtained NSE is about 0.6684 while RMSE of 0.8699 m. The result is under acceptable category with NSE more than 0.5 however the RMSE is very high which is almost a meter high. The overestimation might be due to the changes on the riverbed profile, river Manning roughness and landuse changes.

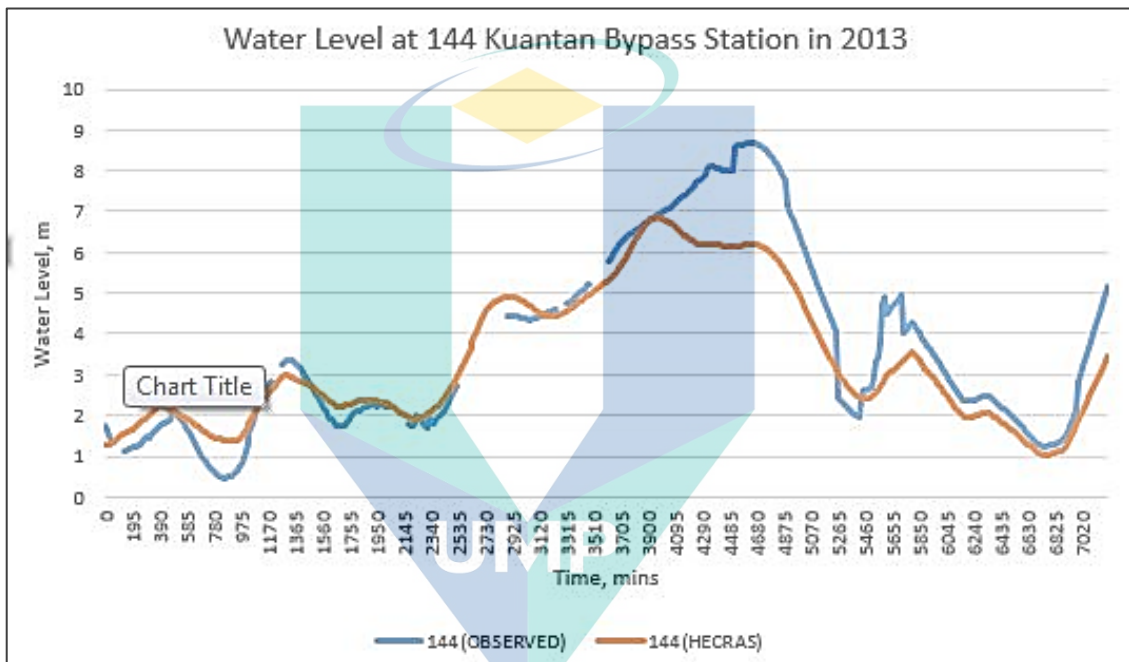


Figure 4.19 The simulated vs observed stage hydrograph on 1st to 5th December 2013 at Kuantan Bypass Station

In Figure 4.19 presents the simulated result slightly underestimation at Kuantan Bypass station. The obtained NSE is about 0.7979 with RMSE of 0.8885 m. Overall, the simulated stage hydrograph is fairly accepted due to NSE more than 0.5 but RMSE is very high.

Lastly, the Table 4.6 shown the summary of the water level prediction as below: All the high RMSE is due to the coarser resolution of floodplain representative model which restricted the water from spilling outside the 1D model. It might also cause by the datum issue of the water level sensor during flooding. Thus, the data obtained might not as accurate as the actual flooding scenario. However, the NSE is still consider satisfactory

where the SRTM-DEM is can be play the role as floodplain area in flood modelling especially at hilly area.

Table 4.6 Summary of model prediction on the 1D water level

Accuracy	Upstream CH43000)	(Bkt	Kenau	Downstream CH144)	(Ktn	Bypass
	2010	2011	2013	2010	2011	2013
NSE	0.699	0.546	0.668	0.714	0.870	0.798
RMSE	0.434	0.273	0.870	0.301	0.191	0.889

4.4.2 Comparison of Flood Inundation Map (FIM) with Historical Flood Event

With the calibrated channel Manning's roughness, the fixed floodplain Manning's roughness, good conveyed 1D model, and selected flood event inflows input, the flood inundation map has been developed. The chosen timestep interval for computation is 2 seconds the same as the 1D unsteady flow simulation setup. The flood inundation maps for the three flood events: a.) 29th December 2010 to 2nd January 2011; b.) 26th to 30th March 2011; c.) 1st to 5th December 2013 were presented in Figure 4.20 to Figure 4.22.

Referring to Figure 4.20, the flood extent occurred surround the downstream of the Sg Kuantan river stretch. The reported flood event on 29th December 2010 to 2nd January 2011 indicated that the floods occurred Sg Balok and Sg Cherating which were outside of Kuantan River Basin. Therefore, the results cannot be compared with the DID flood report. In Figure 4.21, it shows that there is no flood extent occurred. This is also supported by DID flood report that no flood happened between 26th to 30th March 2011.

According to the annually rainfall distribution, the amount of rainfall is rather less during the month of March. Based on Figure 4.22, serious flood occurred at a downstream part of Sg Kuantan with large area of extend. The flood event from 1st to 5th December 2013 has caused severe damages to the citizens of the Kuantan Districts. The simulated result has been justified by comparing with the observed data from DID in term flood locations, flood extent and historical aerial photos.

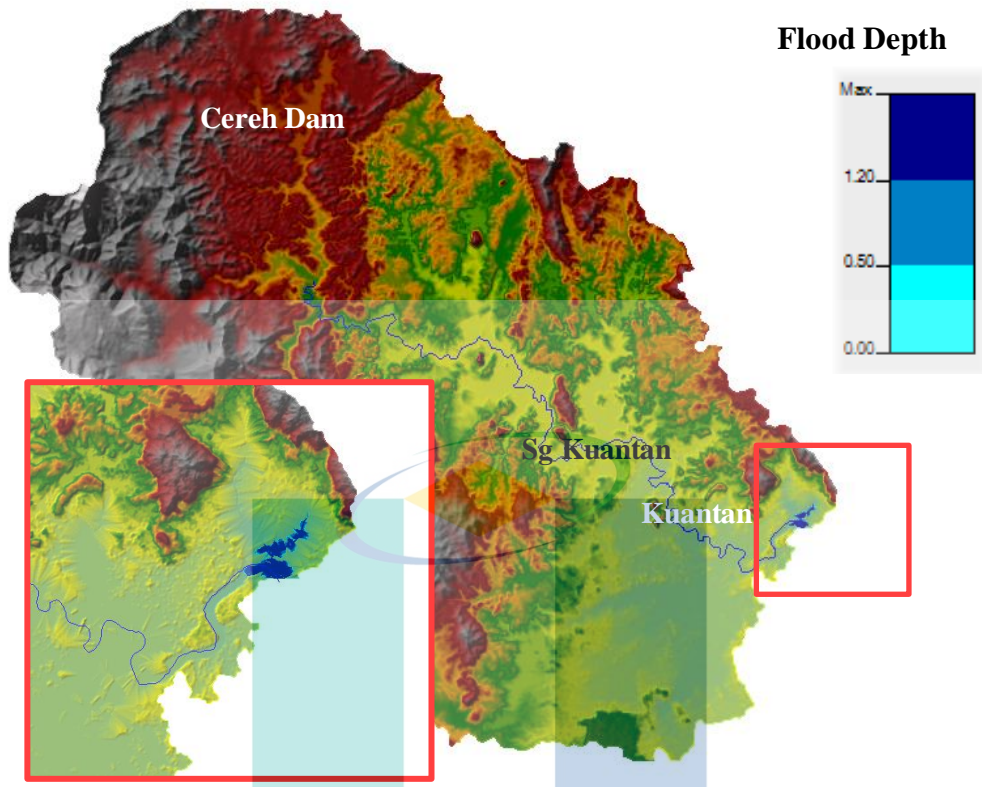


Figure 4.20 Generated FIM on 29th December 2010 to 2nd January 2011

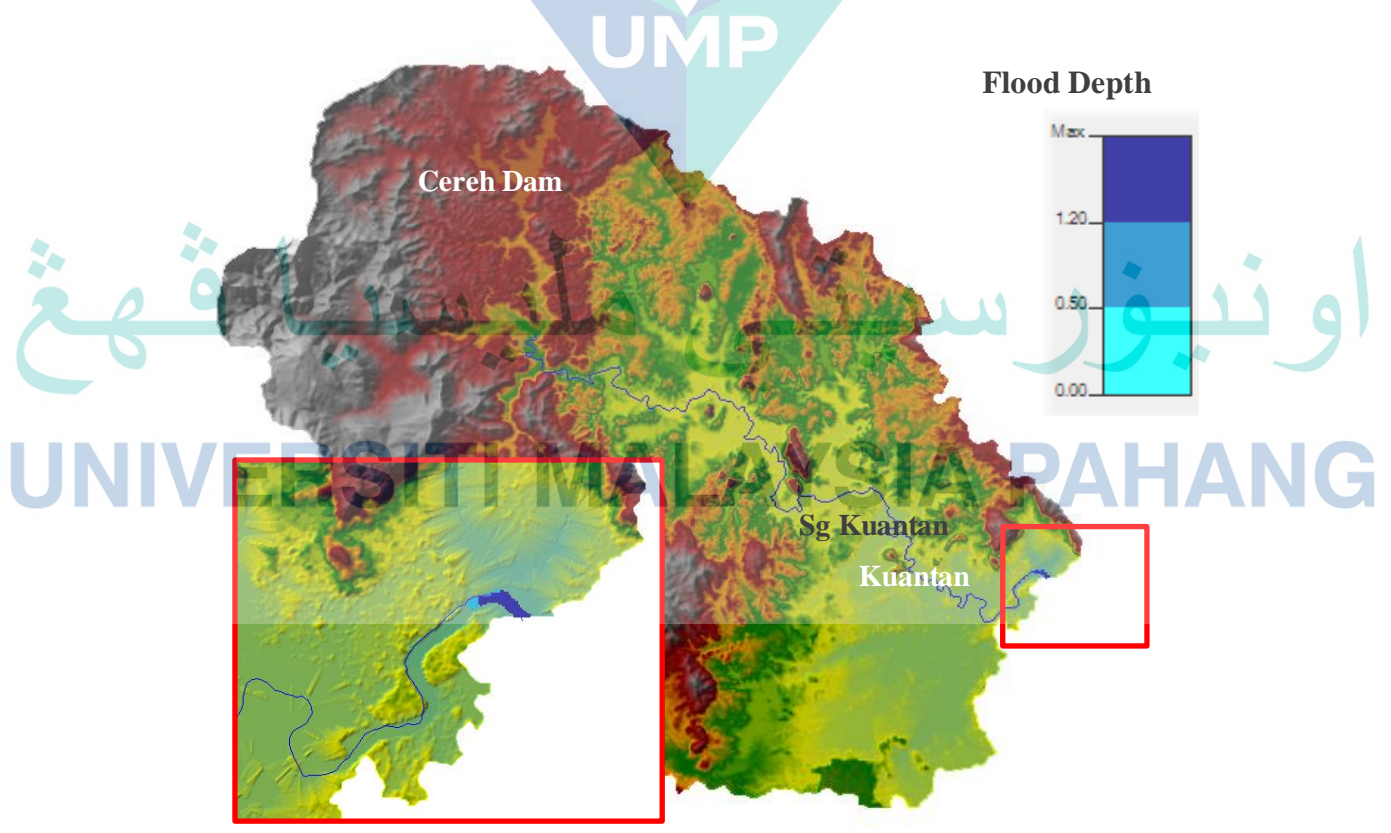


Figure 4.21 Generated FIM on 26th – 30th March 2011

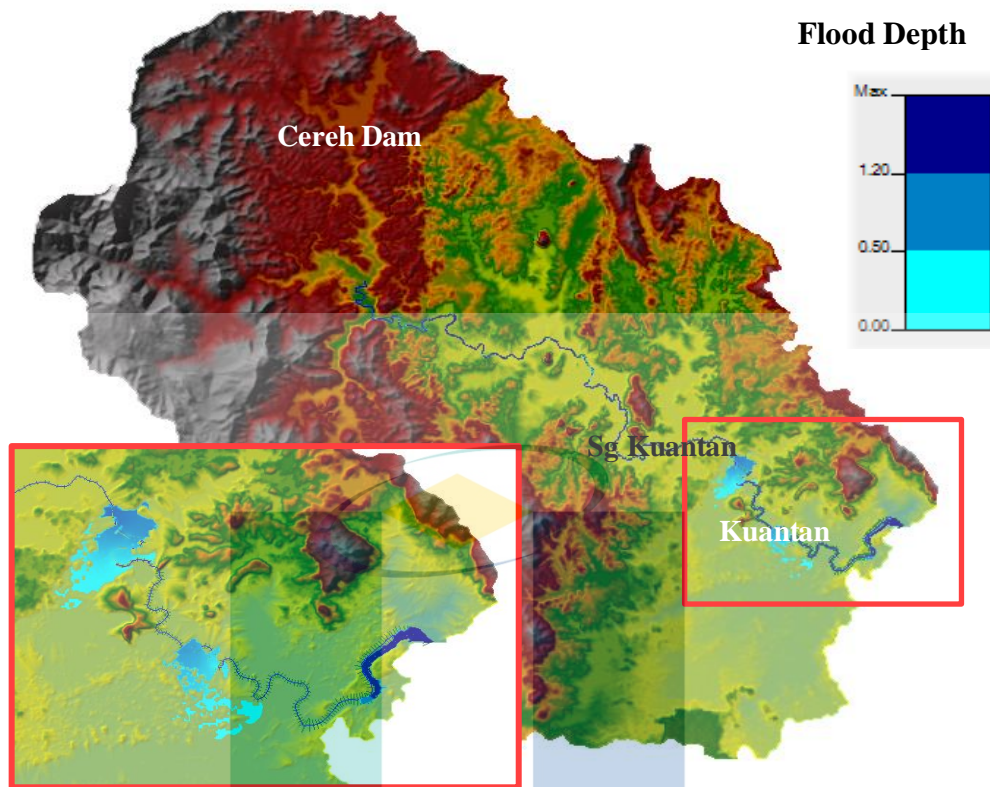
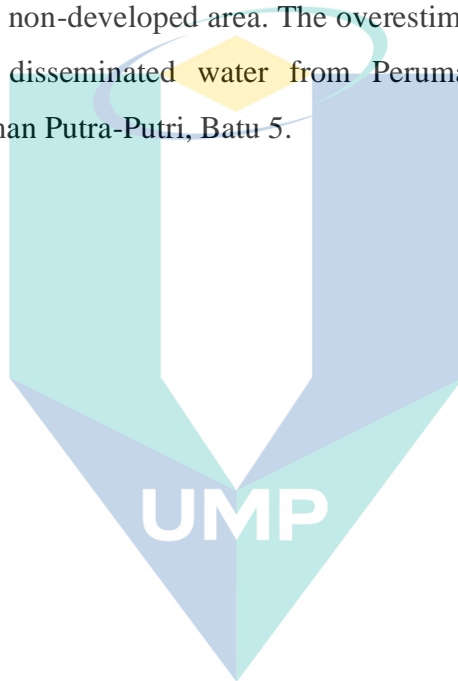


Figure 4.22 Generated FIM on 1st to 5th December 2013

The simulated flood map in year 2013 was compared with the available observed flood information such as FIM collected from DID flood report. Figure 4.23 displays the flooded areas in the year 2013. The flood extent is highlighted in red zones. The generated flood extent in Figure 4.24 has shown that 8 out of 13 locations were within the listed observed flooded region. The 8 flooded locations identified were PAKR Sg Pandan, Sek. Keb. Bukit Rangin, Perkampungan Bukit Rangin, Sg Lembing, Kg Tiram, Sg Isap, Cenderawasih, and Kg. Jawa/Kg. Tengah/Kg. Baru. On the other hand, the model failed to detect other 5 locations including Jalan Bypass Kuantan, Permatang Badak, Kg Selamat, Tok Sira, and Kuantan Megamall area as the flooded region. This is because the locations are situated far away from the riverbank and within a residential zone. The overestimated flood extent presented in the figure was the disseminated water from Jalan Bypass Kuantan and Permatang Badak. Meanwhile, the underestimated flood areas were at the downstream left bank of the lowland urbanized area near the river mouth where the elevation is higher than the river bank. Based on hydraulic result, the simulated flood area was about 43.2 km² while the reported flood map was about 38.4 km². This indicates 12.5% overestimation on the flood extend. In term of depth, the simulation showed flood depth ranges from 0.1 m to 4.0 m.

Figure 4.25 indicates that the simulated flood extent matched 6 out of 8 locations of the observed flood areas. These flooded locations were obtained from the DID report where the matched detected locations at Sg Isap Damai, Sg Isap Jaya, Perkampungan Sg Isap, Cenderawasih, Taman Sepakat, and Taman Tanah Putih Baru. The other 2 places were not detected as the flooded region at Taman Putra-Putri, Batu 5 and Perumahan Permatang Badak. mSince the SRTM-30m is consider rather coarse at flat land (the flooded urbanized areas), the spilled water could not pass through the overestimated zone which was supposed to be low. As a result, the water flows towards the lowland area such as the agricultural and non-developed area. The overestimated flood extent presented in this figure was the disseminated water from Perumahan Permatang Badak and underestimated at Taman Putra-Putri, Batu 5.



اونيورسيتي ملايسيا قهغ

UNIVERSITI MALAYSIA PAHANG

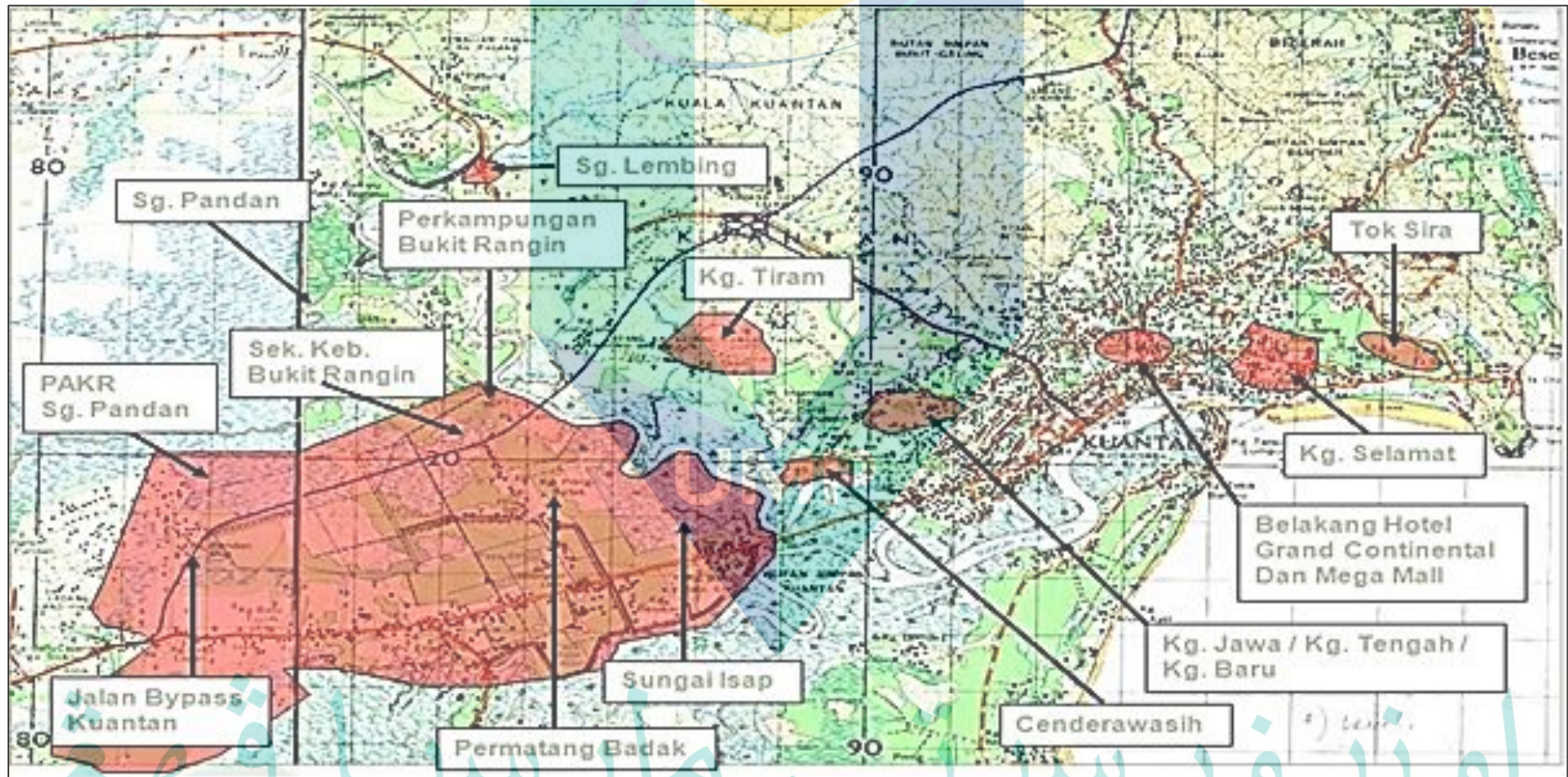


Figure 4.23 Hardcopy of Digital Flood Inundation Map (FIM) in the year of 2013 from DID flood report

Source: Kuantan (2015)



Figure 4.24 Generated flood area from HECRAS (in red filled) with the observed flooded locations from Figure 4-22 (in red line) in the year 2013



Figure 4.25 Generated FIM from HECRAS (in red colour) with the observed flooded locations extracted from DID flood report in the year 2013

HEC-RAS underestimated the flooded regions that occurred within the city and residential area. One of the reasons was due to the poor vertical accuracy of the SRTM-30 m where the elevation data at the flat urban areas was not accurate for flood modelling. It only worked well for flood modelling at hilly or mountainous areas. Thus, the excess water from the river cannot be stored within the urban areas where the elevation information was not adequate. Consequently, the water filled up the lower region land cover such as bare soil, agricultural land, or rural areas causing overestimation of flood extend at this region.

In all, flood inundation map is in acceptable and satisfactory status with 62 % and 75 % similarity matched estimation of flooded regions in Figure 4.24 and Figure 4.25 respectively. The flood inundation maps at several locations for the flood event from 1st to 5th December 2013 were compared to the recorded flood report by DID. From the comparison, it was found that the generated flood extends have 62% to 75% of similarity. The percentages of similarity were obtained by the differences number of matched flooded location per total flooded locations. However, the simulated flood depth performance was fairly good due to the coarse resolution terrain data used. Figure 4.26 to Figure 4.28 were indicated the actual flood and the simulated flood (blue filled area) photos comparison during the flood event at different affected area. The top figure is the historical aerial photos and the bottom figure is the google earth view with the flood extent generated from HEC RAS (highlighted in blue colour).

اونيورسيتي ملايسيا قهغ

UNIVERSITI MALAYSIA PAHANG



Source: Hisyam (2013)



Figure 4.26 Scene 1 at the area around Perkampungan Sg. Isap Perdana and Sg. Isap Damai during a flood event in the year 2013 taken from the historical aerial photos and google earth view



Source: Hananni (2013)



اونيورسيتي ماليسيا قهغ
UNIVERSITI MALAYSIA PAHANG

Figure 4.27 Scene 2 at the area around Sg. Isap during a flood event in the year 2013 from the historical aerial photos and google earth view



Source: Hananni (2013)



Figure 4.28 Scene 3 at Tunas Manja near Sg Isap during a flood event in the year 2013 from the historical aerial photos and google earth view

4.4.3 Flood Inundation Map (FIM) based on Land Use Changes

The changes of five classes of landuse from the year 2010 and 2013 have been analyzed. From the analysis outcome, it was found that the water body, buildup area, and agriculture area have increased to 53.8%, 35.6%, and 2.1% respectively. This also indicate the decrease of the other land used such as forest and bare soil. Since the increment of buildup areas reduced the available pervious land surfaces (reduce infiltration into the soil), it consequently increased the amount of runoff in the urban areas. The simulated flow for the year 2013 rainfall event at Bukit Kenau station based on the landuse in the year 2010 and 2013 were computed as 1657.2 m³/s and 1635.4 m³/s, whereas at Kuantan Bypass station were 3010.7 m³/s and 3607.2 m³/s. It was found that the flow has reduced about 1.3% due to the increase in water bodies at the upstream region. However, the flow has increased about 16.5% at downstream region due to the urbanization occurred. The simulated flow for both scenarios were set as inflow into hydraulic model for 2013 flood event.

Two sets of FIM have been generated using different landuse in the year 2010 and 2013. The flood extents obtained were overlaid onto google earth for visualization and analysis purposes. The simulated flood areas for the landuse in the year 2010 and year 2013 were about 22.5 km² and 44.4 km² respectively as shown in

Figure 4.29 and Figure 4.30. This showed that the flood extent has become wider in year 2013. It is worth to note that the results displayed covered only the downstream area showing the more overflowing and flooding areas due to increase in the developed region.

From the results analyses, it has proved that the landuse changes indeed affected the peak discharge and the flood extent of the lowland areas in the basin. Hence, it is vital to consider the landuse changes into the flood modelling and flood mitigation project to prevent underestimation on flood design structures and management.

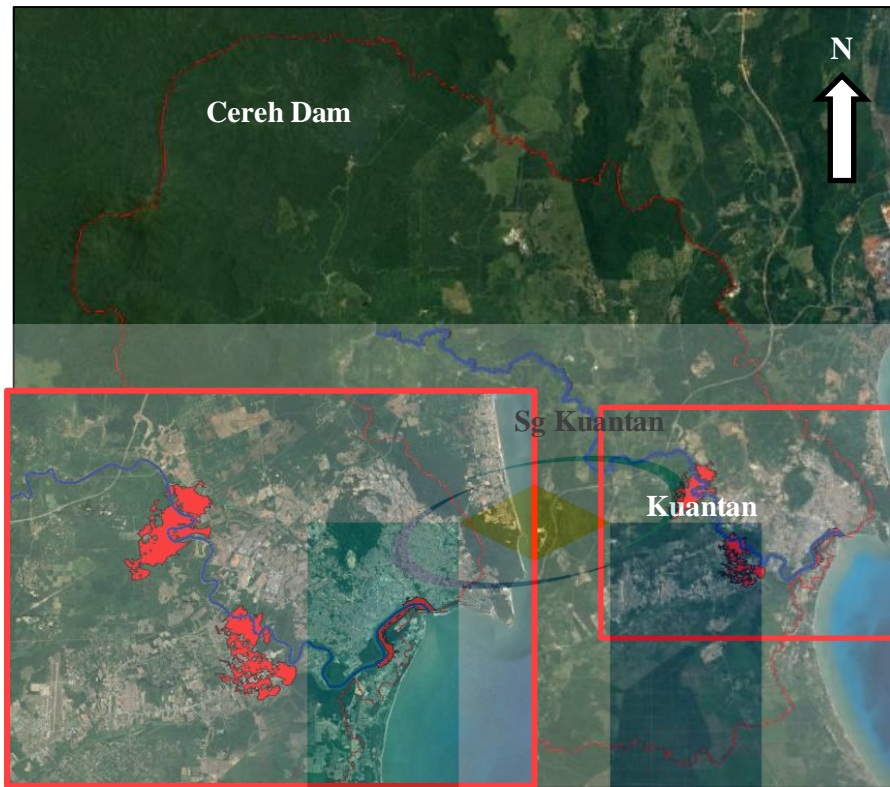


Figure 4.29 Flood Inundation Map based on 2010 landuse

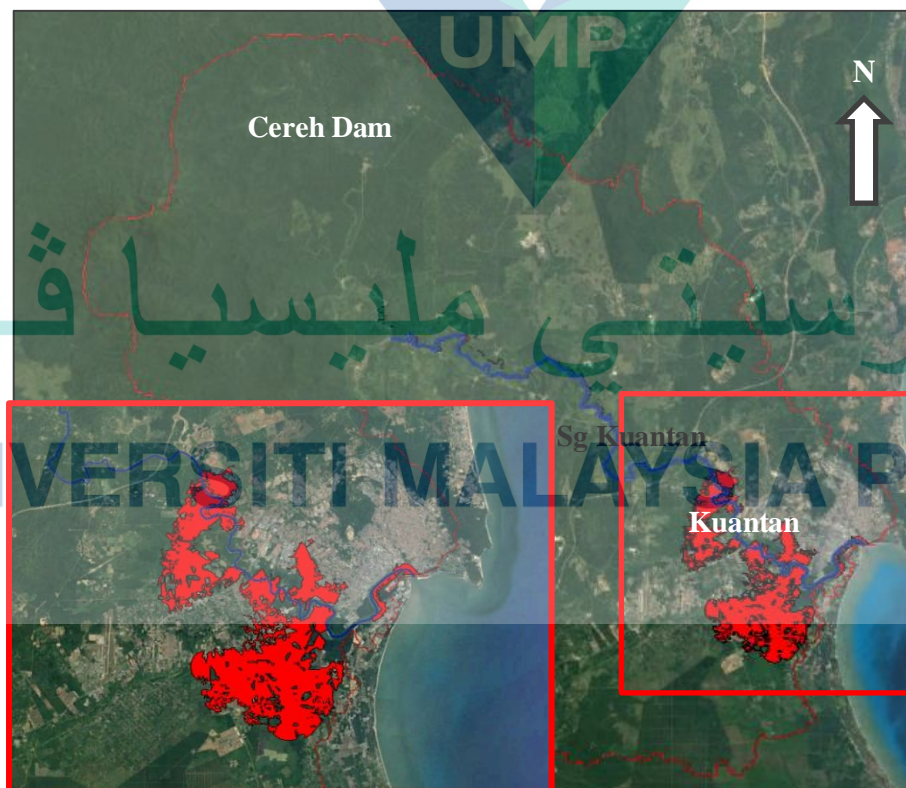


Figure 4.30 Flood Inundation Map based on 2013 landuse

CHAPTER 5

CONCLUSION AND RECOMMENDATIONS

5.1 Introduction

This research involves the analysis of public domain terrain data for flood simulation using public domain hydrologic and hydraulic models. A huge amount of data has been collected and processed based on analytical and statistical approaches. The study results satisfaction outcome in achieving the research objectives.

Firstly, the ArcGIS 10.4 has proven to be a useful tool that can be used to successfully delineate the river basins and river network of Kuantan. It also helped to extract multiple parameters from the SRTM-DEM and create a hydrological database. The CN map, river sub-basins, physical characteristics, and river networks have been generated by using the extension HEC-GeoHMS.

Secondly, the HEC-HMS 4.1 has simulated the flood hydrographs for KRB on the selected flood events where the calibrated hydrographs used were in year 2010 and 2014, and the validated dataset were in the year 2011 and 2013 respectively. Two models evaluation for example the Nash-Sutcliffe Error, NSE and Root Mean Square Error were applied to determine the accuracy of the flood hydrographs. The calibrated hydrographs for the year 2010 and 2014 indicated NSE of 0.752 and 0.540 whereas the validated hydrographs in year 2011 and 2013 showed NSE of 0.589 and 0.682 respectively. Thus, the simulated result can be considered as acceptable.

Thirdly, the HEC-RAS 5.0.3 model has successfully generated FIM for the selected flood events through 1D-2D modelling. The calibration of the water levels has been done in the year 2010 with NSE of 0.699 (Bukit Kenau station) and NSE of 0.714 (KuantanBypass station) as well as validated in the year 2011 and 2013. In year 2011,

the accuracy of NSE at Bukit Kenau station was 0.546 and NSE at KuantanBypass station was 0.870 whereas in the year 2013, the accuracy NSE at Bukit Kenau station was 0.668 and NSE at KuantanBypass station was 0.798. All the simulated water level was considered representative as the observed data as the NSE is more than 0.5.

In the hydraulic modelling aspect, the historical aerial flood photos was referred to give a viable alternative in the absence of the digitized flood extent boundary. The calibrated Manning roughness coefficient was within the ranges based on a suitable value for the riverbed and its floodplain. The channel Manning's roughness ranges from (0.030 – 0.050) and the floodplain Manning's roughness was set to be 0.060. For the assessment of flood inundation map, only the flood area can be assessed not the flood depth as SRTM-DEM 30m is not good to indicate the good terrain in flat area like Kuantan city. The flood prone area was check between the observed and simulated one in term of percentage. The flood extent in 2010 and 2011 were not detected as there is no flood happen in Kuantan whereas there was flood in Kuantan during year 2013. The simulated location which matched with the DID flood report and observed flood region in 2013 with the was 75% and 62% respectively

For the landuse impact towards flood inundation map, two maps have been generated based on landuse in year 2010 and 2013. The flood extent area is bigger in year 2013 (44.4 km²) compare to 2010 (22.5 km²). This incident happened due to higher peak discharge was estimated in year 2013 because approximately 36.5% increment on buildup area (urbanization) since year 2010.

As a conclusion, all the research objectives were achieved and some recommendations has been made for enhancement and improvement in flood modelling results.

5.2 Recommendations

- The SRTM-30 m DEM is good in hydrological modelling but not hydraulic modelling. Thus, a higher resolution DEM, for example, IfSAR-5 m or LiDAR-1 m is suggested to be applied for hydraulic modelling in the urban flat area. Both DEM has a better horizontal and vertical accuracy where LiDAR has approximately 15 cm vertical accuracy which is very fine as the observed topographic data.

- The Manning's roughness coefficient of channel and floodplain can be calculated by using Cowan's method which is required fieldwork. For the channel roughness calculation, the channel base roughness condition, the degree of irregularity, the variation in channel cross-section, the effect of obstruction, the amount of vegetation, and the degree of meandering are being considered in the fieldwork along Sg. Kuantan. Moreover, the floodplain roughness calculation will be focused on the floodplain surface condition, the degree of irregularity, the effect of obstructions, the amount of vegetation, and the degree of meander which is assumed to be 1. By conducting the fieldwork experiment, the Manning's n coefficient can be defined.
- The other tributaries also can be considered in hydraulic modelling by applying for the survey cross-sectional data from DID to obtain a full view of flood extent map. In addition, all the hydraulic structures such as bridges, weirs, and barrage are added into the hydraulic model to get a better result. However, all this hydraulic structures' information must get by fieldwork.
- The flood mitigation solutions need to be proposed to reduce the damage of flooding. Serious analysis can be made by referring to the produced FIM. Some structural method like channelization and enlarge or deepen the drain network around the flooded zones. Besides, levee or flood bank can be applied along the river where water spilled out to prevent flooding to occur again.

All these recommendations can be considered in future studies to improve on flood modelling.

REFERENCES

- Abdulkareem, J., Pradhan, B., Sulaiman, W., & Jamil, N. (2018). Review of studies on hydrological modelling in Malaysia. *Modeling Earth Systems and Environment*, 4(4), 1577-1605.
- Akbari, A. (2011). *Flood modeling using GIS-based watershed hydrological model and remotely sensed data*/Abolghasem Akbari (Doctoral dissertation, University of Malaya).
- Akasah, Z. A., & Doraisamy, S. V. (2015). 2014 Malaysia flood: impacts and factors contributing towards the restoration of damages. *Journal of Scientific Research and Development*, 2(14), 53-59.
- Akbari, A., Mozafari, G., Fanodi, M., & Hemmesy, M. S. (2014). Impact of landuse change on river floodplain using public domain hydraulic model. *Modern Applied Science*, 8(5), 80-86.
- Akbari, A., Samah, A. A., & Daryabor, F. (2016). Raster-based derivation of a flood runoff susceptibility map using the revised runoff curve number (CN) for the Kuantan watershed, Malaysia. *Environmental Earth Sciences*, 75(20), 1-8.
- Alaghmand, S., Abdullah, R., Abustan, I., Said, M. A. M., & Vosoogh, B. (2012). Gis-based river basin flood modelling using HEC-HMS and MIKE11-Kayu Ara river basin, Malaysia. *Journal of Environmental Hydrology*, 20, 1-16.
- Ali, M., Khan, S. J., Aslam, I., & Khan, Z. (2011). Simulation of the impacts of land-use change on surface runoff of Lai Nullah Basin in Islamabad, Pakistan. *Landscape and Urban Planning*, 102(4), 271-279.
- Alias, N. E., Salim, N. A., Taib, S. M., Mohd Yusof, M. B., Saari, R., Adli Ramli, M. W., . . . Ismail, N. (2020). Community responses on effective flood dissemination warnings—A case study of the December 2014 Kelantan Flood, Malaysia. *Journal of Flood Risk Management*, 13(S1), e12552.
- Amini, A., Ali, T. M., Ghazali, A. H. B., Aziz, A. A., & Akib, S. M. (2011). Impacts of land-use change on streamflows in the Damansara Watershed, Malaysia. *Arabian Journal for Science and Engineering*, 36(5), 713-720.
- Bajracharya, S., Shrestha, M., & Shrestha, A. (2017). Assessment of high-resolution satellite rainfall estimation products in a streamflow model for flood prediction in the Bagmati basin, Nepal. *Journal of Flood Risk Management*, 10(1), 5-16.
- Bernama. (2013). Kuantan town almost paralysed, flood situation worsens. *The SUNDAILY*. Retrieved from <http://www.thesundaily.my/news/896679>
- Bhuyian, M. N., Kalyanapu, A., & Hossain, F. (2017). Evaluating conveyance-based DEM correction technique on NED and SRTM DEMs for flood impact assessment of the 2010 Cumberland river flood. *Geosciences*, 7(4), 132.
- Breytenbach, A., & Van Niekerk, A. (2020). Analysing DEM errors over an urban region across various scales with different elevation sources. *South African Geographical Journal*, 102(2), 133-169.

- Brunner, G. W. (2014). *Common model stability problems when performing an unsteady flow analysis*. Davis, CA: USACE Hydrologic Engineering Center.
- Brunner, G. W. (2016). *HEC-RAS, River Analysis System Hydraulic Reference Manual*. Davis, CA: USACE Hydrologic Engineering Center.
- Castro, C. V., & Maidment, D. R. (2020). GIS preprocessing for rapid initialization of HEC-HMS hydrological basin models using web-based data services. *Environmental Modelling & Software*, 130, 104732.
- Chan, N. W. (2015). *Impacts of disasters and disaster risk management in Malaysia: The case of floods*. Resilience and recovery in Asian disasters (pp. 239-265). Springer, Tokyo.
- Chen, D., Shams, S., Carmona-Moreno, C., & Leone, A. (2010). Assessment of open source GIS software for water resources management in developing countries. *Journal of Hydro-environment Research*, 4(3), 253-264.
- Choi, C.-K., Choi, Y.-S., & Kim, K.-T. (2013). Analysis of flood inundation using LiDAR and LISFLOOD model. *Journal of the Korean Association of Geographic Information Studies*, 16(4), 1-15.
- Chong, T., Pan, S., Leong, C., Bahri, S., & Ahmad Khan, A. (2014). *Use of social media in disaster relief during the Kuantan (Malaysia) flood*. 35th International Conference on Information Systems, 14-17 Dec 2014, Auckland, New Zealand.
- Chow, V., Maidment, D. R., & Mays, L. W. (1962). *Applied Hydrology*. *Journal of Engineering Education*, 308, 1959.
- Czubski, K., Kozak, J., & Koleccka, N. (2013). Accuracy of SRTM-X and ASTER elevation data and its influence on topographical and hydrological modeling: case study of the Pieniny Mts. in Poland. *International Journal of Geoinformatics*, 9(2), 7-14.
- De Silva, M., Weerakoon, S., & Herath, S. (2014). Modeling of event and continuous flow hydrographs with HEC-HMS: case study in the Kelani River Basin, Sri Lanka. *Journal Of Hydrologic Engineering*, 19(4), 800-806.
- Di Baldassarre, G., Schumann, G., Bates, P. D., Freer, J. E., & Beven, K. J. (2010). Flood-plain mapping: a critical discussion of deterministic and probabilistic approaches. *Hydrological Sciences Journal–Journal des Sciences Hydrologiques*, 55(3), 364-376.
- Dingman, S. L. (2015). *Physical hydrology*: University of New Hampshire, United States of America Waveland press.
- Domeneghetti, A., Schumann, G. J.-P., & Tarpanelli, A. (2019). Preface: remote sensing for flood mapping and monitoring of flood dynamics: Multidisciplinary Digital Publishing Institute, *Remote Sensing* 11(8), 943.
- Duhan, S., & Kumar, M. (2017). Event and continuous hydrological modeling with HEC-HMS: a review study. *International Journal of Engineering Technology Science and Research*, 4(4), 61-66.
- Edre, M., Hayati, K., Salmiah, M., & SI, S. N. (2015). A case control study on factors associated with leptospirosis infection among residents in flood-prone area, Kuantan: A geographical information system-based approach. *International Journal of Public Health and Clinical Sciences*, 2(3), 151-163.

- El-Shafie, A., Jaafer, O., & Seyed, A. (2011). Adaptive neuro-fuzzy inference system based model for rainfall forecasting in Klang River, Malaysia. *International Journal of the Physical Science*, 6(12), 2875-2888.
- Ernst, J., Dewals, B. J., Detrembleur, S., Archambeau, P., Erpicum, S., & Piroton, M. (2010). Micro-scale flood risk analysis based on detailed 2D hydraulic modelling and high resolution geographic data. *Natural Hazards*, 55(2), 181-209.
- FaghihMina, & Ying, T. P. (2015). GIS techniques for flood modeling and flood inundation mapping. *The Electronic Journal of Geotechnical Engineering*, 20(16), 6795-6805.
- Farran, M. M., & Elfeki, A. M. (2020). Evaluation and validity of the antecedent moisture condition (AMC) of Natural Resources Conservation Service-Curve Number (NRCS-CN) procedure in undeveloped arid basins. *Arabian Journal of Geosciences*, 13(6), 1-17.
- Forkuor, G., & Maathuis, B. (2012). Comparison of SRTM and ASTER derived digital elevation models over two regions in Ghana-Implications for hydrological and environmental modeling. *Studies on Environmental and Applied Geomorphology: InTech*, 220-240.
- Fu, S., Zhang, G., Wang, N., & Luo, L. (2011). Initial abstraction ratio in the SCS-CN method in the Loess Plateau of China. *Transactions of the ASABE*, 54(1), 163-169.
- Gasim, M. B., Toriman, M. E., & Abdullahi, M. G. (2014). Floods In Malaysia historical reviews, causes, effects and mitigations approach. *International Journal of Interdisciplinary Research and Innovations*, 2(4), 59-65.
- Ghani, A. A., Chang, C. K., Leow, C. S., & Zakaria, N. A. (2012). Sungai Pahang digital flood mapping: 2007 flood. *International journal of River Basin Management*, 10(2), 139-148.
- Ghimire, E. (2019). *Evaluation of one-dimensional and two-dimensional HEC-RAS models for flood travel time prediction and damage assessment using HAZUS-MH: A case study of Grand River, Ohio* (Doctoral dissertation, Youngstown State University).
- Goodell, C., & Warren, C. (2014). Flood inundation mapping using HEC-RAS. *Obras y Proyectos*, West Consultant, 2601 25th St SE, Suite 450, Salem, OR 97302.
- Gumindoga, W., Rwasoka, D. T., Nhapi, I., & Dube, T. (2017). Ungauged runoff simulation in upper Manyame Catchment, Zimbabwe: Application of the HEC-HMS model. *Physics and Chemistry of the Earth, Parts A/B/C*, 100, 371-382.
- Hafiz, I., Nor, M. D., Sidek, L. M., Basri, H., Fukami, K., Hanapi, M. N., & Livia, L. (2013). Flood forecasting and early warning system for Dungun River Basin. *Conference Series: Earth and Environmental Science, Putrajaya*, 16, No. 1, p. 012129).
- Hammond, M. J., Chen, A. S., Djordjević, S., Butler, D., & Mark, O. (2015). Urban flood impact assessment: A state-of-the-art review. *Urban Water Journal*, 12(1), 14-29.
- Hananni, A. (2013). 2013 Banjir besar di Kuantan Pahang. Retrieved from <http://amirahhananni.blogspot.my/2013/12/2013-banjir-besar-di-kuantan-pahang.html>

- Hawkins, R. H., Hjelmfelt Jr, A. T., & Zevenbergen, A. W. (1985). Runoff probability, storm depth, and curve numbers. *Journal of irrigation and drainage engineering*, 111(4), 330-340.
- Hilbert, A. (2015). *Rainfall Runoff Simulation Using Modified SCS-CN and HEC-HMS Model in Kuantan Watershed* (Doctoral dissertation, UMP).
- Hirt, C., Filmer, M., & Featherstone, W. (2010). Comparison and validation of the recent freely available ASTER-GDEM ver1, SRTM ver4. 1 and Geodata DEM-9S ver3 digital elevation models over Australia. *Australian Journal of Earth Sciences*, 57(3), 337-347.
- Hisyam, F. (2013). Banjir besar selepas 12 tahun. Retrieved from <http://fadzrulhisyam.blogspot.my/2013/12/banjir-besar-selepas-12-tahun.html>
- Ibarra, S., Romero, R., Poulin, A., Glaus, M., Cervantes, E., Bravo, J., Castillo, E. (2016). Sensitivity analysis in hydrological modeling for the Gulf of Mexico. *Procedia Engineering*, 154, 1152-1162.
- Kabiri, R., Chan, A., & Bai, R. (2013). Comparison of SCS and Green-Ampt methods in surface runoff-flooding simulation for Klang Watershed in Malaysia. *Open Journal of Modern Hydrology*, 3(03), 102.
- Kamran, M., & Rajapakse, R. H. (2018). Effect of watershed subdivision and antecedent moisture condition on HEC-HMS model performance in the Maha Oya basin, Sri Lanka. *International Journal of Engineering Technology and Sciences*, 5(2), 22-37.
- Khattak, M., Anwar, F., Sheraz, K., Saeed, T., Sharif, M., & Ahmed, A. (2016). Floodplain mapping using HEC-RAS and ArcGIS: A case study of Kabul River. *Arabian Journal for Science & Engineering (Springer Science & Business Media BV)*, 41(4).
- Klijn, F., Kreibich, H., De Moel, H., & Penning-Rowsell, E. (2015). Adaptive flood risk management planning based on a comprehensive flood risk conceptualisation. *Mitigation and Adaptation Strategies for Global Change*, 20(6), 845-864.
- Kourtis, I., Bellos, V., & Tsihrintzis, V. (2017). *Comparison of 1D-1D and 1D-2D urban flood models*. Paper presented at the Proceedings of the 15th International Conference on Environmental Science and Technology (CEST 2017), Rhodes, Greece.
- Kuantan, J.P.S.D.R. (2015). *Sub1-Sg.Isap Sg Kuantan saliran daerah Kuantan*. Donna Richardson. Retrieved from <http://slideplayer.com/slide/8537434/>
- Leigh, C., & Low, K. (1978). The flood hazard in peninsular Malaysia: Government policies and action. *Pacific Viewpoint*, 19(1), 47-64.
- Liao, K.-H., Chan, J. K. H., & Huang, Y.-L. (2019). Environmental justice and flood prevention: The moral cost of floodwater redistribution. *Landscape and Urban Planning*, 189, 36-45.
- Maddox, I. (2014). The Risks of Hazard. Retrieved from <http://www.intermap.com/risks-of-hazard-blog/three-common-types-of-flood-explained>
- Majidi, A., & Shahedi, K. (2012). Simulation of rainfall-runoff process using Green-Ampt method and HEC-HMS model (Case study: Abnama Watershed, Iran). *International Journal of Hydraulic Engineering*, 1(1), 5-9.

- Manfreda, S., Leo, M. D., & Sole, A. (2011). Detection of flood-prone areas using digital elevation models. *Journal Of Hydrologic Engineering*, 16(10), 781-790.
- Maxwell, R., Condon, L., & Kollet, S. (2015). A high-resolution simulation of groundwater and surface water over most of the continental US with the integrated hydrologic model ParFlow v3. *Geoscientific Model Development*, 8(3), 923-937.
- Mehebab, S., Raihan, A., Nuhul, H., & Haroon, S. (2015, December). *Assessing flood inundation extent and landscape vulnerability to flood using geospatial technology: a study of Malda district of West Bengal, India*. University of Craiova, Department of Geography. 14(2), 156.
- Miliani, F., Ravazzani, G., & Mancini, M. (2011). Adaptation of precipitation index for the estimation of antecedent moisture condition in large mountainous basins. *Journal Of Hydrologic Engineering*, 16(3), 218-227.
- Mishra, Jain, M., Babu, P. S., Venugopal, K., & Kaliappan, S. (2008). Comparison of AMC-dependent CN-conversion formulae. *Water Resources Management*, 22(10), 1409-1420.
- Mishra, & Singh, V. P. (2013). *Soil conservation service curve number (SCS-CN) methodology* (Vol. 42): Springer Science & Business Media.
- Mohammed, N., Edwards, R., & Gale, A. (2018). Optimisation of flooding recovery for Malaysian universities. *Procedia Engineering*, 212, 356-362.
- Mohor, G., Hudson, P., & Thieken, A. (2020). A comparison of factors driving flood losses in households affected by different flood types. *Water Resources Research*, 56(4), e2019WR025943.
- Moore, J. (Producer). (2012). *Nature and causes of floods and associated secondary hazards*. Retrieved from [https://geographyinactionshss.wikispaces.com/file/view/Nature+and+causes+of+floodi+ng+and+associated+secondary+hazards+\(1\).pdf](https://geographyinactionshss.wikispaces.com/file/view/Nature+and+causes+of+floodi+ng+and+associated+secondary+hazards+(1).pdf)
- Neitsch, S. L., Arnold, J. G., Kiniry, J. R., & Williams, J. R. (2011). *Soil and water assessment tool theoretical documentation version 2009*. Black and Research Center, Texas Water Resources Institute Technical Report No. 406.
- Ng, Z. F., Gisen, J. I., & Akbari, A. (2018, March). Flood inundation modelling in the Kuantan river basin using 1d-2d flood modeller coupled with aster-gdem. *IOP Conference Series: Materials Science and Engineering*, Penang, Malaysia, 318(1), 012024).
- Nor, M., & Rakhecha, P. (2008). *Analysis of a severe tropical urban storm in Kuala Lumpur, Malaysia*. Paper presented at the 11th International Conference on Urban Drainage, Edinburgh, Scotland, UK.
- Olayinka, D. N., & Irivbogbe, H. E. (2017). Flood modelling and risk assessment of Lagos Island and part of eti-osa local government areas in Lagos State. *Journal of Civil and Environmental Systems Engineering*, 15, 106-121.
- Pachepsky, Y. A., Martinez, G., Pan, F., Wagener, T., & Nicholson, T. (2016). Evaluating hydrological model performance using information theory-based metrics. *Hydrology and Earth System Sciences Discussions*, 1-24.

- Paiva, R. C., Collischonn, W., & Tucci, C. E. (2011). Large scale hydrologic and hydrodynamic modeling using limited data and a GIS based approach. *Journal of Hydrology*, 406(3-4), 170-181.
- Pampaniya, N. K. K., & Tiwari, M. K. (2017). Rainfall runoff modeling using remote sensing, GIS and HEC-HMS Model. *Journal of Water Resources and Pollution Studies*, 2(2) 400-405.
- Patel, D. P., Ramirez, J. A., Srivastava, P. K., Bray, M., & Han, D. (2017). Assessment of flood inundation mapping of Surat city by coupled 1D/2D hydrodynamic modeling: a case application of the new HEC-RAS 5. *Natural Hazards*, 89(1), 93-130.
- Pradhan, B., & Youssef, A. (2011). A 100-year maximum flood susceptibility mapping using integrated hydrological and hydrodynamic models: Kelantan River Corridor, Malaysia. *Journal of Flood Risk Management*, 4(3), 189-202.
- Quiroga, V. M., Kure, S., Udo, K., & Mano, A. (2016). Application of 2D numerical simulation for the analysis of the February 2014 Bolivian Amazonia flood: Application of the new HEC-RAS version 5. *RIBAGUA-Revista Iberoamericana del Agua*, 3(1), 25-33.
- Rahman, Balkhair, Almazroui, & Masood. (2017). Sub-catchments flow losses computation using Muskingum–Cunge routing method and HEC-HMS GIS based techniques, case study of Wadi Al-Lith, Saudi Arabia. *Modeling Earth Systems and Environment*, 3(1), 4.
- Rahman, Tarmudi, Z., Rosdy, M., & Muhiddin, F. A. (2017). Flood mitigation measures using intuitionistic fuzzy dematel method. *Malays. J. Geosci.*
- Ramly, S., Tahir, W., Abdullah, J., Jani, J., Ramli, S., & Asmat, A. (2020). Flood estimation for SMART control operation using integrated radar rainfall input with the HEC-HMS Model. *Water Resources Management*, 34(10), 3113-3127.
- Rawat, K. S., Mishra, A. K., Sehgal, V. K., Ahmed, N., & Tripathi, V. K. (2013). Comparative evaluation of horizontal accuracy of elevations of selected ground control points from ASTER and SRTM DEM with respect to CARTOSAT-1 DEM: a case study of Shahjahanpur district, Uttar Pradesh, India. *Geocarto International*, 28(5), 439-452.
- Razi, M., Ariffin, J., Tahir, W., & Arish, N. (2010). Flood estimation studies using hydrologic modeling system (HEC-HMS) for Johor River, Malaysia. *Journal of Applied Sciences*, 10(11), 930-939.
- Reshma, T., Kumar, P. S., Babu, M. R. K., & Kumar, K. S. (2010). Simulation of runoff in watersheds using SCS-CN and muskingum-cunge methods using remote sensing and geographical information systems. *International Journal of Advanced Science and Technology*, 25(31), 31-42.
- Ridolfi, E., Alfonso, L., Di Baldassarre, G., Dottori, F., Russo, F., & Napolitano, F. (2014). An entropy approach for the optimization of cross-section spacing for river modelling. *Hydrological Sciences Journal*, 59(1), 126-137.
- Romali, N., Yusop, Z., & Ismail, A. (2018). *Hydrological modelling using HEC-HMS for flood risk assessment of Segamat Town, Malaysia*. Malaysian Technical Universities Conference on Engineering and Technology 2017, Penang, Malaysia. IOP Conference Series: Materials Science and Engineering, 318(1), 4-10.

- Ros, F. C., Shahrim, M. F. B., & Chuan, D. L. Y. (2019). Estimation of infrastructure demand for flood control in Malaysia, *Malaysia Japan International Institute of Technology (MJIT) Universiti Teknologi Malaysia: Disaster Preparedness & Prevention Centre*, 1-14.
- Sahoo, S. N., & Sreeja, P. (2015). Development of flood inundation maps and quantification of flood risk in an urban catchment of Brahmaputra River. *ASCE-ASME Journal of Risk and Uncertainty in Engineering Systems*, 3(1), 5-10.
- Salajegheh, A., Bakhshaei, M., Chavoshi, S., Keshtkar, A., & Najafi Hajivar, M. (2010). Floodplain mapping using HEC-RAS and GIS in semi-arid regions of Iran. *Desert*, 14(1), 83-93.
- Sardooi, E. R., Rostami, N., Sigaroudi, S. K., & Taheri, S. (2012). Calibration of loss estimation methods in HEC-HMS for simulation of surface runoff (Case Study: Amirkabir Dam Watershed, Iran). *Advances in Environmental Biology*, 6(1), 343-348.
- Satheeshkumar, S., Venkateswaran, S., & Kannan, R. (2017). Rainfall-runoff estimation using SCS-CN and GIS approach in the Pappiredipatti watershed of the Vaniyar sub basin, South India. *Modeling Earth Systems and Environment*, 3(1), 24.
- Shahirah, A., & Saru, M. (2012). *A study on causes of flood at Sungai Isap and Jalan Tun Ismail, Kuantan, Pahang* (Doctoral dissertation, UMP).
- Sobhani, G. (1976). *A review of selected small watershed design methods for possible adoption to Iranian conditions*, 3(2), 2-6.
- Sulaiman, M., El-Shafie, A., Karim, O., & Basri, H. (2011). Real-time flood forecasting by employing artificial neural network based model with zoning matching approach. *Hydrology and Earth System Sciences Discussions*, 8(5), 9357-9393.
- Taib, Z. M., Jaharuddin, N. S., & Mansor, Z. (2016). A review of flood disaster and disaster management in Malaysia. *Int. J. Account. Bus. Manag.*, 4, 97-105.
- Tariq, Q. (2015). First wave of Kuantan flood victims evacuated. *The Star Online*. Retrieved from <http://www.thestar.com.my/news/nation/2015/12/28/first-wave-of-kuantan-flood-victims-evacuated/>
- Tassew, B. G., Belete, M. A., & Miegel, K. (2019). Application of HEC-HMS model for flow simulation in the lake tana basin: the case of gilgel abay catchment, upper blue Nile basin, Ethiopia. *Hydrology*, 6(1), 21.
- Technologies, I. (2012). *The risk of hazard: three common types of flood explained*. Retrieved from <https://www.intermap.com/risks-of-hazard-blog/three-common-types-of-flood-explained#:~:text=Coastal%20flooding%20is%20categorized%20in,threat%20to%20life%20and%20property.>
- Timbadiya, P., Patel, P., & Porey, P. (2011). HEC-RAS based hydrodynamic model in prediction of stages of lower Tapi River. *ISH Journal of Hydraulic Engineering*, 17(2), 110-117.

- USAC, H. (2010). HEC RAS river analysis system, User's Manual, Version 4.1. *US Army Corps of Engineers, Hydraulic Engineering Center, Retrieved from* https://www.hec.usace.army.mil/software/hec-ras/documentation/HEC-RAS_4.1_Users_Manual.pdf
- Verma, A. K., Jha, M. K., & Mahana, R. K. (2010). Evaluation of HEC-HMS and WEPP for simulating watershed runoff using remote sensing and geographical information system. *Paddy and Water Environment*, 8(2), 131-144.
- Vozinaki, A.-E. K., Morianou, G. G., Alexakis, D. D., & Tsanis, I. K. (2017). Comparing 1D and combined 1D/2D hydraulic simulations using high-resolution topographic data: a case study of the Koiliaris basin, Greece. *Hydrological Sciences Journal*, 62(4), 642-656.
- Wang, W., Yang, X., & Yao, T. (2012). Evaluation of ASTER GDEM and SRTM and their suitability in hydraulic modelling of a glacial lake outburst flood in southeast Tibet. *Hydrological Processes*, 26(2), 213-225.
- Yang, Y., Du, J., Cheng, L., & Xu, W. (2017). Applicability of TRMM satellite precipitation in driving hydrological model for identifying flood events: a case study in the Xiangjiang River Basin, China. *Natural Hazards*, 87(3), 1489-1505.
- Yerramilli, S. (2012). A hybrid approach of integrating HEC-RAS and GIS towards the identification and assessment of flood risk vulnerability in the city of Jackson, MS. *American Journal of Geographic Information System*, 1(1), 7-16.
- Zaidi, S. M., Akbari, A., Abu Samah, A., Kong, N. S., Gisen, A., & Isabella, J. (2017). Landsat-5 time series analysis for land use/land cover change detection using NDVI and Semi-Supervised Classification Techniques. *Polish Journal of Environmental Studies*, 26(6), 2833-2840.
- Zaidi, S. M., Akbari, A., & Ishak, W. M. F. (2014). A critical review of floods history in Kuantan River Basin: Challenges and potential solutions. *International Journal of Civil Engineering & Geo-Environment*, 5(1), 40-45.
- Zamri, Z. (2009). *The effect of high tides on sungai damansara using infowork rs.* (Doctoral dissertation, Universiti Teknologi Malaysia).
- Zarrineh, N., Griensven, V. A., Sennikovs, J., Bekere, L., & Plunge, S. (2015). *Regionalisation of parameters of a large-scale water quality model in Lithuania using PAIC-SWAT.* Paper presented at the EGU General Assembly Conference Abstracts, Vienna, Austria, id 607.
- Zema, D. A., Labate, A., Martino, D., & Zimbone, S. M. (2017). Comparing different infiltration methods of the HEC - HMS Model: The case study of the mésima torrent (Southern Italy). *Land Degradation & Development*, 28(1), 294-308.
- Zope, P., Eldho, T., & Jothiprakash, V. (2016). Impacts of land use-land cover change and urbanization on flooding: a case study of Oshiwara River Basin in Mumbai, India. *Catena*, 145, 142-154.

APPENDIX A
SURVEY FIELDWORK PICTURES

a. Rainfall Station



Figure A1 The Manual Method of Rainfall Measurement at Rainfall Station



Figure A2 The Rainfall Data Collection from Tipping Bucket Rainfall Gauge

b. Streamflow Station



Figure A3 The Telemetry Station at Bukit Kenau

c. Water Level Station



Figure A4 The Telemetry Water Level Station at Bukit Kenau

APPENDIX B HYDRAULIC PARAMETERS

TABLE 7: NATURAL CHANNELS AND FLOODPLAINS

Channel	HYDRAULIC ROUGHNESS (MANNING'S n) VALUES		
	Minimum	Normal	Maximum
A. Minor streams (top width at flood stage less than 100 feet)			
1. Streams on plain			
a. Clean, straight, full stage, no rifts or deep pools	0.025	0.030	0.033
b. Same as above, but more stones and weeds	0.030	0.035	0.040
c. Clean, winding, some pools and shoals	0.033	0.040	0.045
d. Same as above, but some weeds and stones	0.035	0.045	0.050
e. Same as above, lower stages, irregular slopes and sections with more ineffective flow area	0.040	0.048	0.055
f. Same as d. but more stones	0.045	0.050	0.060
g. Sluggish reaches, weedy, deep pools	0.050	0.070	0.080
h. Very weedy reaches, deep pools, or floodways with heavy stand of timber and underbrush	0.075	0.100	0.150
2. Mountain streams, no vegetation in channel, banks usually steep, trees and brush along banks submerged at high stages			
a. Bottom: gravels, cobbles, and few boulders	0.030	0.040	0.050
b. Bottom: cobbles with large boulders	0.040	0.050	0.070
B. Floodplains			
1. Pasture, no brush			
a. Short grass	0.025	0.030	0.035
b. High grass	0.030	0.035	0.050
2. Cultivated areas			
a. No crop	0.020	0.030	0.040
b. Mature row crops	0.025	0.035	0.045

Channel	HYDRAULIC ROUGHNESS (MANNING'S n) VALUES		
	Minimum	Normal	Maximum
c. Mature field crops	0.030	0.040	0.050
3. Brush			
a. Scattered brush, heavy weeds	0.035	0.050	0.070
b. Light brush and trees, in winter	0.035	0.050	0.060
c. Light brush and trees, in summer	0.040	0.060	0.080
d. Medium to dense brush, in winter	0.045	0.070	0.110
e. Medium to dense brush, in summer	0.070	0.100	0.160
4. Trees			
a. Dense willows, summer, straight	0.110	0.150	0.200
b. Cleared land with tree stumps, no sprouts	0.030	0.040	0.050
c. Same as above, but with heavy growth of sprouts	0.050	0.060	0.080
d. Heavy stand of timber, a few down trees, little undergrowth, flood stage below branches	0.080	0.100	0.120
e. Same as above, but with flood stage reaching branches	0.100	0.120	0.160
C. Major streams (top width at flood stage more than 100 feet). The n values are less than those of minor streams with similar description because banks offer less effective resistance.			
1. Regular section with no boulders or brush	0.025	0.060
2. Irregular and rough section	0.035	0.100

Figure B1 The Manning's n Coefficient of Natural Channel and Floodplains

APPENDIX C
HYDROLOGICAL PARAMETERS

a. Rainfall Data

Table C1 The Rainfall Data on 29th December 2010 – 2nd January 2011 Flood Event at Each Rainfall Stations

Date Time	Site 3731018 Jkr. Gambang at Pahang, mm	Site 3732020 Paya Besar at Kuantan, mm	Site 3732021 Kg. Sg. Soi at Pahang, mm	Site 3832015 Ranc. Pam Paya Pinang at Pahang, mm	Site 3833002 Pej. Jps. N. Pahang at Pahang, mm	Site 3930012 Sg. Lembing Pccl Mill at Pahang, mm	Site 3931013 Ldg. Nada at Pahang, mm	Site 3931014 Ldg. Kuala Reman at Pahang, mm
29/12/2010 0:00	0	0	0	0	0	0	0	0
29/12/2010 0:15	0	0	0	0	0	0	0	0
29/12/2010 0:30	0	0	0	0	0	0	0	0
29/12/2010 0:45	0	0	0	0	0	0	0	0
29/12/2010 1:00	0	0	0	0	0	0	0	0
29/12/2010 1:15	0	0	0	0	0	0	0	0
29/12/2010 1:30	0	0	0	0	0	0	0	0
29/12/2010 1:45	0	0	0	0	0	0	0	0
29/12/2010 2:00	0	0	0	0	0	0	0	0

b. Streamflow Data

Table C2 The Streamflow Data on 29 December 2010 – 2 January 2011 Flood Event at Bukit Kenau Station

Date Time	Site 3930401 Bukit Kenau at Pahang, m ³ /s
29/12/2010 0:00	34.8
29/12/2010 0:15	34.8
29/12/2010 0:30	34.8
29/12/2010 0:45	34.8
29/12/2010 1:00	34.8
29/12/2010 1:15	34.8
29/12/2010 1:30	34.8
29/12/2010 1:45	34.8
29/12/2010 2:00	34.8
29/12/2010 2:15	34.8
29/12/2010 2:30	34.8
29/12/2010 2:45	34.8
29/12/2010 3:00	34.8
29/12/2010 3:15	35.2
29/12/2010 3:30	35.8
29/12/2010 3:45	34.8
29/12/2010 4:00	34.8
29/12/2010 4:15	35.2
29/12/2010 4:30	35.8
29/12/2010 4:45	34.8
29/12/2010 5:00	34.8

c. Water Level Data

Table C3 The Water Level on 29 December 2010 – 2 January 2011 Flood Event at Kuantan Bypass Station

Date Time	Site 3832420 Kuantan Bypass at Pahang, m
29/12/2010 0:00	0.78
29/12/2010 0:15	0.86
29/12/2010 0:30	0.94
29/12/2010 0:45	1
29/12/2010 1:00	1.08
29/12/2010 1:15	1.14
29/12/2010 1:30	1.16
29/12/2010 1:45	1.18
29/12/2010 2:00	1.21
29/12/2010 2:15	1.24
29/12/2010 2:30	1.25
29/12/2010 2:45	1.26
29/12/2010 3:00	1.27
29/12/2010 3:15	1.29
29/12/2010 3:30	1.29
29/12/2010 3:45	1.3
29/12/2010 4:00	1.28
29/12/2010 4:15	1.27
29/12/2010 4:30	1.23
29/12/2010 4:45	1.17
29/12/2010 5:00	1.09

d. HEC-HMS Parameters

Table C4 The HEC-HMS Hydrologic Loss and Transform Parameters on 29 December 2010 – 2 January 2011 Flood Event

Subbasin	Ia, mm	CN	%	Lag time, min
W1000	0	27.91	5	237.32
W1010	0	25.90	5	211.39
W1020	0	26.50	5	127.05
W1030	0	33.56	5	120.89
W1040	0	27.90	5	139.47
W1050	0	27.98	5	122.8
W1060	0	29.21	5	169.22
W1070	0	27.96	5	197.55
W1080	0	30.20	5	111.65
W1090	0	34.02	5	34.215
W1100	0	30.06	5	182.48
W1110	0	29.50	5	136.17
W1120	0	27.56	5	37.969
W1130	0	29.64	10	184
W1140	0	30.44	5	112.3
W1150	0	30.37	5	103.84
W1160	0	29.28	10	131.54
W1170	0	30.96	20	166.7
W1190	0	31.40	40	146.64
W1200	0	26.63	15	234.02
W1210	0	35.00	60	66.603
W1220	0	29.42	5	260.22
W1240	0	35.54	40	98.37
W1250	0	36.45	60	44.723
W1260	0	35.09	50	98.351
W1270	0	35.82	65	114.7
W1280	0	33.14	25	309.51
W1290	0	31.10	20	321.83
W1300	0	33.70	5	2.0039
W1310	0	28.40	5	110.83
W1320	0	34.46	15	301.06
W1330	0	35.14	10	258.21
W1340	0	29.32	5	87.289
W1350	0	32.60	10	106.59
W1360	0	30.66	5	333.34
W1370	0	29.81	5	394.31
W1380	0	31.78	10	109.07
W1400	0	29.18	5	186.24
W1410	0	29.43	5	72.514

W1450	0	30.26	15	61
W1460	0	29.92	5	65.583
W1500	0	28.27	10	227.16
W1510	0	32.84	5	90.405
W1550	0	36.21	50	124.1
W1560	0	29.40	30	167.95
W700	0	28.86	5	115.91
W710	0	28.32	5	121.9
W720	0	32.28	5	103.01
W730	0	32.07	5	38.38
W740	0	28.27	5	98.988
W750	0	28.40	5	78.298
W760	0	27.92	5	103.45
W770	0	33.69	5	55.503
W780	0	30.94	5	66.671
W790	0	31.85	5	188.92
W800	0	30.84	5	157.97
W810	0	28.72	5	132.52
W820	0	31.00	5	103.54
W830	0	28.57	5	189.72
W840	0	28.25	5	136.54
W850	0	28.44	5	153.48
W860	0	32.26	5	127.8
W870	0	26.84	5	205.87
W880	0	28.57	5	104.26
W890	0	28.17	5	87.534
W900	0	32.29	5	115.44
W910	0	27.60	5	85.345
W920	0	28.83	5	216.72
W930	0	29.56	5	107.57
W940	0	27.96	5	67.672
W950	0	28.01	5	71.313
W960	0	31.63	5	68.454
W970	0	24.36	5	160.53

Table C5 The HEC-HMS Muskingum-Cunge Routing Method Parameters on 29 December 2010 – 2 January 2011 Flood Event

Reach	Length,m	Slope	n	Width,m	Side slope
R1420	1341.7	0.005217	0.055	100	0.1
R1470	3139.3	0.005415	0.055	50	1
R1520	1346.1	0.005	0.055	100	0.1
R1570	2136.5	0.005	0.055	150	0.1
R160	8637.7	0.001737	0.055	50	1
R180	11606	0.005601	0.055	50	1
R20	5003.8	0.004996	0.055	50	1
R210	4247.4	0.003296	0.055	50	1
R220	8507.5	0.000705	0.055	50	1
R230	3809.6	0.000262	0.055	50	1
R240	3205.3	0.000936	0.055	100	0.1
R250	1677.5	0.001788	0.055	50	1
R270	2659.2	0.002256	0.055	50	1
R280	3976.7	0.007293	0.055	50	1
R290	3064.1	0.000653	0.055	100	0.1
R300	9701.4	0.000825	0.055	100	0.1
R320	2785.5	0.0002	0.055	50	1
R340	4588.4	0.005	0.055	50	1
R360	825.53	0.005	0.055	100	0.1
R370	7127.9	0.005	0.055	100	0.1
R380	2033.5	0.005	0.055	50	1
R40	1946.3	0.013872	0.055	50	1
R400	6207.8	0.000322	0.055	50	1
R440	1325	0.0005	0.055	50	1
R470	9083.7	0.00011	0.055	100	0.1
R490	2680.4	0.001865	0.055	100	0.1
R520	4593.2	0.001	0.055	100	0.1
R530	825.98	0.0001	0.03	350	0.1
R540	5427.6	0.000368	0.03	150	0.1
R560	522.77	0.005	0.03	250	0.1
R570	6265.9	0.000958	0.03	300	0.1
R590	30.804	0.0005	0.03	50	1
R600	2717.7	0.0005	0.055	50	1
R640	8958.1	0.000335	0.055	50	1
R670	5694.3	0.002283	0.055	50	1
R690	20632	0.001163	0.055	50	1
R70	4801.9	0.005	0.055	50	1
R90	4140	0.002657	0.055	50	1